

Exploration of the physiological role of the endogenous CXCR4 inhibitor
EPI-X4 on hematopoiesis and immunology in mice

Dissertation
zur Erlangung des Doktorgrades
der Naturwissenschaften

vorgelegt beim Fachbereich Biowissenschaften
der Johann Wolfgang Goethe - Universität
in Frankfurt am Main

von
Eva Maria Danner
aus Worms

Frankfurt 2020

D30

vom Fachbereich Biowissenschaften der

Johann Wolfgang Goethe - Universität als Dissertation angenommen.

Dekan: Prof. Dr. Sven Klimpel

Gutachter: Prof. Dr. Virginie Lecaudey

Prof. Dr. Halvard Bönig

Datum der Disputation:

Table of contents

Zusammenfassung	4
1. Introduction	9
1.1. CXCR4/CXCL12 axis	9
1.2. EPI-X4.....	11
1.3. Mouse models.....	14
1.4. Aims of this work	16
2. Material and methods.....	17
2.1. Material	17
2.2. Methods	20
2.2.1. EPI-X4-targeting strategy	20
2.2.2. Mice	21
2.2.3. Genotyping.....	21
2.2.4. Mobilization of hematopoietic cells	23
2.2.5. Recovery from hematopoietic stress	23
2.2.6. Transplantation of hematopoietic cells	24
2.2.7. Preparation of blood and organs	24
2.2.8. Lysis of erythrocytes.....	24
2.2.9. Preparation of spleen or bone marrow cell suspensions.....	24
2.2.10. Blood analysis (CBC)	25
2.2.11. Plasma preparation	25
2.2.12. Methylcellulose assay (CFU-C assay)	25
2.2.13. BM-fluid collection	26
2.2.14. Induction of Peritonitis	26
2.2.15. DSS-induced Colitis	26
2.2.16. OVA challenge (based on Kato <i>et al.</i> , 2001).....	26

2.3.	Flow cytometry (FACS) based methods	27
2.3.1.	Cell surface protein analyses	27
2.3.2.	Intracellular staining	27
2.3.3.	Cytokine measurements.....	28
2.4.	Biomolecular methods.....	28
2.4.1.	Mass spectrometry for EPI-X4 detection	28
2.4.2.	Determination of RNA/DNA-contents	29
2.4.3.	Measurement of CXCL12 concentrations.....	29
2.4.4.	LPS measurements.....	29
2.4.5.	Histology of colon samples.....	30
2.4.6.	Stool sample collection.....	31
2.5.	Statistics.....	31
3.	Results	32
3.1.	Generation of EPI-X4 mutant mice	32
3.2.	Hematopoietic cells during homeostasis.....	33
3.3.	EPI-X4 alters T-cell distribution	37
3.4.	HSPC mobilization is independent of EPI-X4	37
3.5.	Engraftment of HSPC is normal after transplantation	42
3.6.	Regeneration after hematopoietic stress is independent from EPI-X4	47
3.7.	Immune reaction to peritonitis is not dependent on EPI-X4	52
3.8.	No role for EPI-X4 in DSS-induced colitis.....	55
3.9.	Microbiome changes in EPI-X4 deficient mice.....	59
3.10.	Pathogen defense is not influenced by EPI-X4.....	60
3.11.	Response to orally presented allergen is influenced by EPI-X4.....	61
4.	Discussion.....	63
4.1.	Divergent findings in different Ala-EPI-X4 mouse models.....	63
4.2.	EPI-X4 in the context of immature hematopoiesis	65
4.3.	Impact of EPI-X4 on lymphopoiesis.....	69

4.4. EPI-X4 in the context of inflammation.....	71
5. Conclusion	75
Literature	76
Abbreviations	88
Table of Figures	91
Tables	93
Appendix	94
Acknowledgements	117
Curriculum vitae	118

Zusammenfassung

Die CXCR4/CXCL12-Achse ist von entscheidender Bedeutung für die Entstehung und Aufrechterhaltung einer gesunden, reifen Hämatopoese. Erstmals beschrieben wurde der später als CXCR4 bezeichnete Rezeptor 1996 allerdings als Co-Rezeptor für den Eintritt humaner HIV-Viren in Lymphozyten. Ein großes Interesse bestand daraufhin darin, sowohl natürliche Inhibitoren des G-Protein gekoppelten Rezeptors zu identifizieren, als auch synthetische herzustellen, um einen Eintritt des Virus in den menschlichen Organismus zu verhindern bzw. seine Ausbreitung zu unterbinden. Zahlreiche potentielle Liganden wurden seitdem entwickelt, die an CXCR4 binden, jedoch längst nicht mehr nur als HIV-Inhibitoren. Als wichtigster Vertreter der natürlich vorkommenden CXCR4-Liganden spielt CXCL12 im hämatopoetischen System eine zentrale Rolle. Ursprünglich als B-Zell-Wachstumsfaktor *in vitro* identifiziert, wurde schnell seine Schlüsselfunktion für die Retention von hämatopoetischen Stammzellen im Knochenmark erkannt. Darüber hinaus ist er für die Migration von Blutzellen von entscheidender Bedeutung. Ein weiterer natürlich vorkommender CXCR4-Ligand, der 2015 von Zirafi und Kollegen erstmals beschrieben wurde, fand sich im Hämofiltrat von Dialysepatienten. Der im weiteren Verlauf als EPI-X4 bezeichnete CXCR4-Antagonist wurde als Spaltprodukt von Albumin identifiziert, welches über viele Spezies hochkonserviert ist. Diese Eigenschaft interpretieren wir als Hinweis auf eine relevante physiologische Funktion des Peptids. Die Bedingungen, unter denen EPI-X4 von Albumin abgespalten wird, wurden experimentell als sauer ermittelt: EPI-X4 entsteht durch gezielte partielle Proteolyse im sauren Milieu von Neutrophilenelelastasen und Cathepsinen. Da die Halbwertszeit von natürlich vorkommendem EPI-X4 beim Menschen vermutlich sehr kurz ist, sind *in vivo*- und darauffolgende *in vitro*-Analysen schwierig durchzuführen. *In-vitro*-Spike-Analysen von synthetischem EPI-X4 in humanem Plasma ergaben eine Halbwertszeit von nur 17 Minuten. Die geringen auftretenden Konzentrationen erschweren die Problematik zusätzlich. In dieser Arbeit sollen deshalb im Mausmodell *in vivo*-Analysen durchgeführt werden, um die Effekte von potentiell entstehendem EPI-X4 in verschiedenen experimentellen Ansätzen aufzudecken. Ein probates, hier verwendetes Mittel, ist die Analyse einer *Knock-out* (KO)-Maus. Die für die Bindung an CXCR4 entscheidende Aminosäure von EPI-X4, das am N-Terminus gelegene Leucin, wurde durch Alanin ersetzt, welches die Entstehung von EPI-X4 unterbindet und zusätzlich dessen Bindung an CXCR4 verhindert. Zwei verschiedene Methoden zur Mausgenerierung wurden hierfür verwendet: Ein klassischer Basenaustausch mittels homologer Rekombination (HR) und ein solcher durch die CRISPR/Cas (CC) Methode. Beide Verfahren stellen zuverlässige Wege dar, um eine Punktmutation im Genom herzustellen, wie sie für die nicht funktionale EPI-X4-Variante, im weiteren Verlauf als Ala-EPI-X4 bezeichnet, benötigt wird.

Sequenzierungen der mutierten Basen und der angrenzenden genomischen Regionen bestätigten den erfolgreichen Basenaustausch (CTA → GCA) und die Integrität der angrenzenden Bereiche in beiden Mausmodellen; beider Mäuse Albuminspiegel im Plasma war normalwertig. Die für CC eingesetzten embryonalen Stammzellen waren von reiner C57Bl/6-Abstammung, wohingegen mittels HR erzeugte mutagene Mäuse zunächst auf C57Bl/6-Hintergrund rückgekreuzt werden mussten. Eine SNP-Analyse bestätigte die erfolgreiche Rückkreuzung. Mit Hilfe dieser beiden Mausmodelle können nun Analysen im EPI-X4-defizienten Modell durchgeführt werden, die im Umkehrschluss Informationen über die organismische Wirkung von EPI-X4 beinhalten. Zunächst wurde in beiden Modellen die physiologisch normale reife und unreife Hämatopoese charakterisiert. Hierbei zeigte sich kein signifikanter systematischer Einfluss von EPI-X4 auf reife Leukozyten (WBC), lediglich eine leichte Lymphozytose in der HR-Variante. Ein Trend zu erhöhter Lymphozytenzahl konnte auch in der CC-Ala-Variante ermittelt werden, jedoch ohne statistische Signifikanz zu erreichen. Entgegen diesem Trend fand sich bei beiden KO-Modellen eine verringerte Zahl an regulatorischen T-Zellen (Tregs) in der Peripherie, was ein Hinweis auf eine (mutmaßlich indirekte) immunregulatorische Wirkung von EPI-X4 sein könnte, wohingegen die relative Verteilung anderer T- und auch B-Zellen unauffällig war. Ein Einfluss von EPI-X4 ist hier anzunehmen, da in Vergleichsgruppen der wildtypischen (WT) Mäuse beider KO-Stämme durchgehend normale Treg-Zahlen zu finden waren; Einflüsse der potentiell unterschiedlichen genetischen Hintergründe der Stämme sind hier vermutlich auszuschließen. Im weiteren Verlauf der homöostatischen Analyse der Hämatopoese der Ala-EPI-X4-Mäuse zeigten sich keine signifikanten Unterschiede zu wildtypischen Mäusen. Sowohl reife als auch unreife Zellen zeigten, außer in der T- und B-Zelllinie, keine zahlenmäßigen oder funktionalen Auffälligkeiten, weder im Blut, noch in der Milz oder im Knochenmark. Analysen der Zellzyklusaktivität unterschiedlicher Unreifestufen wiesen ebenfalls keine Auffälligkeiten auf. Diese Daten einer normalen, von einer C57Bl/6-Maus zu erwartenden Ergebnisse dienen als Grundlage zur Bewertung und Analyse von durchgeführten hämatopoetischen Stressmodellen. Hierfür wurden zunächst hämatopoetische Stamm- und Vorläuferzellen (HSPC) mobilisiert: Der bereits erwähnte CXCR4-Antagonist AMD3100 wurde den Ala-EPI-X4-Mäusen sowie den WT-Kontrollen einmalig verabreicht. Serielle Blutentnahmen spiegelten den Anstieg bis zwei Stunden und den anschließenden Abfall von HSPC bis vier Stunden nach Administration wieder. Obwohl eine AMD3100-Gabe mutmaßlich ein Milieu für erfolgreiche EPI-X4-Abspaltung induziert, schien diese Art der Mobilisierung unabhängig von EPI-X4 zu sein. Die heutzutage klinisch relevante Methode zur Stammzellmobilisierung, eine fünftägige G-CSF-Gabe, wurde ebenfalls in EPI-X4-defizienten Mäusen durchgeführt. Obwohl der genaue Wirkmechanismus

von G-CSF bis heute nicht vollständig aufgeklärt ist, wurde gezeigt, dass das HSPC-Milieu im Knochenmark stark beeinträchtigt wird. Die Zerstörung von Gefäßen sowie potentiellen Nischenzellen wie Osteoblasten und Osteoclasten führt zu einer Verringerung der CXCL12-Konzentration. Ebenfalls werden relevante Konzentrationen von Proteasen freigesetzt, die vorhandenes CXCL12 spalten und damit unwirksam werden lassen. Da die CXCR4/CXCL12-Achse unverzichtbar für die Retention von HSPC im Knochenmark ist, kommt es bei einem Ungleichgewicht von Rezeptor zu Ligand sowie bei Rezeptordefekten unweigerlich zu Störungen in der unreifen Hämatopoese. Im Falle einer G-CSF-Gabe, also einer Unterbrechung des Signalweges, kommt es zum Egress von HSPC in die Peripherie. Zusätzlich wird die Proliferation letzterer durch eine Aktivierung des G-CSF-Rezeptors angeregt, weshalb nach fünftägiger G-CSF-Gabe eine große Anzahl HSPC im Blut und in der Milz zu finden sind. Charakteristischerweise halbiert sich etwa die Zahl der verbleibenden Stammzellen im Knochenmark durch kombinierte Effekte von Differenzierung und Mobilisierung. Alle diese beschriebenen Effekte auf HSPC können sowohl in wildtypischen als auch in EPI-X4-defizienten Mäusen beobachtet werden. Dabei unterscheiden sich die KO-Mäuse weitestgehend weder untereinander noch zu ihren WT-Kontrollen. Jedoch sind in CC-Ala-Mäusen um etwa 25% erhöhte Granulozytenzahlen im Knochenmark zu finden, was durch potentiell verlängerte Retention im Knochenmark, gesteigerte Überlebensdauer oder höhere Proliferationsraten bedingt sein könnte. Der unauffällige Phänotyp der HR-Ala-Mäuse spricht für einen subtilen Effekt von EPI-X4 im Mobilisierungsgeschehen, der von eventuell vorhandenen genetischen Differenzen überdeckt wird. Um potentielle Auswirkungen von EPI-X4 im Knochenmark weiter zu untersuchen, wurde ein weiteres Stressmodell gewählt, welches ebenfalls mutmaßlich die Bedingungen zur EPI-X4-Generierung schafft: Subletale Bestrahlung der Mäuse sorgt für Schäden an allen Zellarten im Knochenmark, es wird ein steriles entzündliches Milieu kreiert. Unter diesen Umständen wurde die Regeneration von Blutzellen analysiert. Es zeigten sich keine nennenswerten Unterschiede sowohl in der akuten Phase des Schadens als auch in regelmäßigen Blutentnahmen während der Regenerierung. Einzig verminderte IL-10-Level konnten in beiden EPI-X4-KO-Modellen gefunden werden. IL-10 als antiinflammatorisches Zytokin wird von T-Zellen des Organismus als Antwort auf Entzündungen freigesetzt. Verminderte IL-10 Levels weisen auf eine geringere Intensität der Entzündung hin. Unterschiede in der IL-10-Konzentration zeigten sich ebenfalls in anderen von uns gewählten Entzündungsmodellen, die nicht die unreife Hämatopoese involvieren. Da EPI-X4 ein Spaltprodukt von Serumalbumin ist und demzufolge im Organismus systemisch verfügbar, liegt die Vermutung nahe, dass auch andere CXCR4-abhängige Prozesse von EPI-X4 moduliert werden. Die Beschreibung von natürlich vorkommendem EPI-X4 in Vaginal- und

Rektalschleimhaut zeigt seine Entstehung an Schleimhautbarrieren auf. Ala-EPI-X4-Mäuse werden deshalb auf deren Durchlässigkeit untersucht: LPS-Konzentrationen als Marker für eindringende pathogene Bakterien wurden im Plasma untersucht. Hierbei zeigten sich keine Unterschiede zwischen den Gruppen, eine Störung scheint hier nicht vorzuliegen. Zusätzlich wurde die Zusammensetzung des Mikrobioms im Darm untersucht, da beschrieben wurde, dass sich Mikrobiom und die Integrität der Darmschleimhaut gegenseitig beeinflussen. Ein Einfluss von EPI-X4 auf die vorhandenen Mikroben ist daher denkbar. Zahlreiche Krankheiten wie Diabetes oder Übergewicht sind mit veränderter Zusammensetzung der Mikroben im Darm assoziiert und eine wechselseitige Kausalität wird diskutiert, weshalb das Mikrobiom heute große Aufmerksamkeit genießt. Im Falle der EPI-X4-defizienten Mäuse liegt zwar keine offensichtliche pathologische Veränderung vor, dennoch konnte in männlichen HR-Ala-Mäusen die Abwesenheit des Proteobakteriums *Parasutterella* nachgewiesen werden. Da diese Beobachtung jedoch ausschließlich auf die männlichen Mäuse begrenzt ist, die Anzahl der beta-Proteobakterien im Allgemeinen bei unter 1% liegt und bereits gezeigt wurde, dass *Parasutterella* auch bei Zusammenhaltung von Mäusen nicht zwangsläufig alle Mäuse besiedelt, sind diese Ergebnisse mit Vorbehalt zu interpretieren. Eine größere Anzahl Ala-EPI-X4-Mäuse muss hier in Zukunft analysiert werden, um valide, relevante Aussagen zu treffen. Um eine mögliche Defizienz der Barrierefunktion weiter zu testen, wurden zwei Stressmodelle gewählt: Zunächst wurde den Mäusen eine akute, sterile Peritonitis zugefügt, woraufhin die Anzahl und Zusammensetzung der ins Peritoneum einströmenden Leukozyten analysiert wird. Da CXCR4-exprimierende Leukozyten über eine erhöhte CXCL12-Konzentration zu Entzündungsorten geleitet werden, ist die Annahme eines Einflusses von EPI-X4 hierauf denkbar. In diesem gewählten Ansatz zeigten sich keine Auffälligkeiten, weder in der Influxkinetik noch in der Art der infiltrierenden Zellen. Ein Einfluss von EPI-X4 ist hier entweder nicht vorhanden, oder aber das Modell war zu hart und verdeckte subtilere Effekte von EPI-X4. Dessen Entstehung wird ebenfalls durch die entzündlichen Gegebenheiten favorisiert. Die potentiell vorhandenen Unterschiede in EPI-X4-defizienten Mäusen zu ihren wildtypischen Kontrollen könnten durch tiefere Analysen veranschaulicht werden. Ähnliche Ergebnisse zeigten sich auch im Colitis-Stressmodell. Hierbei wird sowohl WT als auch EPI-X4-defizienten Mäusen über sieben Tage Dextran-sulfat (DSS) über das Trinkwasser verabreicht, welches zu einer akuten Entzündung des Kolons führt. Die Schwere der Entzündung kann anhand von Entzündungsmarkern im Blut und der Beurteilung von histologischen Schnitten des Kolons erfolgen. Mithilfe standardisierter Scorings wurden proximale und distale Abschnitte des Kolons gemäß des Schweregrads der Entzündung beurteilt. Hierbei waren keine Unterschiede von EPI-X4-defizienten Mäusen zu ihren WT Kontrollen zu beobachten. Ebenso zeigten sich im

Peripherblut keine nennenswerten Unterschiede. Einzig die IL-10-Konzentration, wie bereits erwähnt, unterschied sich in der CC-KO-Maus von den anderen behandelten Tieren: Deutlich niedrigere IL-10-Konzentrationen deuten auf eine weniger ausgeprägte Entzündung hin, wobei pathologisch keine Unterschiede im Kolon auszumachen sind. Ebenso war die IL-10-Konzentration in HR-Ala-Mäusen gleich derer in WT-Mäusen, was zunächst widersprüchlich scheint. Ein subtileres Modell der Colitis scheint besser geeignet, um die wahrscheinlich geringen Effekte von EPI-X4 an dieser Stelle aufzudecken. Anstelle einer akuten, starken DSS-Behandlung, könnte eine niedriger dosierte, dafür wiederkehrende Behandlung über mehrere Wochen eine chronische Entzündung auslösen, welche den Effekt des Fehlens von EPI-X4 möglicherweise besser zu Tage treten lässt. Insgesamt sollte bei zukünftigen Experimenten darauf geachtet werden, dass EPI-X4 vermutlich nur sehr subtil die CXCR4-Signalachse moduliert, dementsprechend sollten die Versuche angepasst werden. Insgesamt lässt sich sagen, dass EPI-X4 ein hochkonservierter, natürlich vorkommender CXCR4-Antagonist ist, der eine vermutlich eher kleine Rolle für die unreife Hämatopoese spielt, jedoch an Schleimhautbarrieren einen relevanten Einfluss haben könnte: Zum einen als potentieller Inhibitor für den Eintritt von X4-tropen Hi-Viren, wie Zirafi *et al.* beschrieben, zum anderen als Modulator der Darmbarriere, wie in den hier verwendeten Modellen getestet. Ebenso scheint EPI-X4 sich auf T-Lymphozyten auszuwirken, insbesondere auf regulatorische T-Zellen, da deren Anzahl bei Fehlen des Peptids um etwa 30% reduziert ist.

1. Introduction

1.1. CXCR4/CXCL12 axis

C-X-C chemokine receptor type 4 (CXCR4), also known as fusin or CD184, is a seven-transmembrane G-protein coupled receptor (GPCR) [1, 2] which is expressed on the surface of immature and mature hematopoietic cells. It was first identified as one of the co-receptors for HIV-entry [3] and soon shown to be expressed on and being important for hematopoietic cells. Experiments in CXCR4 deficient mice show a heavily disturbed hematopoiesis [4, 5], while other organs are healthy and not dependent on the receptor after birth. Additionally, CXCR4 expression on hematopoietic stem and progenitor cells (HSPC) was shown to be critical for survival and for bone marrow (BM) retention of the latter [6, 7]. CXCR4 signals via activation of G α i-proteins when activated by one of its ligands which is typically C-X-C motif chemokine ligand 12 (CXCL12) [8, 9], but also nonclassical ligands have been described, as ubiquitin [10] or HMGB1 [11]. Binding of CXCL12 induces receptor phosphorylation followed by internalization and activation of several signal transduction pathways, e.g. phosphoinositide 3-kinase/protein kinase B which accounts for cell proliferation, angiogenesis, and survival [12]. Moreover, CXCR4 activation induces cell migration by chemotaxis. CXCL12 is expressed by human BM endothelium, regulated by hypoxia inducible factor-1 (HIF-1) and shown to directly cooperate with α 4 β 1 integrin and α L β 2 integrin in inducing the arrest of circulating progenitors especially on vascular endothelium [7]. Activation of integrins by CXCR4/CXCL12 interaction was thus proposed to account for cell adhesion. In the immature hematopoietic compartment, these cellular functions influence the retention of HSPC in the BM [13] as well as their capacity of self-renewal [14]. Deregulation of CXCR4/CXCL12 axis was shown to perturb renewal of HSPC, localization and quiescence as well as HSPC overall survival [15, 16]. Much of what is known about the function of CXCR4 in immature hematopoiesis has been deduced from experimentation with models of CXCR4 deficiency, disrupted CXCR4 signaling or pharmacological inhibitors of CXCR4 signaling. Thus the claim of CXCR4 mediating retention of HS(P)Cs in bone marrow largely hinges on the observation that the viral entry inhibitor of X4-tropic Hi-virus "AMD3100" induced accumulation of immature cells in blood [17]. By blocking CXCR4 or down-regulating CXCL12, HSPC are forced to exit the BM into the blood stream. The exaggeration of the physiological egress using substances enabling HSPCs to leave their niches is called mobilization. In clinical practice, standard regimen for mobilization of HSPC is a five-day treatment with granulocyte colony-stimulation factor (G-CSF) [18, 19]. AMD3100 which is a highly selective CXCR4 antagonist and interferes with binding of all known CXCR4 ligands, was developed as pharmacological mobilizing agent for use in combination with G-CSF in G-CSF-

refractory patients [20, 21]. The CXCR4 paradigm was later also assessed in the context of mobilization with G-CSF [22]. In spite of synergistic mobilization between G-CSF and AMD3100 it was concluded that G-CSF-mediated mobilization significantly targets in multi-faceted ways CXCR4-dependent retention: Proteases are cleaving and hence, de-activating CXCL12. At the same time, depletion of sources of CXCL12 (such as osteoblasts) happens, leading to a weakening of trans-endothelial CXCL12 gradients between BM and blood, attenuating the retentive force of CXCR4 and allowing HSPC egress [23, 24].

The role of CXCR4/CXCL12 axis was shown to be important for neutrophil development and their egress out of the BM [25]. The number of neutrophils in peripheral blood is tightly regulated through the balance of neutrophil production, release from the BM and clearance out of the circulation [26]. Again, a role of CXCR4 for a healthy neutrophil equilibrium was implied from observations made in CXCR4^{-/-} and CXCL12^{-/-} mice. Their fetal circulation was shown to have elevated neutrophil numbers, and in parallel they failed to establish BM myelopoiesis [27]. Moreover, in a syndrome where the intracellular domain of CXCR4 is truncated, namely the WHIM syndrome, causing exaggerated receptor signaling, low neutrophils counts are detected in the periphery due to abnormal retention thereof in the BM [28, 29]. Taken together, these data point to an important role of CXCR4/CXCL12 signaling axis for maintaining neutrophil homeostasis as a key retention signal.

With respect to B-cells in the context of which the main CXCR4 ligand was first described [30], CXCR4 expression has been shown to be critical for lymphocyte development [4, 27]. B-cell precursors are produced in the BM where CXCR4 accounts for retention of the latter until they (are ready to) migrate to the spleen [31]. Mice deficient in CXCL12 or CXCR4 lack B-cell lymphopoiesis [4]; precursor B cells are released into the blood stream prematurely. Thus, a reduction of the mature B cell compartments in the spleen is detected, resulting in low numbers of mature, functional B lymphocytes. Surprisingly, though, the CXCR4 gain-of-function mutant alluded to above similarly has got strongly reduced B-cell numbers ([32] and own, unpublished observation). The role for T-cell function is somewhat different: Migration of immature T cells to the thymus and their subsequent maturation in there is a CXCR4 dependent process [33]. Tight regulation of CXCR4 expression during maturation stages was shown to be important for correct differentiation [34]. In mice, high levels of CXCR4 expression remain detectable on mature CD4⁺ and CD8⁺ T cells, pointing at a continued role of CXCR4 in mature T cell function [35]. For these and all other immune cells, CXCL12 remains a potent, albeit not necessarily specific chemoattractant which is generated at almost all sites of injury and largely independent of the type of injury, as part of a DAMP (Damage-associated molecular patterns) response [36, 37].

Dependent on co-secreted factors, leukocytes are sequentially recruited to injured tissues. Deregulation of CXCR4/CXCL12 signaling is thus associated with numerous pathological conditions, including various types of cancers, chronic inflammatory diseases and immunodeficiencies.

1.2. EPI-X4



Figure 1: Model of EPI-X4 and its binding to CXCR4 receptor. EPI-X4 exhibits a lasso-like structure with Leu408 as critical amino acid. Its binding to CXCR4 was modeled by Zirafi et al., 2015.

Using a large functional peptide screen for natural inhibitors of HIV in hemodialysis fluid of patients in renal failure, a large consortium led by Jan Münch (Ulm, Germany) recently discovered a peptide subsequently called “EPI-X4”, endogenous peptide inhibitor of CXCR4 [38]. Functional assays showed that the peptide selectively inhibits infection of primary T-lymphocytes with CXCR4-tropic, but not CCR5-tropic HI-virus. Sequencing by Edman degradation revealed an amino acid sequence of the peptide of LVRYYTKKVPQVSTPTL, which maps to amino acid positions 408-423 of human albumin. In silico analyses predicted, and specific experiments later confirmed, that EPI-X4 is cleaved from mature albumin by proteases of the cathepsin family under acidic conditions. Serum albumin is commonly considered a non-specific carrier molecule for water insoluble compounds, both endogenous and pharmacological [39], as well as it is largely responsible for the oncotic pressure of plasma [40]. It was not previously imputed in any very specific functions, which, together with its high conservation score over various mammals, points at a highly specific and important role in an organism. EPI-X4 was synthesized and its properties carefully assessed in biochemical, cell culture and *in vivo* assays which conclusively show that EPI-X4 is a highly specific antagonist of CXCR4 by directly

interacting with the second extracellular loop of the receptor, a moiety which is also targeted by some pharmacological CXCR4 antagonists as well as the natural CXCR4 antagonist polyphemusin [41]. Structure prediction suggested an internal loop-like configuration of EPI-X4 in which the N-terminally leading amino acid, leucine, should bear a critical role. An alanine screen was performed to address this question experimentally and indeed, the only single amino acid replacement by alanine which leads to complete loss of antagonistic activity was the Leu-Ala-substitution at position 408. Loss of the first-position leucine was shown to inhibit the exhibition of its lasso-like structure which is indispensable for EPI-X4 binding to the CXCR4 receptor. By contrast, introduction of isoleucine instead of leucine generated a slightly more potent peptide, although whether the effect was due to higher receptor affinity or peptide stability was not clear and was not pursued. These variants, Ala-EPI-X4 and Ile-EPI-X4, will be of relevance later on. Detection of EPI-X4 by itself was already highly remarkable in that it established an entirely novel paradigm, i.e. generation of bioactive peptides by cleavage not from a typical precursor peptide but a functionally entirely remote large protein.

Now, the peptidome of hemodialysis fluid may not necessarily represent a physiological peptidome, both because it is derived from plasma of patients with kidney failure and because neutrophils are trapped in and activated on the dialysis membrane. Whether, therefore, EPI-X4 was “only” yet another CXCR4 inhibitor for potential pharmacological applications generated *ex vivo* on a non-physiological interface or a (patho)physiological endogenous receptor antagonist was not clear. Subsequently, however, EPI-X4 was found, among others, in vaginal lavage fluid, rectal mucosa and gastric content of neonates, providing evidence of its natural occurrence *in vivo*. To begin to address its physiological role, *in silico* homology studies were performed. Albumin itself is a fairly highly conserved protein, with a conservation score across a large panel of mammalian species in excess of 75% [42]. EPI-X4, however, and the amino acids N- and C-terminally thereof (the putative peptidase cleavage sites), has a remarkable conservation score of 98%. Closer analysis of the variants identifies as the only reproducible variant, present in 7 of the 20 analyzed species, substitution of Leu408 by Ile408 – as earlier mentioned, the hyperactive variant of EPI-X4. Only one species, the guinea pig, lacks a branched-chain amino acid in position 408, where it is replaced by alanine, generating an inactive variant of EPI-X4. Its evolutionary age, therefore, suggested conserved, and presumably meaningful, functions of the peptide.

defects. The constant interaction between intestinal epithelial cells and microbes is usually maintained by tight-junction proteins, thickness and composition of the mucus layer, presence of antimicrobial factors and, critically, (activity of) immune cells [50]. If the barrier gets disturbed, microbes can invade the host's intestine and provoke an immune reaction, leading to increased T-cell numbers, inflammatory processes and elevated cytokine productions. Thus, the immune system must maintain a fine balance between protection against entry of bacteria (causing potentially lethal sepsis) and over-reaction of the immune system in response to the bacteria and the PAMPs (Pathogen-associated molecular patterns) they generate (causing inflammatory bowel disease). Moreover, the intestine is a large interface for contact with environmental antigens which instruct specific immunological responses; acute inflammatory reactions to (largely) non-pathogenic abundant environmental antigens could lead to allergic reactions [51]. Therefore, generation of tolerance to environmental antigens (regulatory T-cell responses) is another important function of the mucosal immunological barrier. Seeking, therefore, to analyze a potential role of EPI-X4 as a "guardian" of mucosal tolerance, mice with an Ala-EPI-X4 variant were generated to explore this hypothesis in model of mucosal challenge.

1.3. Mouse models

Mouse models are a common method for either performing *in vivo* translational experiments that are not representative in cell culture models or as first/small organism models [52]. If a mouse is selected as model organism, it is important to choose the best-suited genetic background for the researcher's scientific question [53]. Therefore, various well-known and well-defined strains are commercially available serving a broad field of applications. In case a distinct gene is studied, a typical method is the generation of a knock-out mouse: the gene of interest is modified with a frameshift or stop mutation, by replacing with a neo cassette or a complete deletion. All of these methods should lead to a non-functional gene, a so-called knock-out (KO) variant. Also, distinct mutations in a gene of interest can be inserted, restrictions to different organs/expression patterns can be chosen or reporter genes inserted, making the mouse a powerful model. There are several ways to generate a genetically modified mouse. The most common method is homologous recombination with gene-targeting vectors in embryonic stem cells (ES cells). Homologous recombination was first described as a mechanism for DNA repair in mammalian cells, but also as the process by which eukaryotes make gamete cells [54]. As a genetic tool it has been discovered in the 1980s, leading to the potential of introducing targeted mutations into mouse ES cells [55]. Here, a vector is cloned *in vitro* that contains the part of the gene with the desired mutation, mostly together with an antibiotics resistance gene to facilitate clone selection. Introduction of this vector into ES cells leads to homologous recombination of the inserted

sequence with genomic DNA, introducing the new sequence to the cell's genome. Positive clones can subsequently be selected via antibiotic and genetic screening. Mutated ES cells can then be injected into blastocysts and transferred to pseudo-pregnant foster mice. At the end, for a stably mutated mouse strain germline transmission has to be ascertained.

A method that has recently come to large attention is the CRISPR/Cas system. Discovered as a defense mechanism of bacteria to excise palindromic virus DNA that has been inserted into the genome [56], it was developed to a powerful tool for effective gene modification in mammalian cells [57]. A schematic representation of the mechanism is shown in Figure 3. In brief, a guide RNA is inserted into ES cells to target the DNA sequence of interest together with the Cas9 protein. A length of 18-22 bp and specific recognition sequence (protospacer adjacent motif, PAM) for Cas9 nuclease activity are crucial for effective manipulation. Cas9 and the inserted RNA will then form a ribonucleoprotein complex guiding the nuclease to the particular site of interest where it will exhibit its nuclease activity. The DNA strands are cleaved and will be repaired by non-homologous end joining. At this point, a specific modification can be inserted by injection of a template DNA that will serve as a template and thus force homologous recombination. Thus, scar-free nucleotide exchanges, gene deletions or gene insertions are possible. The risk, or disadvantage, of this otherwise quick, inexpensive and technically simple technique is that off-target damage is highly likely to occur and to go unnoticed, whereas ectopic insertion of long homology sequences is unlikely and easy to detect.

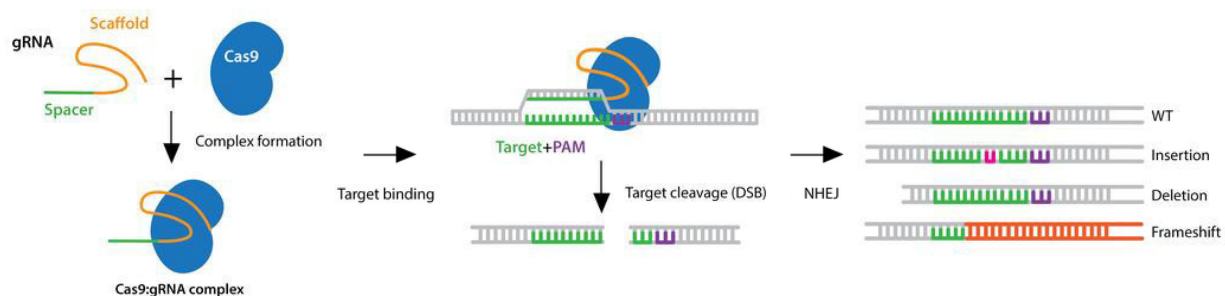


Figure 3: Schematic representation of CRISPR/Cas induced genome editing. After gRNA transfection together with Cas9 protein expression in cells, a Cas9:gRNA complex is formed. It binds its target and induces a double-strand break. Subsequent modifications of DNA can include insertions, deletions and frameshift mutations. Picture modified after <https://www.addgene.org/guides/crispr/>.

1.4. Aims of this work

We hypothesize that EPI-X4 has a non-redundant physiologic role. We further posit that, given that leukocytes, both mature and immature, are the only postnatally CXCR4-dependent cell species and that EPI-X4 was found at mucosal interfaces (stomach, rectal mucosa, vaginal lavage), EPI-X4 may play a role in mucosal tolerance.

We therefore queried the composition of the immature and mature hematopoietic system, the immature hematopoietic system under proliferative stress, the intestinal mucosal barrier under toxic stress, and reaction to an environmental antigen (the highly allergenic avian eggwhite protein ovalbumin, OVA), in two different strains of EPI-X4 competent (wild-type) and EPI-X4 mutated mice.

2. Material and methods

2.1. Material

Table of antibodies used for flow cytometry analysis of mature and immature hematopoietic cells.

Table 1: Antibodies used for flow cytometry stainings.

<i>Murine antigen (reactivity)</i>	<i>Clone</i>	<i>Fluorochrome</i>	<i>Manufacturer</i>
7-AAD			BioLegend
CD117 (c-kit)	2B8	APC-Cy.7	BioLegend
CD117 (c-kit)	ACK2	PE-Cy.7	BioLegend
CD11b	M1I70	PE	BioLegend
CD127	A7R34	BV605	BioLegend
CD150	TC15-12F12.2	APC	BioLegend
CD197	4B12	PerCP-Cy5.5	BioLegend
CD25	7D4	FITC	BioLegend
CD3	17A2	eFluor450	BioLegend
CD3	17A2	AlexaFluor700	BioLegend
CD3	17A2	FITC	BD Bioscience
CD3	145-2CM	APC	BioLegend
CD4	GK1.5	APC-Cy.7	BioLegend
CD44	IM7	AlexaFluor700	BioLegend
CD45	30-F11	PacificBlue	BioLegend
CD45	30-F11	eFluor450	invitrogen
CD45.1	A20	APC-Cy.7	BioLegend
CD45.2	104	FITC	eBioscience
CD45R (B220)	RA3-6B2	PE-Cy.7	BioLegend
CD48	HM48-1	PE-Cy.7	BioLegend
CD62L	MEL-14	PE	BD Bioscience
CD8	53-6.7	AlexaFluor594	BioLegend
FoxP3	MF-14	PE	BioLegend
Gr-1	RB6-8C5	APC-Cy.7	BioLegend

Gr-1	RB6-8C5	APC	BioLegend
Ki67	SolA15	eFluor450	invitrogen
Lineage cocktail		PacificBlue	BioLegend
Lineage cocktail		APC	BD Bioscience
Sca-1	D7	BV510	BioLegend
Sca-1	D7	PE	BioLegend
Ter-119	Ter-119	FITC	BioLegend

Media and reagents used for cell culture, flow cytometry staining and washing of cells:

Red Blood Cell Lysis Buffer, Sigma Aldrich, Darmstadt, Germany

Methyl cellulose MethoCult™ GF M3434, Stemcell Technologies, Vancouver, Canada

RPMI medium 1640, gibco, Carlsbad, USA

DMEM GlutaMAX –I medium, gibco, Carlsbad, USA

Fetal calf serum, PAA Laboratories, Pasching, Germany

Penicillin/Streptomycin, Thermo Fisher, Darmstadt, Germany

Dulbecco's Phosphate Buffered Saline, gibco, Carlsbad, USA

Bovine serum albumin, VWR International, Radnor, USA

0.9% NaCl, BBraun, Melsungen, Germany

Other reagents used:

Albumin from chicken egg white (OVA), Merck, Darmstadt, Germany

Agarose, VWR, Radnor, Pennsylvania, United States

TAE-Buffer: Tris-HCl, Merck, Darmstadt, Germany

Acetic acid, Roth, Karlsruhe, Germany

EDTA, Merck, Darmstadt, Germany

RPMI+++ is RPMI basic medium, 500ml supplemented with

+ FCS, 50 ml to a final concentration of 9%

+ PenStrep (10,000 U/ml Penicillin, 10,000 µg/ml Streptomycin), 5 ml to a final concentration of 1%

+ Glutamate, 5 ml

2.2. Methods

2.2.1. EPI-X4-targeting strategy

To generate inactive mutants of EPI-X4, the first amino acid which is crucial for CXCR4-binding was targeted. Two different approaches, homologous recombination and CRISPR/Cas9-mediated mutagenesis, were taken for carrying the mutations into the germline, but the same two bases were exchanged in exon 11 of the albumin gene: The naturally occurring leucine at position 408 on exon 11 in the mouse albumin gene was exchanged for alanine (EPI-X4-Ala) because, according to an earlier alanine screen of EPI-X4, this should generate a mouse with an albumin variant devoid of the predicted cleavage sites for EPI-X4 generation and further predicted to lack antagonistic function at the CXCR4 [38]. Two point mutations were inserted (CTA->GCA) in BAC DNA (RPC123.C, Thermo Fisher, Darmstadt, Germany). For the generation of HR EPI-X4-Ala mice, homologous recombination according to standard protocols was performed [58]. pGEM-T Easy vector (Promega, Madison, WI, USA) was used to clone the corresponding albumin fragment and site-directed mutagenesis (QuikChange II, agilent, Santa Clara, California, USA) was used to insert the nucleotide changes [59]. A neo-cassette was added to facilitate screening. After cloning of successfully mutated parts into a gene transfer vector pGK12 (a generous gift from T. Wunderlich, Köln, Germany), ES cells from CB20 mice were transfected [60]. Double-selection via G418 and ganciclovir [61] as well as southern blot were performed to screen for positive clones. Positive ES cells were injected into blastocysts and transferred into pseudo-pregnant foster mice for further development. Creation of CC EPI-X4-Ala mice was performed by ingenious targeting laboratory (Ronkonkoma, NY, USA) using CRISPR/Cas technology for inserting the point mutations [62]. A targeting vector was designed and electroporated into FLP C57Bl/6 ES cells. These cells were then screened by Sanger sequencing [63] and correctly mutated cells were injected into blastocysts followed by transfer into pseudo-pregnant foster mice. Pups with black coat color were screened for the desired mutation. Sanger sequencing was performed for both HR and CC EPI-X4 Ala mice to confirm successful mutagenesis.

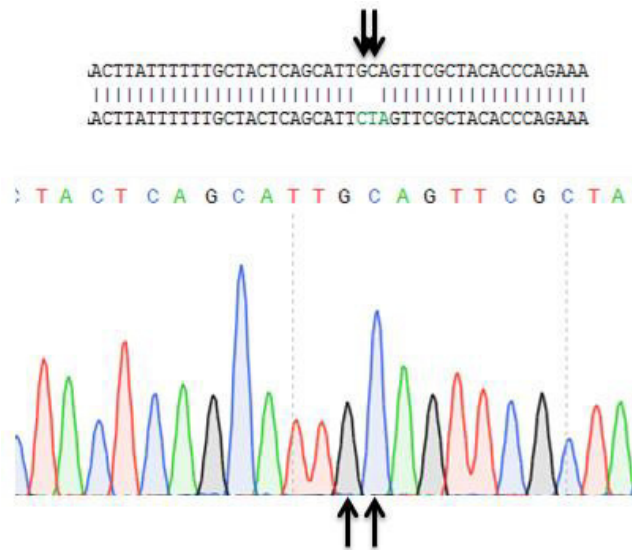


Figure 4: Sanger sequencing of Ala-mutants. The exchange of two bases (CTA → GCA) leading to the desired Ala-mutation was confirmed by Sanger sequencing (seqlab, Göttingen, Germany).

2.2.2. Mice

B6.126-Alb^{tmL408A1/Hbb} (“HR-Ala”-) mice were backcrossed for ten generations to a C57Bl/6J background [64] and then identified as genetically pure C57Bl/6J mice by Jackson Genome Scanning service (Bar Harbor, ME, USA). B6.126-Alb^{tmL408A2/Hbb} (“CC-Ala”-) mice were purchased from ingenious targeting laboratory (Ronkonkoma, NY, USA) already on a C57Bl/6J background. For transplantation experiments, B6.SJL-*Ptprc*^a*Pep3*^b/BoyJ (JAX stock #002014; CD45.1) “Ly5.1” mice were used as BM donors [65]. Mice were bred and housed in filter-top cages with food and water *ad libitum* under non-SPF conditions. Both male and female mice were used for experiments, unless otherwise stated. All animal experiments were performed in accordance with the agreement of national animal protection and approved by the municipal animal welfare authority (Regierungspräsidium Darmstadt, F27/1004).

2.2.3. Genotyping

Ear tag samples from three-week old mice were lysed in 100 µl DirectPCR Lysis Reagent (Viagen Biotech, Los Angeles, California, USA) with 200 µg/ml of Proteinase K (AppliChem, Darmstadt, Germany) *o/n* and heat inactivated at 85 °C for 45 min. 0.5 µl of crude DNA was used per genotyping reaction using RedExtract-N-Amp (Merck, Darmstadt, Germany) according to the manufacturer’s recommendations. A classical four-primer SSP PCR was designed to distinguish WT and Ala-mutant mice [66]. The innermost bases of the WT or Ala-mutant primers recognized either the two WT (CT) or the two mutant (GC) bases, respectively.



Figure 5: Schematic representation of the SSP-PCR used for mouse genotyping. Mice were genotyped using a classical four-primer strategy with one primer being specific for the WT allele (“WT-rev”), a second primer recognizing only the Ala variant (“Ala-fwd”).

The following primers were used for both HR and CC mutants: Alb-rev: 5'-CCCAGCCCTGTAACTTTGT- 3', Ala-fwd: 5'-CTTATTTTTTGCTACTCAGCATTGC-3', WT-rev: 5'-GCTTTCTGGGTGTAGCGAACTAG- 3' and Alb-fwd: 5'-TGCCATTGGGTTAGAGAAATG- 3' leading to fragments of 460 bp (Alb-fw to Alb-rev), 309 bp (WT) and 155 bp (mutant).

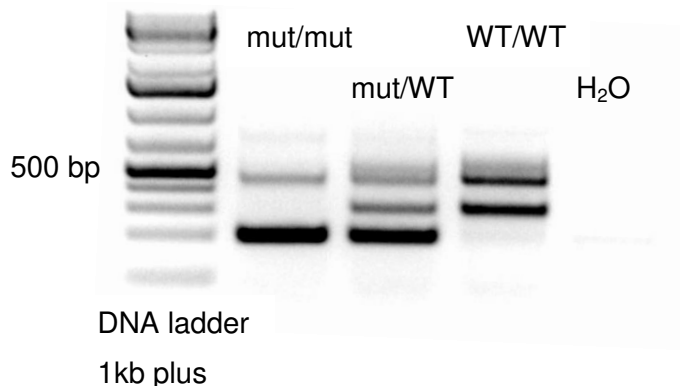


Figure 6: Genotyping of HR Ala and CC Ala mutant strains. Ear biopsies were prepared as described. Crude DNA was used for SSP-PCR. The resulting fragments were loaded on a 2% agarose gel together with a marker.

2.2.4. Mobilization of hematopoietic cells

To test responses to mobilizing agents, mice received either a single bolus injection of AMD3100 *i.p.* at the indicated doses in a volume of 100 μ l saline followed by subsequent peripheral blood drawings. Alternatively nine consecutive applications of rhG-CSF over five days (100 μ g/kg bodyweight q12h *i.p.*), as previously described [67, 68] were performed. One hour after the ninth dose of rhG-CSF, peripheral blood, spleen and bone marrow were collected and analyzed for mature and immature cell content using phenotypic and functional *in vitro* assays, as described below.

2.2.5. Recovery from hematopoietic stress

To achieve sub-lethal myelosuppression, mice were irradiated with a single dose of 4.5 Gy [69] using a caesium source with a dose rate of 0.75 Gy/min (Biobeam 2000, Gamma-Service Medical, Leipzig, Germany). Recovery of peripheral blood cell counts was serially monitored over six weeks. For examination of BM and spleen reconstitution, mice were sacrificed ten days after irradiation and analyzed for immature and mature hematopoietic cells. 5-Fluorouracil (5-FU; medac, Hamburg, Germany) was given as a bolus injection of 250 mg/kg BW *i.p.* as an alternative to irradiation [70]. Regeneration of hematopoietic cells was monitored accordingly.

2.2.6. Transplantation of hematopoietic cells

Host function of EPI-X4-Ala mice or WT controls was assessed by *i.v.* transplantation of WT BM cells into lethally irradiated hosts. Donor Ly5.1 mice were sacrificed by cervical dislocation and femurs and tibiae were harvested. BM cells were obtained as described in 2.2.9 and resuspended in 0.9 % NaCl at a concentration of 1 M/ml. Recipient mice were irradiated with a single myeloablative dose of 9.5 Gy [65] using a caesium source as described before. Within 4 hours of irradiation, mice received intravenous transplants of unmanipulated (not HSPC-enriched) BM cell suspensions of donor mice (200,000 cells/mouse) into the lateral tail vein. Engraftment kinetics were analyzed by drawing blood twice weekly starting 14 days after transplantation. Mice were sacrificed for final analysis 16 weeks after transplantation.

2.2.7. Preparation of blood and organs

Blood was drawn from wake mice by puncturing the *Vena maxillaris* with a 20 G cannula. It was collected in tubes containing potassium/EDTA (Microvette CB 300 K2E, Sarstedt, Nürnberg, Germany) and stored at room temperature until needed. Inner organs were harvested after painless death by cervical dislocation. The body was fixed and, after midline longitudinal extra-fascial incision, the skin was mobilized laterally to both sides from cranially of the jugulum all the way to the feet, then femora and tibiae were bluntly extracted. Connective tissue was carefully removed to minimize extramedullary cell contaminations. To isolate the spleen, the abdominal wall was opened. Bones and spleen were collected in PBS/0.5 % BSA or PBS only and stored on ice until further use unless mentioned otherwise.

2.2.8. Lysis of erythrocytes

Prior to leukocyte cytometry or seeding into colony assays, red blood cells were lysed using a hypotonic solution of ammoniumchloride [71]. Whole blood was washed with PBS/0.5 % BSA (400*g, 5 min, RT) and resuspended in 2 ml lysis buffer. The suspension was incubated at 37 °C for five minutes and then washed again with PBS/0.5 % BSA to remove lysed erythrocytes. Leukocyte cell pellets were resuspended in 200 µL RPMI+++ medium and plated into methylcellulose as described in 2.2.12.

2.2.9. Preparation of spleen or bone marrow cell suspensions

Splenocytes were isolated by gentle blunt extrusion from the capsule with 20 G cannulas into PBS/0.5 % BSA. Cell suspension was filtered through a 40 µm filter to remove aggregates and spun down at 400*g for 5 minutes at RT. Pellets were resuspended in 2 ml of PBS/0.5 % BSA. To isolate bone marrow, bones were flushed with PBS/0.5 % BSA using a 23 G cannula, filtered through a 40 µm filter and washed once for removal of remaining bone particles.

2.2.10. Blood analysis (CBC)

All whole blood samples as well as bone marrow and spleen cell suspensions were analyzed for a complete blood count (CBC) including RBC and indices, platelets and indices as well as WBC and 4-way differential with an automatic veterinary hemocytometer (Hemavet 950, Drew Scientific, Miami Lakes, Florida, USA). 50 µl of sample was used. Daily control (MULTI-TROL™) was run to check the cytometer's performance.

2.2.11. Plasma preparation

To generate cell-free plasma samples for cytokine analysis, peripheral blood was centrifuged for 15 min at 3500*g at 4 °C to separate cells from plasma. The cell-free plasma (supernatant) was pipetted off carefully avoiding red blood cells and buffy coat. It was snap frozen and stored in aliquots at ≤ -80 °C until needed. All further experiments were performed on samples thawed only once.

2.2.12. Methylcellulose assay (CFU-C assay)

To determine and quantify the number of functional progenitor cells in a test sample *in vitro* a defined amount expected to yield 20-100 CFU-C is plated into 2 ml of semi-solid methylcellulose medium supplemented with myeloid growth factors SCF, Il-3, Il-6 and EPO (MethoCult™ GF M3434, Stemcell Technologies, Vancouver, Canada) [72]. After one week incubation at 37 °C, 5 % CO₂ and humidified atmosphere distinct colonies are formed. They can be enumerated under an inverted light microscope with 2.5x magnification and differentiated based on color and morphology with respect to their myeloid lineage, i.e. BFU-E (burst-forming unit – erythroid), CFU-G (colony forming unit – granulocyte), CFU-M (colony forming unit – monocyte/macrophage), CFU-GM (colony forming unit – granulocyte/monocyte/macrophage) and CFU-GEMM (colony forming unit – granulocyte/erythrocyte/monocyte/macrophage/megakaryocyte).

Blood: The volume of blood plated varied, depending on the treatment of the mice: In order to count and classify the colonies, the number of colonies should be < 100 per plate, so the volume of blood was adjusted based on expected outcomes. Blood from untreated mice served as a control to estimate the plausibility of the observations. Blood was lysed and washed before plating in order to minimize contamination with erythrocytes. The pellet was suspended in 200 µl of RPMI+++.

Spleen/Bone marrow: 5x10⁴ BM WBC or 2x10⁵ splenocytes (according to CBC count) were suspended in 200 µl of RPMI+++.

The cell suspensions were then added to 2 ml of methylcellulose, vigorously mixed and 1.1 ml each were plated on two 35-mm tissue culture dishes.

2.2.13. BM-fluid collection

Bone marrow from one femur and one tibia was flushed with 500 μ l PBS followed by cell removal by centrifugation at 400*g for 5 min. The supernatant called 'BM fluid' was snap frozen and stored at \leq 80 °C for cytokine arrays. The residual cell pellet was divided into two tubes, to be used for further analysis of protein and RNA content. Total mRNA was isolated from the BM-cell-pellets using the RNeasy® Plus Mini Kit (Qiagen, Hilden, Germany) according to the manufacturer's recommendations. All experiments were performed using samples thawed only once.

2.2.14. Induction of Peritonitis

To induce a sterile inflammation of the peritoneum, mice received injections of 1 mL of autoclaved, aged 4 % Brewer's Thioglycolate Broth Medium (Merck, Darmstadt, Germany) into the peritoneal cavity. Alterations in cellular and inflammatory mediator composition in the blood and in the peritoneum were assessed after 8 h, 24 h and 48 h by drawing blood and flushing the peritoneal cavity with 3 ml of sterile 0.9 % NaCl [73].

2.2.15. DSS-induced Colitis

In order to induce an acute inflammation of the colon, healthy 14-16 week old mice were given 3 % Dextran Sulfate Sodium Salt (MP Biomedicals, Solon, Ohio, USA) in autoclaved drinking water [74]. After seven days mice were weighed, exsanguinated and sacrificed for organ collection. Blood, BM and spleen were prepared as described. Colon and rectum from appendix to anus was washed using a blunt 20 G needle flushing with PBS/0.5 % BSA, cut open longitudinally on one side, rolled and fixed using formaldehyde (Merck, Darmstadt, Germany) for further histological analysis [75].

2.2.16. OVA challenge (based on Kato *et al.*, 2001)

To challenge B- and T-cell activation and reaction to foreign antigens, we used a common model of ovalbumin (OVA)-sensitization. Mice received 100 μ l of a 0.5 mg/ml OVA Grade III (Thermo Fisher, Waltham, Massachusetts, USA) absorbed on 20 mg/ml Imject Alum Adjuvant (Thermo Fisher, Waltham, Massachusetts, USA) suspension weekly for sensitization over three weeks [76]. To challenge sensitized mice, mice received 50 mg OVA in PBS via oral gavage once or 40 μ g every other day for two weeks starting three weeks after sensitization. After the last dose, mice were sacrificed and generation of antigen-specific cytotoxic T-cells was analyzed using OVA-specific MHC class I (H-2 Kb) dextramers directed against SIINFEKL which corresponds to

OVA amino acids 257-264 (Cat. No. KL-JD2163-PE; immudex, Copenhagen, Denmark) conjugated to PE in whole blood samples and OVA-IgE-ELISA (BioLegend, San Diego, California, USA) in plasma [77].

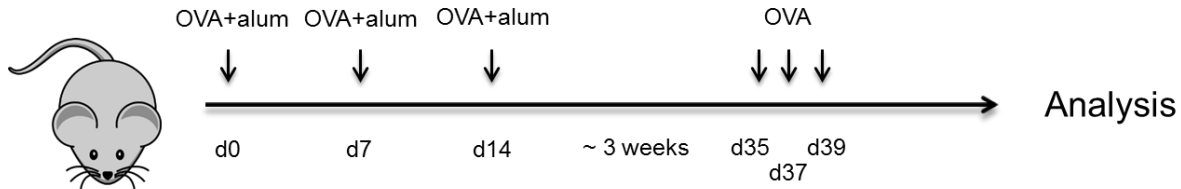


Figure 7: Schematic representation of OVA immunization and challenge regimen. Mice were immunized using three doses of OVA+alum every seven days followed by an oral challenge with OVA in saline after three weeks. Analysis was performed two to five days after the last dose.

2.3. Flow cytometry (FACS) based methods

2.3.1. Cell surface protein analyses

Quantification of bone marrow and spleen HSPC was performed according to standard protocols using titrated amounts of antibodies for each marker [78]. Hematopoietic cells in blood, BM and spleen were enumerated using multi-parametric flow cytometry for informative markers for mature (CD45, CD3, B220, Ter-119, CD11b, Gr-1) and immature (lineage, c-kit, sca-1, CD48 and CD150) subsets. Antibodies used are listed in Table 1. Acquisition was done with FACS LSR Fortessa II equipped with a four-laser standard filter set-up with 13 fluorescence channels in addition to FSC and SSC (Becton-Dickinson, Heidelberg, Germany). Data analysis was performed using FACS Diva 7 (BD) and FlowJo 10 (BD).

2.3.2. Intracellular staining

Cell cycle analysis as well as quantification of regulatory T cells was performed after fixation and permeabilization of hematopoietic cells. For information about cell cycle states, BM and spleen cells suspensions were stained with informative surface markers for immature subsets (lineage, c-kit, sca-1, CD48 and CD150), washed with PBS/0.5 % BSA to remove antibody excess, fixed and permeabilized using Foxp3/Transcription Factor Staining Buffer Set (Thermo Fisher, Carlsbad, CA, USA). Staining of Ki67 as a proliferation marker followed. Ten minutes before measurement, cells were incubated with 10 μ l 7-AAD to allow for relative DNA quantification in order to distinguish between G1 and G2/S/M phases, then filtered through a 40 μ m strainer to remove aggregates. For counting of regulatory T cells, splenic cells and peripheral blood were

stained using murine consensus Treg cell markers (CD45, CD3, CD4, CD25 and CD127) [79]. After fixation and permeabilization, cells were stained with Foxp3 antibody to identify regulatory T cells. Data acquisition and analysis was done as described before.

2.3.3. Cytokine measurements

Detection and quantification of inflammatory cytokines was performed using LEGENDplex Mouse Inflammation Panel 13-plex (BioLegend, San Diego, California, USA) according to the manufacturer's recommendations. Plasma samples were diluted 1:1, bone marrow fluids were used as undiluted samples. Data acquisition and analysis was done as described before.

2.4. Biomolecular methods

Standard molecular biology methods were performed according to the protocols of Sambrook *et al.*, 1989 [80].

2.4.1. Mass spectrometry for EPI-X4 detection

Plasma samples were analyzed regarding their EPI-X4 content after acidification by Armando A. Rodriguez (group of Sebastian Wiese, Ulm, Germany). A 5 μ L-aliquot of every mouse plasma sample or 20 μ M peptide in water were mixed with 1.5 mL 0.1% TFA and stirred for 5 seconds. A volume of 15 μ L (1 pmol peptide) from every diluted sample was separated for mass spectrometric analysis.

Samples were measured using an Orbitrap Elite Hybrid mass spectrometry system (Thermo Fisher Scientific, Bremen, Germany) online coupled to an U3000 RSLCnano (Thermo Fisher Scientific) employing an Acclaim PepMap analytical column (75 μ m \times 500 mm, 2 μ m, 100 Å, Thermo Fisher Scientific) at a flow rate of 250 nL/min. Using a C18 μ -precolumn (0.3 mm \times 5 mm, PepMap, Dionex LC Packings, Thermo Fisher Scientific), samples were pre-concentrated and washed with 0.1% TFA for five minutes at a flow rate of 30 μ L/min. The subsequent separation was carried out using a binary solvent gradient consisting of solvent A (0.1% FA) and solvent B (86% ACN, 0.1% FA). The column was initially equilibrated in 5% B. In a first elution step, the percentage of B was raised from 5 to 15% in 5 min, followed by an increase from 15 to 40% B in 30 min. The column was washed with 95% B for 4 min and re-equilibrated with 5% B for 19 min. The mass spectrometer was equipped with a nanoelectrospray ion source and distal-coated SilicaTips (FS360-20-10-D, New Objective, Woburn, MA, USA). The instrument was externally calibrated using standard compounds (LTQ Velos ESI Positive Ion Calibration Solution, Pierce, Thermo Scientific, Rockford, USA). The system was operated using the following parameters: spray voltage, 1.5 kV; capillary temperature, 250 °C; S-lens RF level, 68.9%. XCalibur 2.2 SP1.48 (Thermo Fisher Scientific) was used for data-dependent tandem

mass spectrometry (MS/MS) analyses. Full scans ranging from m/z 370 to 1700 were acquired in the Orbitrap at a resolution of 30,000 (at m/z 400) with automatic gain control (AGC) enabled and set to 10^6 ions and a maximum fill time of 500 ms. Up to 20 multiply-charged peptide ions were selected from each survey scan for collision induced fragmentation (CID) in the linear ion trap using AGC set to 10,000 ions and a maximum fill time of 100 ms. For MS/MS fragmentation, a normalized collision energy of 35% with an activation q of 0.25 and an activation time of 30 ms was used.

For visualization in XCalibur Qual Browser (Thermo Fisher Scientific, Bremen, Germany), eXtracted Ion Chromatograms (XICs) of the most intense isotope (± 20 ppm), as theoretically predicted, at $z=2$ were calculated. Using default parameters within the QualBrowser, peak areas were calculated and exported. For absolute peptide concentration calculation, peptide peak areas were compared to the injections with 1 pmol.

2.4.2. Determination of RNA/DNA-contents

RNA concentration was determined using NanoDrop200c (PepLab Biotechnologie GmbH, Erlangen, Germany). With the extinction rate E260/E280 and the spectrum, the purity of isolated nucleic acid was assessed. Isolated RNA was reverse transcribed into cDNA using the iScript cDNA Synthesis Kit (Bio-Rad, Munich, Germany) according to the manufacturer's recommendations. Unless mentioned otherwise, the amount of RNA was 1 μ g per reaction.

2.4.3. Measurement of CXCL12 concentrations

BM fluids and plasma samples were analyzed regarding their CXCL12 content using Mouse CXCL12/SDF-1 alpha Quantikine ELISA (R&D systems, Minneapolis, Minnesota, USA) according to the manufacturer's recommendations.

2.4.4. LPS measurements

LPS concentrations in plasma after sublethal whole-body irradiation were measured using Endosafe Nexgen-PTS (Charles River Laboratories, Wilmington, Massachusetts, USA) according to the manufacturer's instructions. LPS concentrations in plasma of homeostatic mice were measured by the UC Davis Mouse Biology Program (Davis, California, USA) using a LPS-detection kit (Biometec GmbH, Greifswald, Germany) according to the manufacturer's recommendations.

2.4.5. Histology of colon samples

Standard hematoxylin and eosin (H&E) stains were performed on colon samples from colitis experiments. Colons were therefore rolled and embedded in paraffin wax for 48 h at 4 °C. Samples were subsequently sliced every 200 µm in 4 µm sections using a microtome (Microm HM335E, GMI Inc, Ramsey, Minnesota, USA) and subsequently rehydrated. Staining using hematoxylin (Gill No 1, Sigma-Aldrich, Darmstadt, Germany) and 2% eosin solution Y (Sigma-Aldrich) were performed according to standard protocols [81]. For staining of goblet cells a standard alcian blue staining [82] was performed according to the manufacturer's recommendations (Merck, Darmstadt, Germany). Mounting of samples after dehydration was performed using Roti Histokitt II (Roth, Karlsruhe, Germany). The stained colon tissues were examined using an Axio Scope microscope under 20x magnification. Detailed pictures were taken using AxioCam MRc5 microscope camera (both Zeiss, Oberkochen, Germany) and subsequently assembled using Adobe Photoshop (Adobe, San Jose, California, USA). The same software was used for editing and evaluation of the images. Table 2 depicts the criteria for histopathology scoring, based on Dieleman *et al.*, 1998 [83]:

Table 2: Histopathology scoring system for DSS-induced colitis model. Histopathology Scoring Pattern (based on Dieleman *et al.*, 1998 [83]).

Feature	Severity Score & Description	Area Score Based on Percentage Affected
Inflammation	0 None	
	1 Slight	
	2 Moderate	
	3 Severe	Score 1: 1-25% area involved
Extent of Damage	0 None	Score 2: 26-50% area involved
	1 Mucosa	Score 3: 51-75% area involved
	2 Mucosa and submucosa	Score 4: 76-100% area involved
	3 Transmural	
Crypt Damage	0 None	
	1 Basal 1/3 Damaged	
	2 Basal 2/3 Damaged	
	3 Only surface epithelium intact	
	4 Entire crypt and epithelium lost	

2.4.6. Stool sample collection

To assess possible differences in mucosal barrier function that are reflected in the microbiome, stool samples were analyzed for bacterial composition [84]. Littermate mice of all genotypes were housed together until sample collection. Then, mice were separated and housed individually for 48 hours with low, dust-free bedding. Stool was collected into 1.5 ml tubes using forceps and frozen at -80 °C until further analysis. Microbiome analysis was performed by the UC Davis Mouse Biology Program (Davis, California, USA) according to their standard protocol: Total DNA was extracted using PowerFecal kit (Qiagen, Venlo, Netherlands). Sample libraries were prepared and analyzed by barcoded amplicon sequencing. High-throughput sequencing was performed with Illumina MiSeq paired end 250-bp run (San Diego, California, USA).

2.5. Statistics

Descriptive statistics and Student's t-tests were calculated using Excel (Microsoft, Redmond, Washington, USA) or GraphPad Prism 5 (GraphPad Software, Inc., La Jolla, California, USA); two-way ANOVA with Bonferroni posttest was calculated using GraphPad Prism 5. For non-normally distributed data non parametric Mann-Whitney-U-test was calculated using SPSS (IBM, Armonk, New York, USA). For microbiome analysis of stool samples, the data derived from sequencing was processed using QIIME2 for 16S based microbiota analyses (QIIME 2 Development Team (2017)). Demultiplexed paired end sequences that already had barcodes and adapters removed were analyzed using Qiime 2 version 2018.4. For quality filtering and feature (OTU) prediction, DADA2 [85] was used. Representative sequences were aligned using MAFFT [86]. A phylogenetic tree of the aligned sequences was made using FastTree 2 [87]. OTUs/features were taxonomically classified using a pre-trained Naive Bayes taxonomy classifier. The classifier was trained using the Silva 128 97% OTUs [88] for the 319F-806R region. Tables of taxonomic counts and percentage (relative frequency) were generated. Diversity analyses were run on the resulting OTU/feature .biom tables to provide both phylogenetic and non-phylogenetic metrics of alpha and beta diversity [89]. Additional data analysis (PLS-DA) and statistics were performed with R.

Unless stated otherwise, results are presented as mean \pm SEM, n.s. $p \geq 0.05$, * $p < 0.05$, ** $p < 0.01$, *** $p < 0.001$.

3. Results

3.1. Generation of EPI-X4 mutant mice

To generate EPI-X4 deficient mice, we targeted the first amino acid of the peptide in its molecule of origin, serum albumin. The first amino acid of EPI-X4 is leucine; as we previously showed in a HR Alanine screen, its replacement by alanine disrupts all activity at the CXCR4, essentially creating a null mutant [38]. We moreover predicted that replacement of leucine for alanine should disrupt the cleavage site for EPI-X4 from albumin altogether, but experimental evidence proved otherwise. Ala-EPI-X4 mutated mice are born at Mendelian ratios, are healthy and without any obvious physical impairments. Investigations of EPI-X4 contents in acidified plasma samples revealed the generation of Ala-EPI-X4 and complete lack of normal EPI-X4 in plasma from mutated mice. We thus have evidence that Ala-EPI-X4 is still cleaved, against our predictions, but demonstrate that the non-functional variant of EPI-X4 is generated. The Ala-EPI-X4 mouse is thus a suitable tool for unraveling the physiological role of EPI-X4. Surprisingly, in CC Ala mice the amount of cleaved EPI-X4 was up to five times higher than in HR Ala and up to 25 times higher than in WT mice.

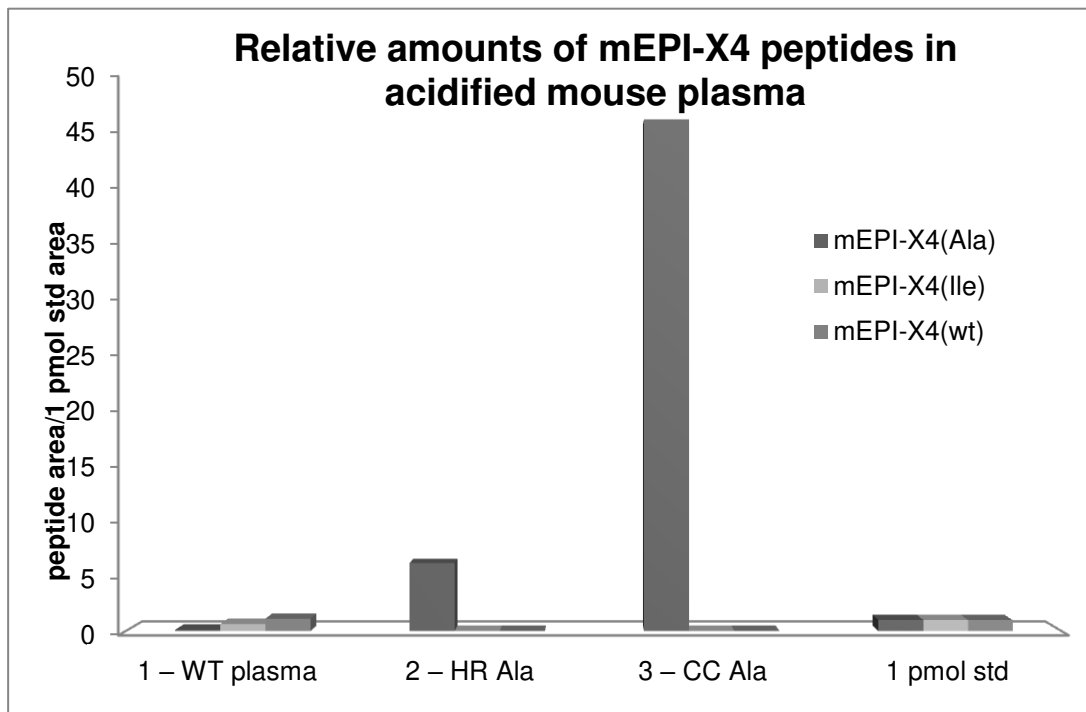


Figure 8: Relative amounts of mEPI-X4 peptides in acidified mouse plasma. Plasma from WT, HR Ala and CC Ala mice was acidified and EPI-X4 generation was measured via mass spectrometry. Generation of EPI-X4 in CC Ala plasma was significantly higher compared to HR Ala and WT mice.

3.2. Hematopoietic cells during homeostasis

Given the prominent role of CXCR4 as retention signal for immature hematopoietic cells, signal for egress and return of neutrophils to the BM, and inducer of B-cell maturation and trafficking, we first assessed the immature hematopoiesis of both Ala-variants and WT controls in young adult mice under homeostatic conditions. Hematopoietic progenitor cells were counted and analyzed in phenotypical (LSK-SLAM) (Figure 9) and functional (CFU-C) (Figure 10) investigations in all hematopoietic organs. Immature cell counts were found to be at similar levels in all compartments, trending to differ between the Ala-variants. The CC mutant trended to have larger cell numbers in spleen analysis. All values obtained represent normal and expected values of healthy C57Bl/6 mice.

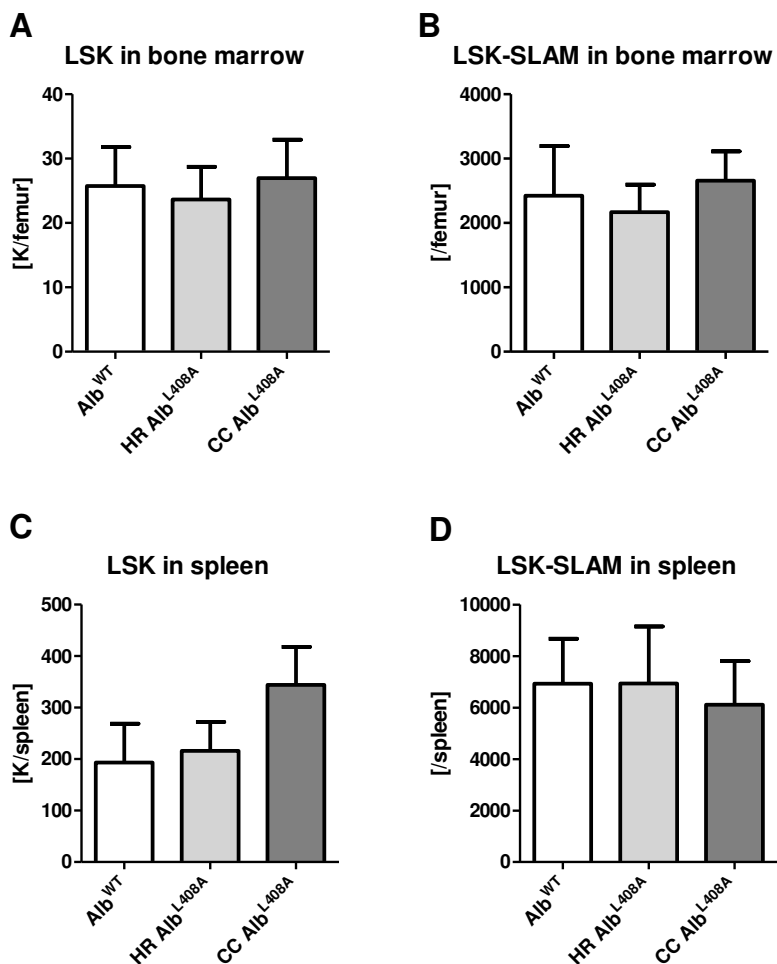


Figure 9: Phenotypical analysis of progenitor cells in BM and spleen under steady-state conditions. LSK progenitor cells were counted in BM (A) as well as more immature cells, termed LSK-SLAM (B), via flow cytometry. The same was performed for splenic LSK (C) and LSK-SLAM (D) cells. None of the investigated properties were found to differ between genotypes. $n \geq 10$.

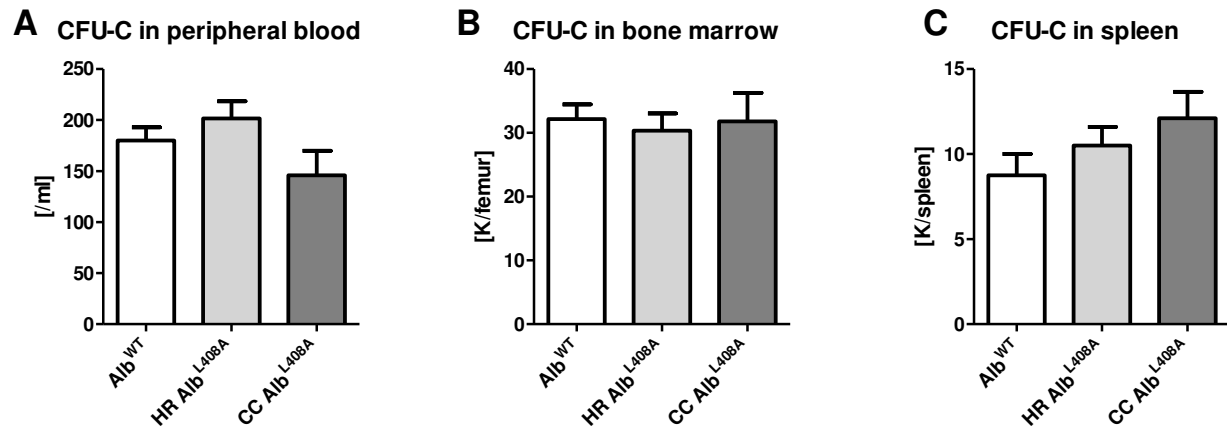


Figure 10: Functional analysis of hematopoietic progenitor cells under steady-state conditions. Immature hematopoietic cells were counted in peripheral blood (A), BM (B) and spleen (C) by CFU-C assays.

Across all hematopoietic organs, mature cells were found in very similar numbers and distributed equally through all lineages in every strain, except for the number of lymphocytes in peripheral blood: HR Ala-mice had higher B- and T-cells counts and thus showed an increased number of total white blood cells when compared to WT mice. By contrast, leukocytosis could not be detected in CC Ala mice. Contrary to the increased number of leukocytes in blood, we find granulocytes in BM of HR Ala mice to a lesser extent compared to WT mice. This was also not the case in CC Ala mice which showed the same distribution of mature cells as WT mice throughout all lineages. Splenic cell counts were indistinguishable among genotypes.

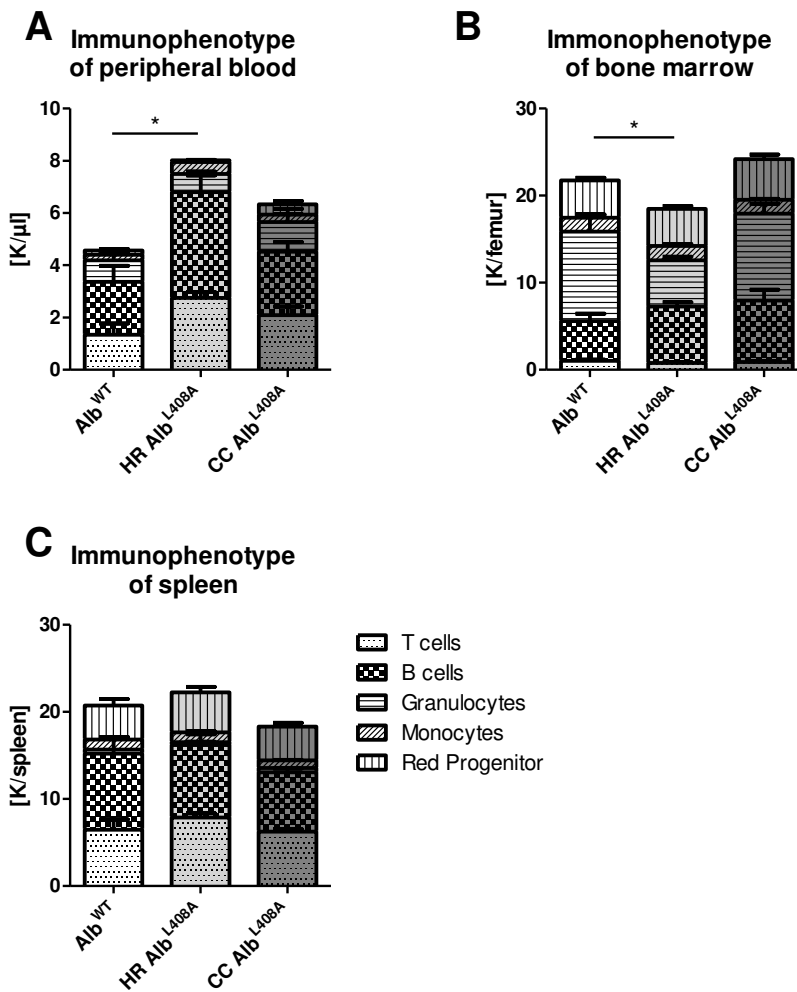


Figure 11: Phenotypical analysis of mature hematopoietic cells under steady-state conditions. Mature cells from peripheral blood (A), BM (B) and spleen (C) were analyzed using flow cytometry staining. HR Ala mice showed significantly higher lymphocyte counts in peripheral blood, whereas the total amount of cells in BM was diminished due to a reduced number of granulocytes. No differences could be detected in spleen. CC Ala mice were indistinguishable from their WT counterparts. $n \geq 10$ mice per group, * $p < 0.05$.

Higher proliferation rates of progenitor cells in the BM are associated with increased numbers of mature cells in peripheral blood. The most immature cells assessed here, so-called LSK cells, usually tend to have very low proliferation rates as they represent early HSPC. When dividing, these cells will give rise to more differentiated, but still immature progenitor cells. In contrast, cells low for lineage markers (linlow) cells represent more mature progenitor cells which will give rise to distinct mature hematopoietic cells. We thus assessed cell cycle states of immature LSK cells in all three genotypes as well as cycling activity of linlow cells (Figure 12). Analysis did not reveal any differences between the strains in any of the subsets examined in BM or spleen.

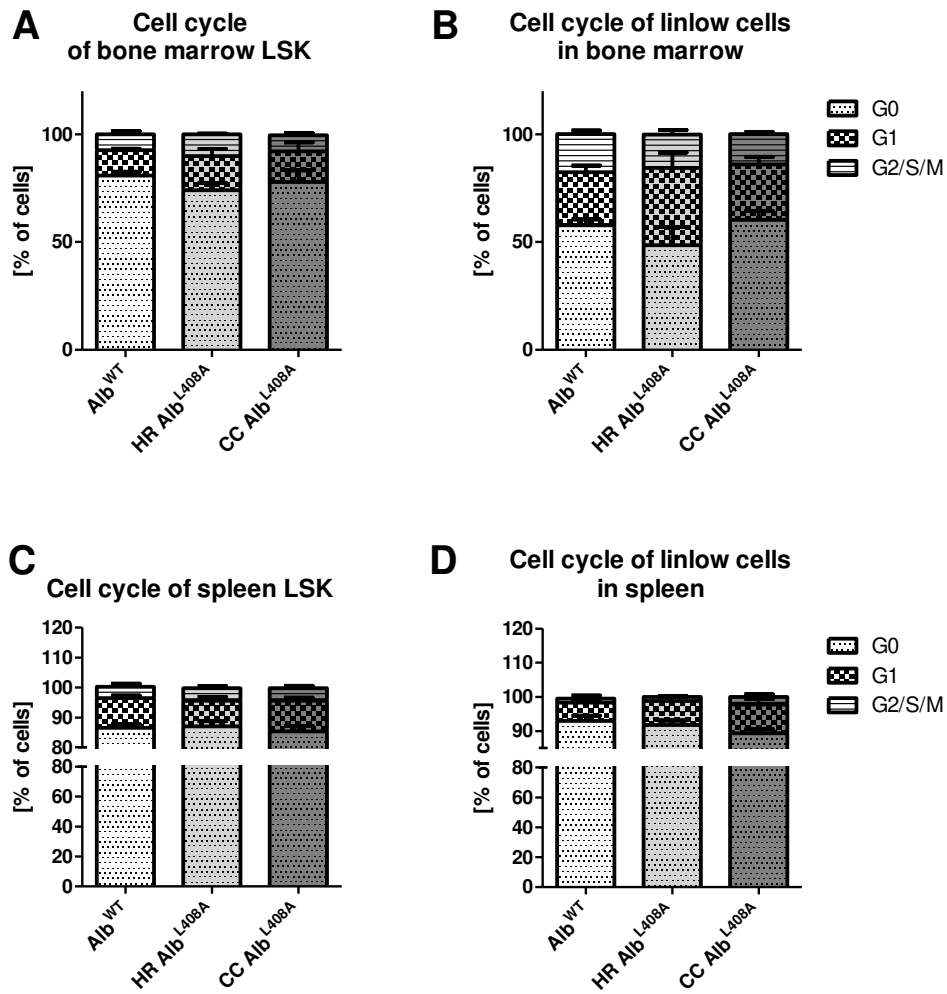


Figure 12: Cell cycle analysis of hematopoietic cells in BM and spleen under steady-state conditions. Immature LSK cells of BM (A) and more mature linlow cells (B) were analyzed regarding their cell cycle state in flow cytometric analysis. We distinguished between G0, G1 and G2/S/M phases using Ki67 and 7-AAD. The same was performed for splenic LSK (C) and linlow (D) cells. $n \geq 10$ mice per group.

3.3. EPI-X4 alters T-cell distribution

Immature T cells are derived from HSPC in the BM of mice from where they are released into the periphery. T cell maturation subsequently occurs in the thymus yielding CD4+ and CD8+, all CD3+ T cells with their corresponding subgroups. A crucial role of CXCR4 in T cell development is demonstrated as CXCR4 is expressed on pre-mature T cells, guiding them to the thymus, and remains expressed during maturation [34, 90]. But CXCR4 is not only important for T cell maturation; it also enhances responses of peripheral T cells to T cell receptor (TCR) signals [91].

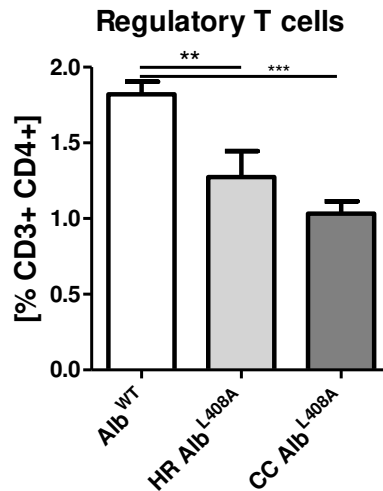


Figure 13: Regulatory T cell counts in peripheral blood under steady-state conditions. Whole peripheral blood was RBC lysed and T cells were analyzed via flow cytometry. Regulatory T cells were found to be diminished in both HR and CC Ala mutants. $n \geq 5$ mice per group, ** $p < 0.01$, *** $p < 0.001$.

Conceivably, EPI-X4 could interfere with these processes leading to an altered distribution of T cells due to potential effects on their maturation. We examined T cell subpopulations in peripheral blood of EPI-X4-Ala and WT mice. All genotypes showed comparable distributions of mature T cells in the investigated subsets except for regulatory T cells. We found them to be diminished by 30 % in both HR and CC Ala mice compared to their WT littermates.

3.4. HSPC mobilization is independent of EPI-X4

Mobilization of HSPC out of the BM into the periphery can be achieved by disruption of the CXCR4/CXCL12-axis. AMD3100, a bicyclam small molecule used for boosting poor mobilizers in the clinic, targets CXCR4 directly, competing with potential EPI-X4 binding sites [92]. It induces rapid yet only modestly efficient mobilization of HSPC [93]. Mice of all genotypes received a single bolus injection of AMD3100 i.p., leading to peak mobilization of HSPC after two

hours. Blood was drawn at the indicated time points and analyzed with regards to white blood cell (WBC) and HSPC count. Already one hour after administration, 1.5-fold elevated levels of WBC can be detected in peripheral blood, reaching its maximum, approximately two-fold, after two hours. Baseline levels are reached again within four hours. Identical kinetics, albeit much larger –fold increase, are detected for HSPC: All mice reached maximum CFU-C numbers two hours after injection of AMD3100 with an increase to 1200 CFU-C/ml compared to 150 CFU-C/ml under homeostatic conditions. The increase in immature cells is more pronounced than that of mature cells, but a significant drop in HSPC is detected at four hours after injection reaching almost baseline values. This shows that mobilization is short-lived and HSPC are cleared rapidly out of the blood stream. Overall, the same pattern, including cell numbers, was observed in the two EPI-X4 mutants for mature and immature cells.

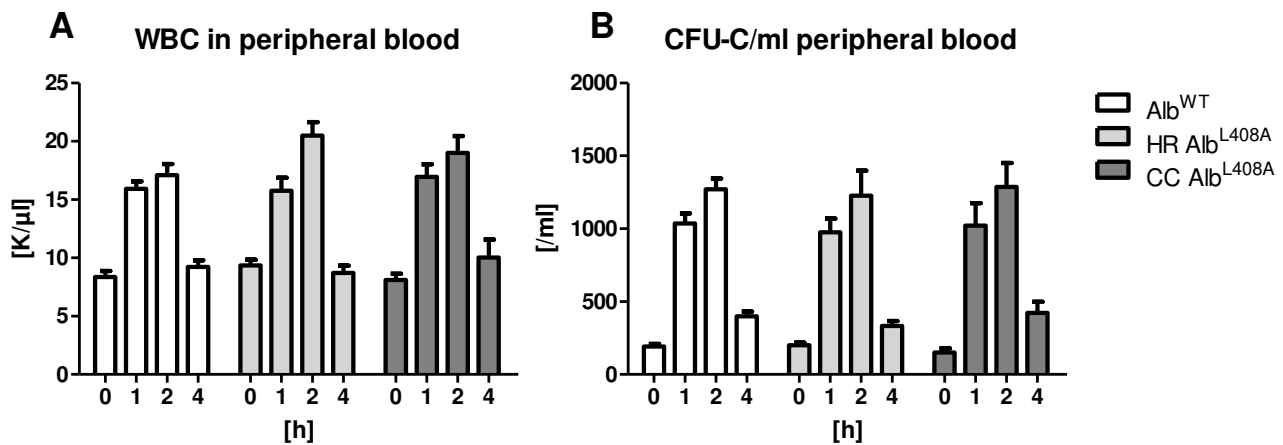


Figure 14: Mobilization outcome after AMD3100 administration. Mice received a bolus injection of AMD3100 in saline, leading to rapid mobilization kinetics. White blood cells were counted at the indicated time-points (A). A CFU-C assay was performed additionally in all genotypes (B). No differences in mobilization outcome could be detected between the mice. $n \geq 10$ mice per group.

Next, we assessed the mobilization potential by administering the standard regimen of nine doses q12h of rhG-CSF to our mice. Such a five-day regimen is the current clinical standard for mobilization in healthy HSPC donors [94, 95]. The exact mechanism of action of G-CSF during BM mobilization is not fully understood yet, but evidence was presented that at first HSPC are forced to proliferate [96]. Later on, a proteolytic, possibly also hypoxic and hence, acidic milieu,

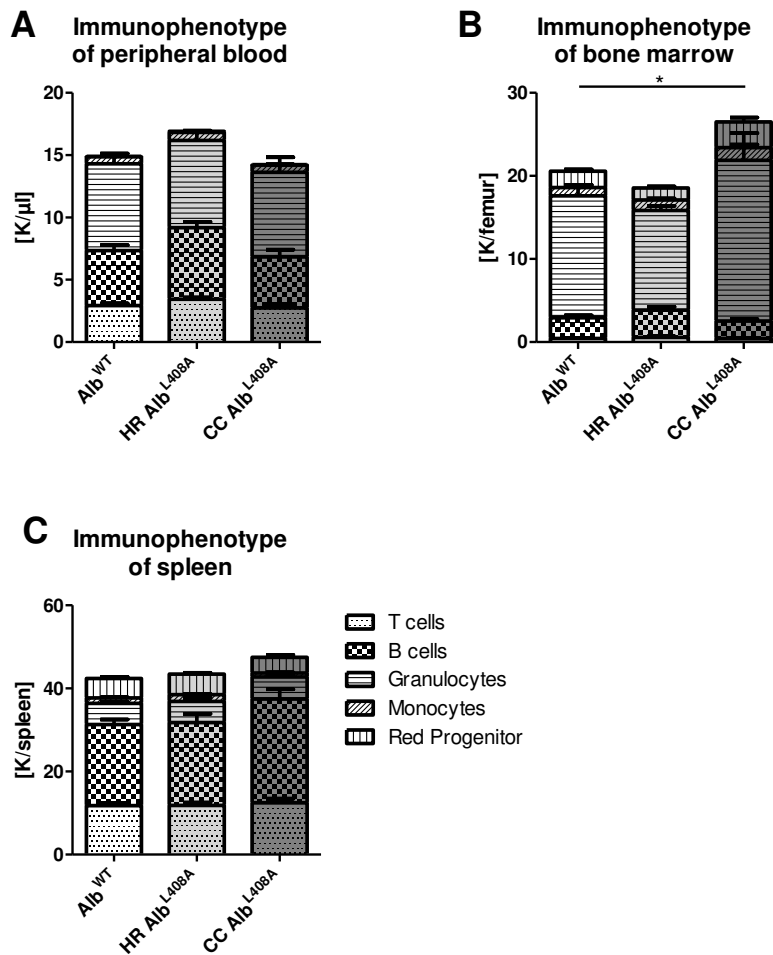


Figure 15: Mature hematopoietic cell count after G-CSF induced mobilization. Mature cells from peripheral blood (A), BM (B) and spleen (C) were analyzed via flow cytometry. An increase in granulocytes was detected in BM of CC Ala mice which remains the only remarkable difference. $n \geq 10$ mice per group, * $p < 0.05$.

probably established by G-CSF-activated neutrophils, cleaves retention factors, allowing for HSPC egress. The established conditions could thus provide the appropriate conditions for neutrophil elastases or cathepsins to cleave EPI-X4. To assess a possible contribution of EPI-X4 to G-CSF-induced mobilization, mice were treated with G-CSF and sacrificed one hour after the last dose. Analyses of mature and immature hematopoietic cells as well as cell cycle analysis of HSPC were performed. Mature cells were counted in every hematopoietic organ, showing an

accumulation of granulocytes in BM of CC Ala mice. The smallest number of respective cells was found in HR Ala mice. Mature cell counts in peripheral blood and spleen were found to be equal as expected.

Functional examination of immature cells in peripheral blood showed a rise up to 4000 CFU-C/ml as expected from WT C57Bl/6 mice in all genotypes (Figure 16). For BM LSK a depletion of about half of BM HSPC after G-CSF administration is described in the literature [97]; we could confirm this observation in WT and HR Ala mice, but found 50% higher CFU-C counts in BM of CC Ala mice. These observations were confirmed by phenotypical examination (Figure 17). Expected CFU-C numbers were also detected in spleen analysis of WT mice. In CC Ala mice colony counts were significantly elevated, which could not be confirmed by phenotypical analysis, but a trend towards higher levels was seen as well.

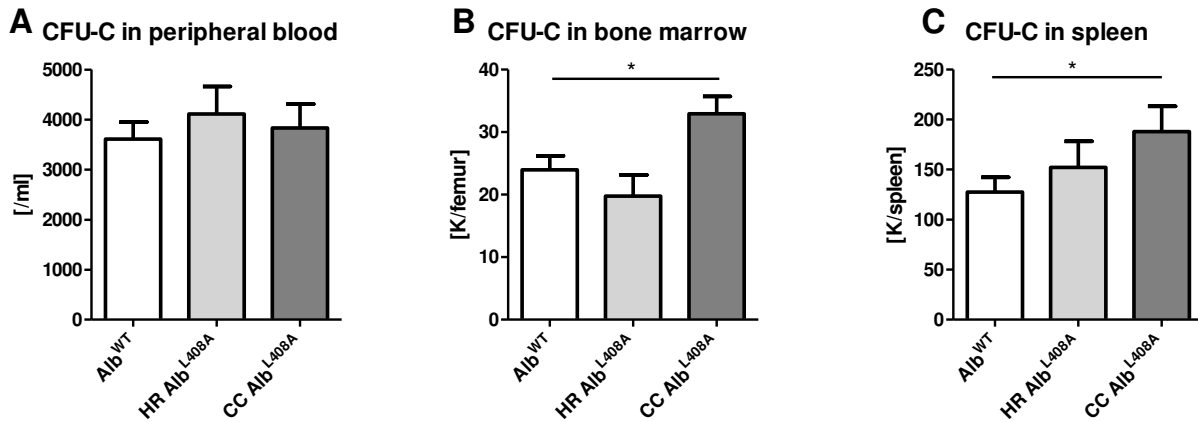


Figure 16: Functional analysis of hematopoietic progenitor cells after G-CSF-induced mobilization. Immature hematopoietic cells were counted in peripheral blood (A), BM (B) and spleen (C) by CFU-C assays. CC Ala mice had significantly higher HSPC counts in BM and spleen, while in peripheral blood, no differences in neither strain were detectable. $n \geq 10$ mice per group, * $p < 0.05$.

Higher proliferation rates of progenitor cells could account for elevated levels of HSPC after G-CSF regimen. However, cell cycle analysis performed on LSK and linlow cells in BM and spleen could not detect any differences between the strains after mobilization. The accumulation of granulocytes accompanied by HSPC in BM of CC Ala mice is the only detectable difference that has appeared.

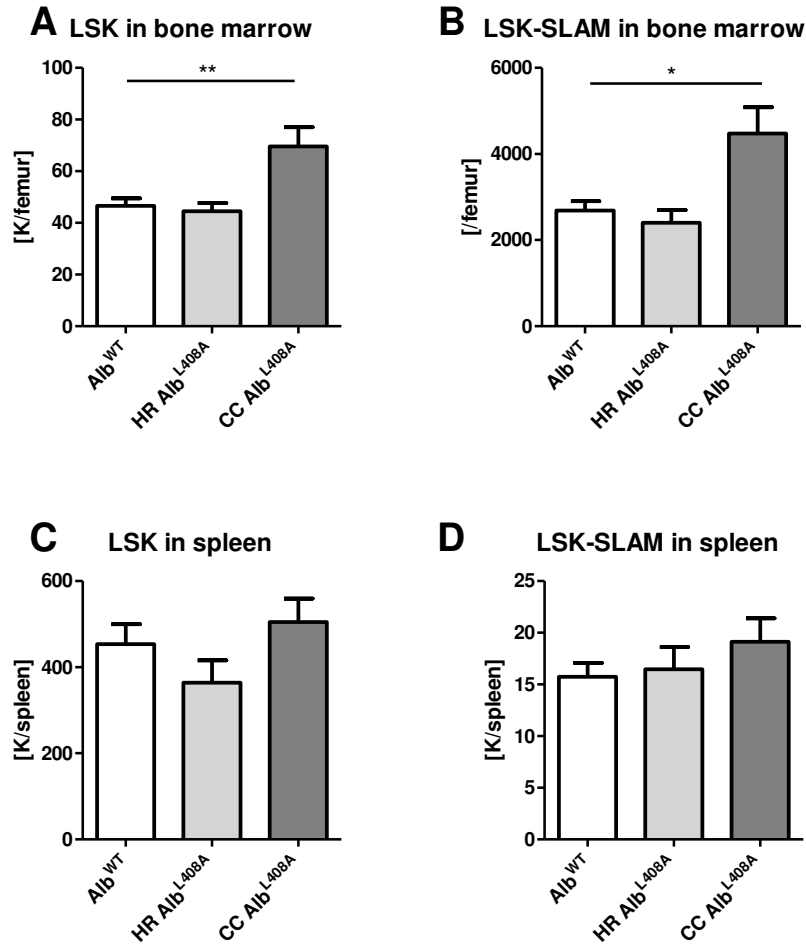


Figure 17: Phenotypical analysis of immature hematopoietic cells after G-CSF-induced mobilization. LSK (A) and LSK-SLAM (B) cells were counted via flow cytometry in BM of G-CSF-treated mice. The total number of progenitor cells was found to be significantly higher in CC Ala mice than in WT littermates. HSPC counts in HR Ala mice were not altered. In spleen, LSK (C) as well as LSK-SLAM (D) numbers were not found to differ between genotypes. $n \geq 10$ mice per group, * $p < 0.05$, ** $p < 0.01$.

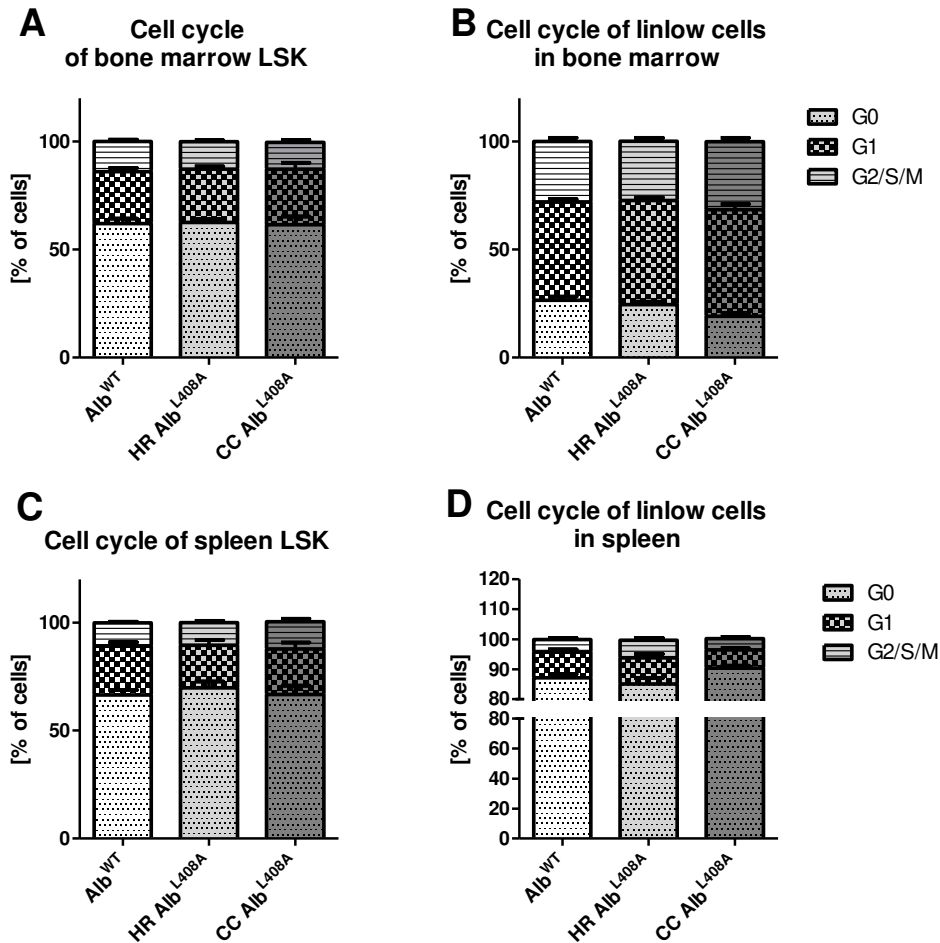


Figure 18: Cell cycle analysis after G-CSF-induced mobilization. Immature LSK cells of BM (A) and more mature linlow cells (B) were analyzed regarding their cell cycle state in flow cytometric analysis. We distinguished between G0, G1 and G2/S/M phases using Ki67 and 7-AAD. The same was performed for splenic LSK (C) and linlow (D) cells. Cell cycle activity in all types of cells of both organs rose after G-CSF administration, but did not differ between genotypes. $n \geq 10$ mice per group.

3.5. Engraftment of HSPC is normal after transplantation

Before receiving HSPC transplantation a patient is treated with chemotherapy or radiotherapy to clear the BM of malignant cells, suppress immune responses, and provide a cytokine milieu conducive to establishment of donor hematopoiesis [98]. A dose of 9.5 Gy total body irradiation, which is used in the corresponding mouse model, leads to a comparable elimination of progenitor cells from the BM and immunosuppression in our mice. At the same time, an inflammatory environment is generated which could, according to our hypothesis, lead to the

generation of EPI-X4 in WT mice. Homing, the initial interaction of HSPC with BM environment, was not altered in Ala mice. Experiments performed by us and other groups [99, 100], where 10 M whole BM cells are transplanted into lethally irradiated mice and the recovery in hematopoietic organs is monitored 20 hours later, did not show any dependency on CXCR4. Thus, we did not necessarily expect an effect of EPI-X4 on homing capacity of Ala mice, and indeed this is what was observed (data not shown); availability of these data is nevertheless critical because it provides the baseline for comparison of engraftment data, since differential engraftment in the context of impaired homing would imply different mechanisms than in mice with normal homing. However, due to the disturbed niche environment and potential inflammation signals during HSPC recovery after transplantation, we were interested in a possible role of EPI-X4 for HSPC engraftment. Mice of either genotype were lethally irradiated and reconstituted with healthy WT whole BM cells. Engraftment analysis was started two weeks after transplantation and continued for six weeks, monitoring leukocyte and red blood cell numbers in peripheral blood. No differences were detected in neither Ala-strain compared to WT mice with respect to WBC or RBC engraftment.

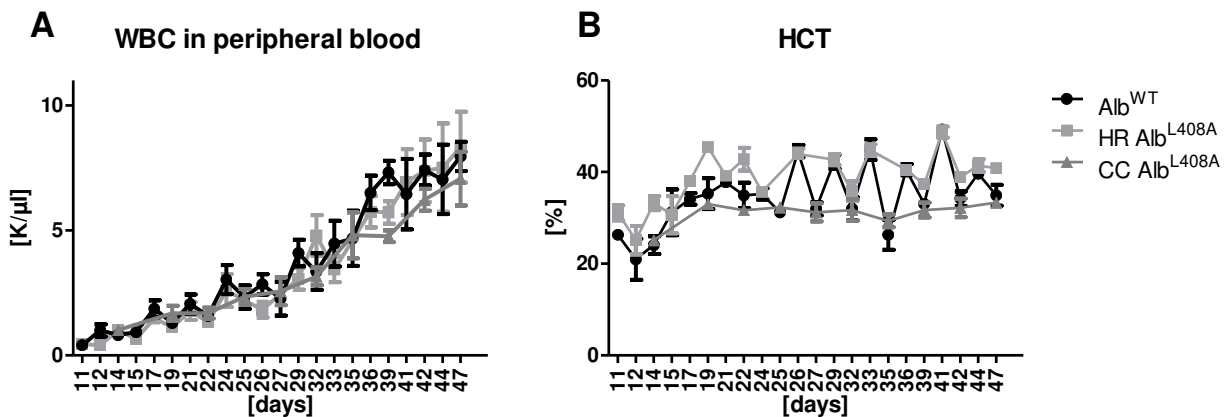


Figure 19: Engraftment analysis after transplantation regimen. Lethally irradiated mice were reconstituted with 200.000 total BM-cells of WT donors. Engraftment of WBC (A) and hematocrit (HCT) (B) was monitored over six weeks. All mice engrafted equally to normal homeostatic cell counts. n ≥ 4 mice per group.

Sixteen weeks after transplantation, when hematopoiesis is considered fully established, end-point analysis was performed as described before. Mature cell counts were found to be equal in peripheral blood and in BM of all strains of mice. Splenic cells were diminished in CC Ala mice by half in all subgroups compared to WT littermates.

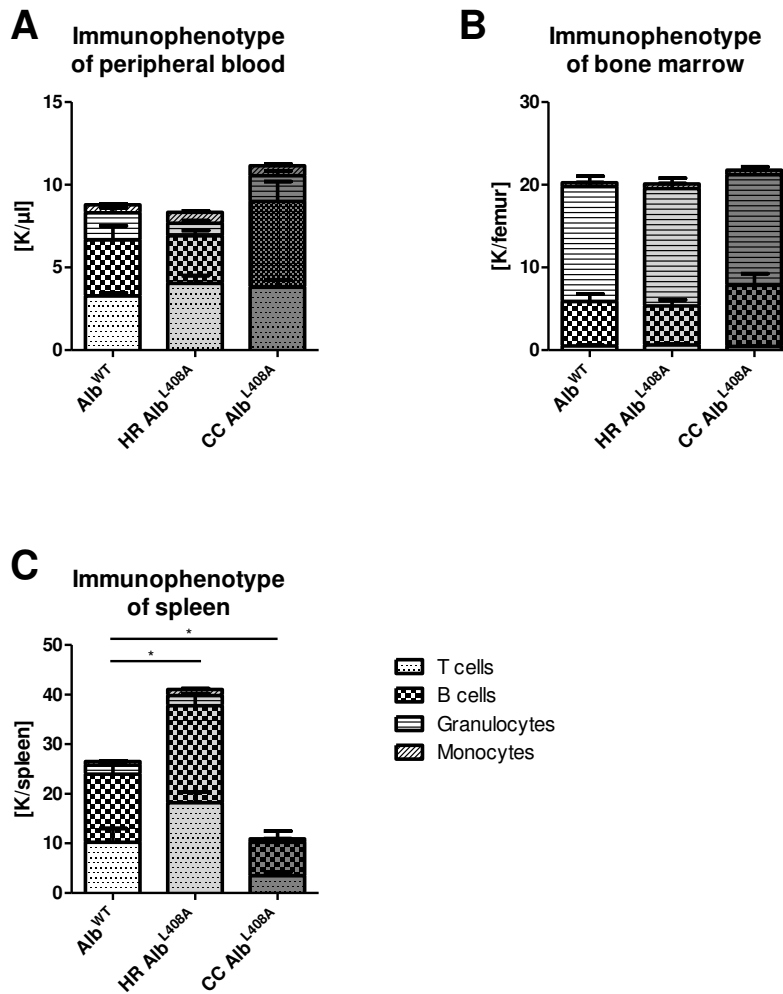


Figure 20: Mature hematopoietic cell count after transplantation. Mature cells from peripheral blood (A), BM (B) and spleen (C) were analyzed via flow cytometry after donor hematopoiesis was considered fully established. Cell counts and distributions were not altered in peripheral blood and BM between genotypes, but differed significantly in spleen. Total cell numbers were elevated in HR Ala mice, while they were strongly diminished in CC Ala mutants compared to WT mice. Cell distributions were not changed. $n \geq 4$ mice per group, * $p < 0.05$.

The same trend is seen in the examination of immature cells in phenotypical assays in spleen. On the other hand, immature cell counts of CC Ala mice were not found to be lowered by functional analysis in any hematopoietic organ. Analysis did not reveal any differences between HR Ala mice and WT ones; neither did the final cell cycle analysis performed. However, splenic cells of CC Ala mice showed less proliferation than WT ones. Interestingly, the previously found leukocytosis in HR Ala mice was absent after transplantation. Overall, the engraftment capacity of EPI-X4-Ala mice can be considered normal.

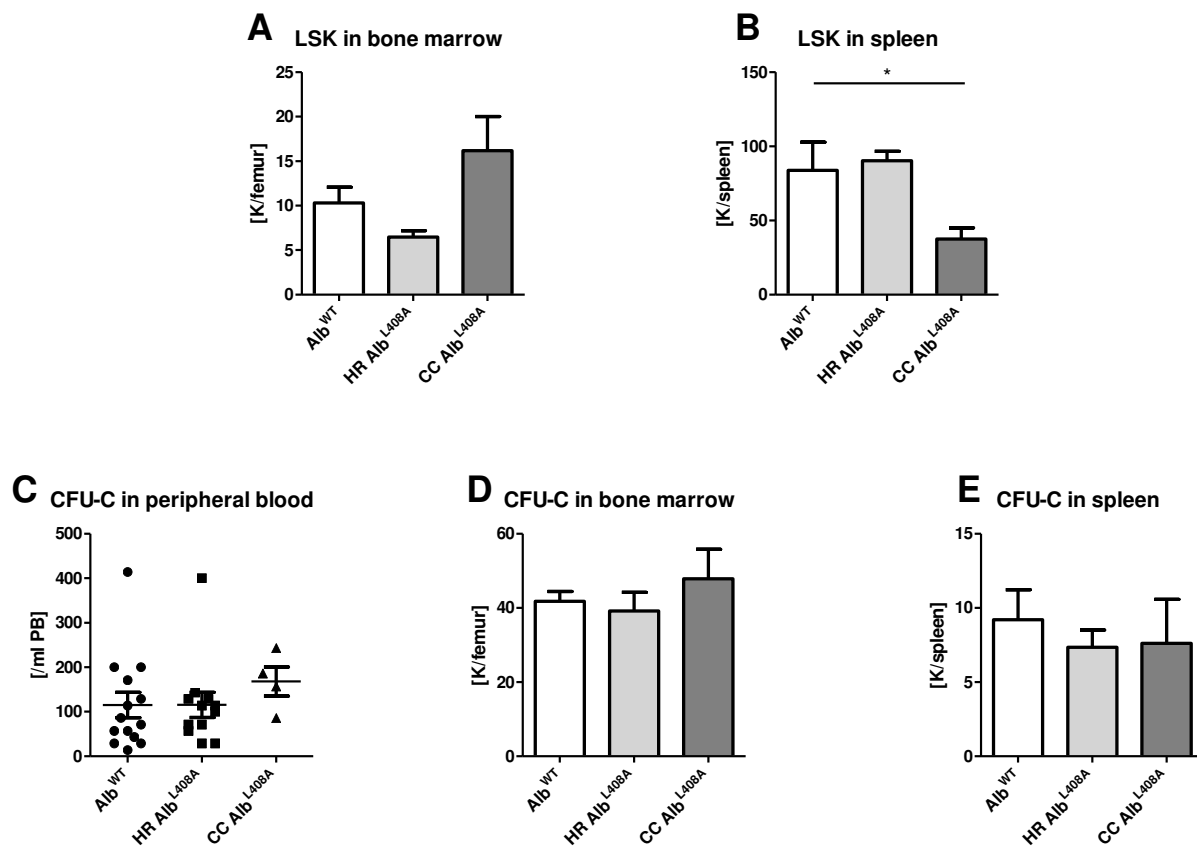


Figure 21: Phenotypical and functional analysis of HSPC after transplantation. Immature hematopoietic cells were analyzed in BM (A) and spleen (C) of transplanted mice via flow cytometry when donor hematopoiesis was considered fully established. LSK cells were significantly diminished in spleen of CC Ala mutants, while they trended towards higher numbers in BM compared to WT mice. Functional analysis of progenitor cells in peripheral blood (C), BM (D) and spleen (E) does not confirm this observation. In CFU-C assays, all mice had similar HSPC numbers in all organs independently from their genotype. $n \geq 4$ mice per group, * $p < 0.05$.

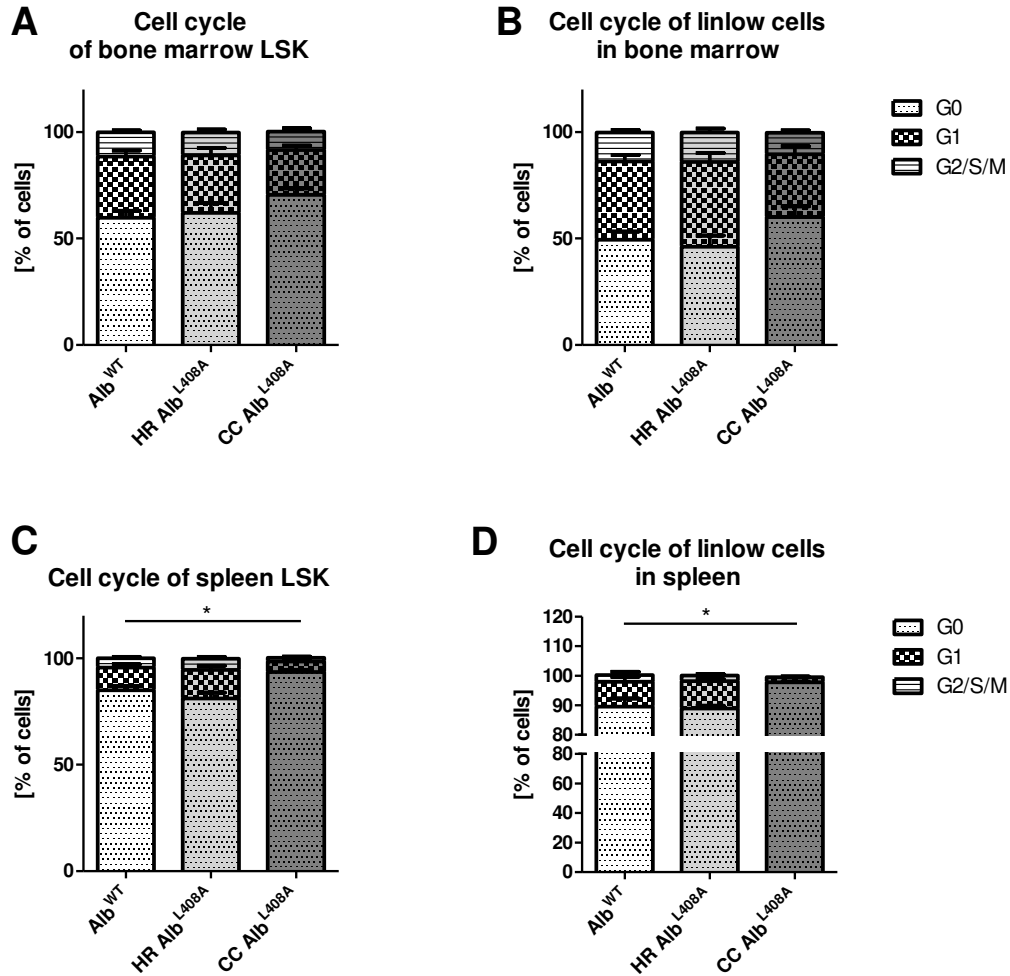


Figure 22: Cell cycle analysis after transplantation. Immature LSK cells of BM (A) and more mature linlow cells (B) were analyzed regarding their cell cycle state in flow cytometric analysis after re-establishing a stable hematopoiesis after transplantation. We distinguished between G0, G1 and G2/S/M phases using Ki67 and 7-AAD. The same was performed for splenic LSK (C) and linlow (D) cells. Significantly higher fractions of all immature cells were found to be in G0 phase of in spleen of CC Ala mice. $n \geq 3$ mice per group, * $p < 0.05$.

3.6. Regeneration after hematopoietic stress is independent from EPI-X4

Sub-lethal whole body irradiation induces apoptosis of cycling cells. This effect manifests as a transient near-complete WBC aplasia in peripheral blood (Figure 23) after three days and a drop in RBC count after seven, in agreement with the life spans and irradiation-resistance of mature WBC and RBC [101]. BM HSPC are thus forced to proliferate to repopulate the peripheral blood with mature hematopoietic cells. At the same time, irradiation harms the BM environment, which could lead to the generation of EPI-X4, similar to the lethal irradiation setting described in 3.5. As no direct detection of putatively generated EPI-X4 is feasible due to its limited detectability only by mass spectrometry and in larger fluid volumes, investigations need to be performed indirectly. To examine the possibility that EPI-X4 is generated and impacts on HSPC proliferation after mild injury, mice of either strain were irradiated with 4.5 Gy and hematopoietic reconstitution was monitored until recovery. Regeneration of WBC was found to be the same in all genotypes (Figure 23), negating a role of EPI-X4 in regeneration from radiotoxicity.

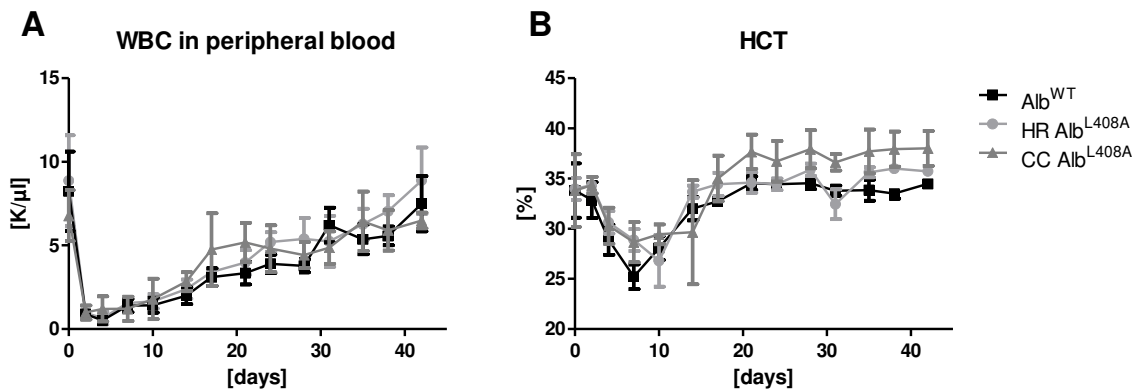


Figure 23: Engraftment analysis after sublethal irradiation. Mice were irradiated with 450 cGy and allowed to recover for six weeks. Hematopoietic engraftment of WBC (A) and hematocrit (HCT) (B) was monitored over seven weeks. All mice recovered equally to normal homeostatic cell counts. $n \geq 5$ mice per group.

To gain insight into the early kinetics of recovery, a second cohort of mice was sacrificed ten days after irradiation and hematopoietic organs were analyzed regarding immature HSPC.

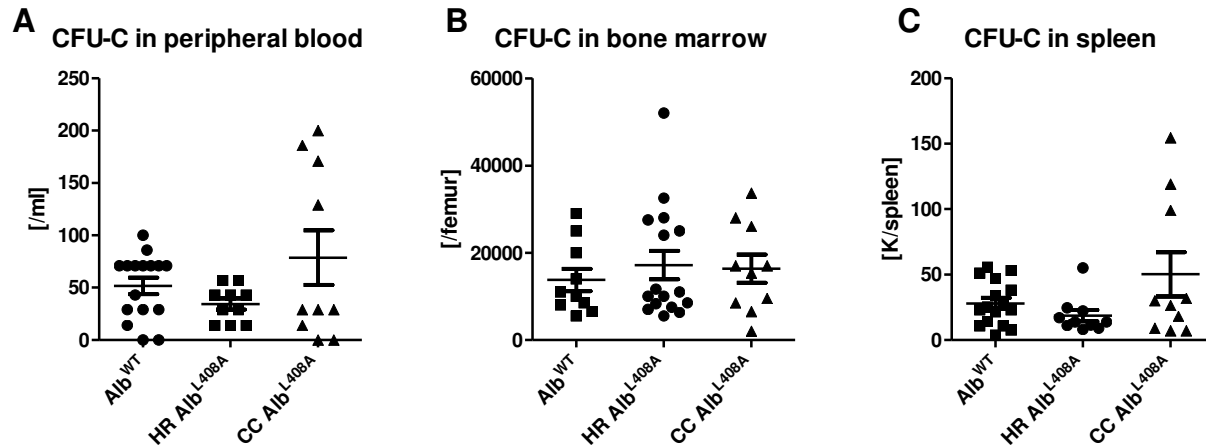


Figure 24: Functional analysis of HSPC after sublethal irradiation. Ten days after low-dose irradiation, peripheral blood (A), BM (B) and splenic cells (C) were plated into methylcellulose and counted. CFU-C counts were diminished in all types of mice in all organs as expected, but did not differ between genotypes. $n \geq 10$ mice per group.

At that point of time, proliferation rates of BM HSPC are high, while strongly elevated levels of inflammatory markers (Figure 25) can be detected in plasma. EPI-X4 could thus potentially be generated in this setting and affect hematopoietic regeneration in a meaningful way.

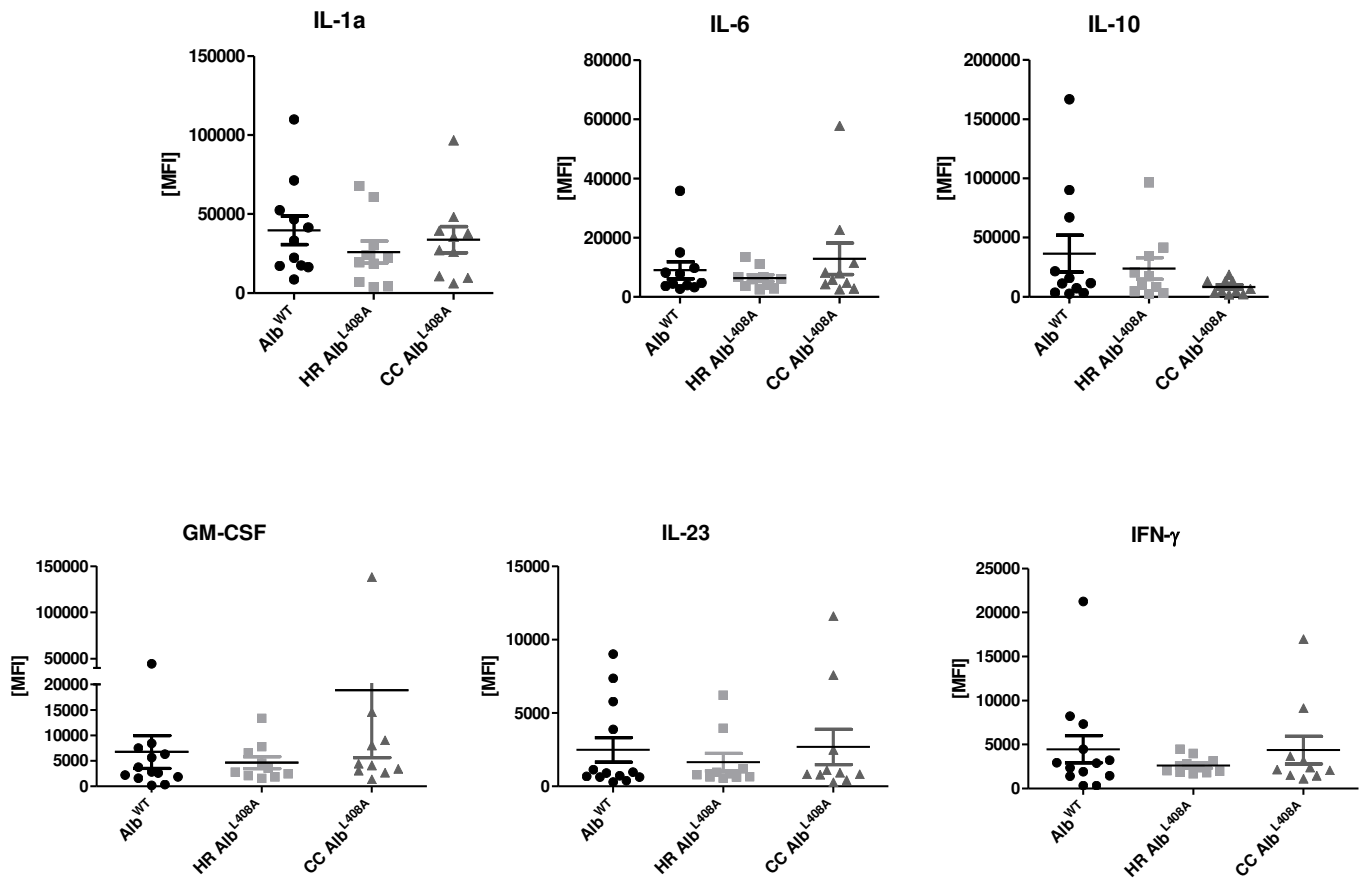


Figure 25: Inflammatory cytokine measurements after sublethal irradiation. Levels of selected inflammatory cytokines were measured using a bead-based technology via flow cytometry. Markers of acute inflammation were elevated in all types of mice. IL-10 trended towards lower levels in CC Ala mice. $n \geq 10$ mice per group.

We found similar levels of HSPC in BM of all mice in phenotypical as well as in functional analyses, and relatively elevated numbers in spleen and peripheral blood only in CC Ala mice compared to WT mice. Slightly higher proliferation rates of linlow cells spleen of CC Ala mice could account for this observation.

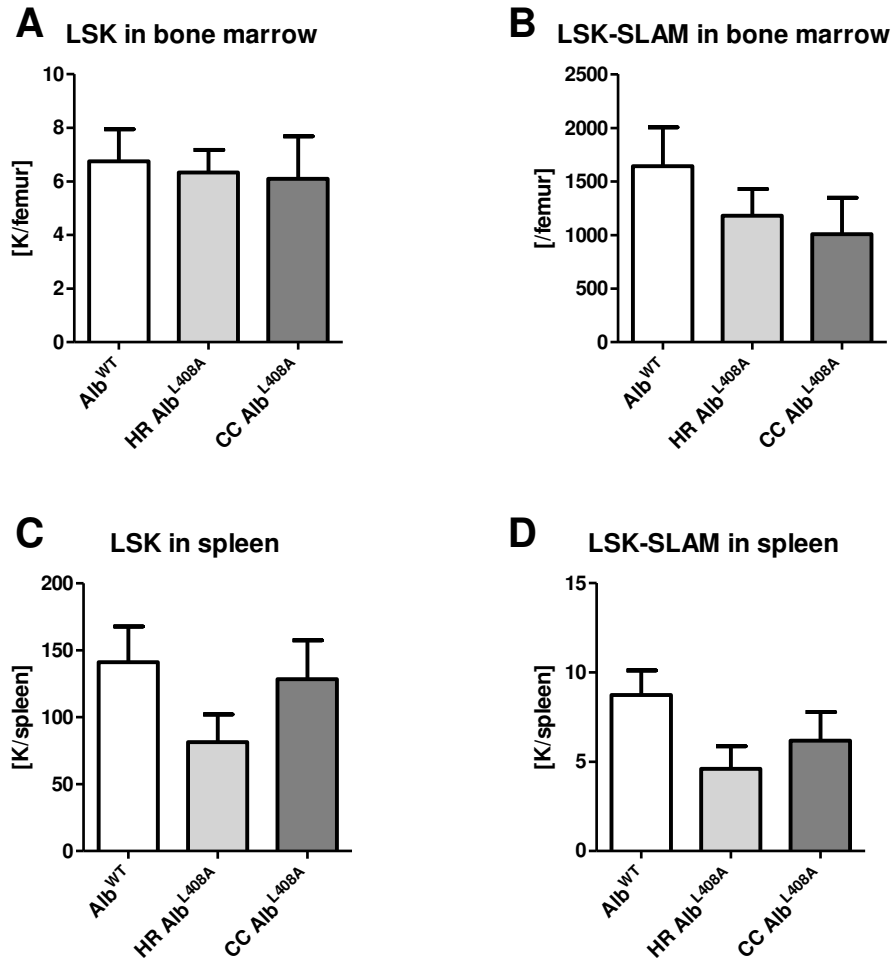


Figure 26: Phenotypical analysis of immature hematopoietic cells after sublethal irradiation. LSK progenitor cells were counted in BM (A) as well as LSK-SLAM cells (B), via flow cytometry. The same was performed for splenic LSK (C) and LSK-SLAM (D) cells. None of the obtained values of Ala mutant mice differed from their WT littermates. $n \geq 10$ mice per group.

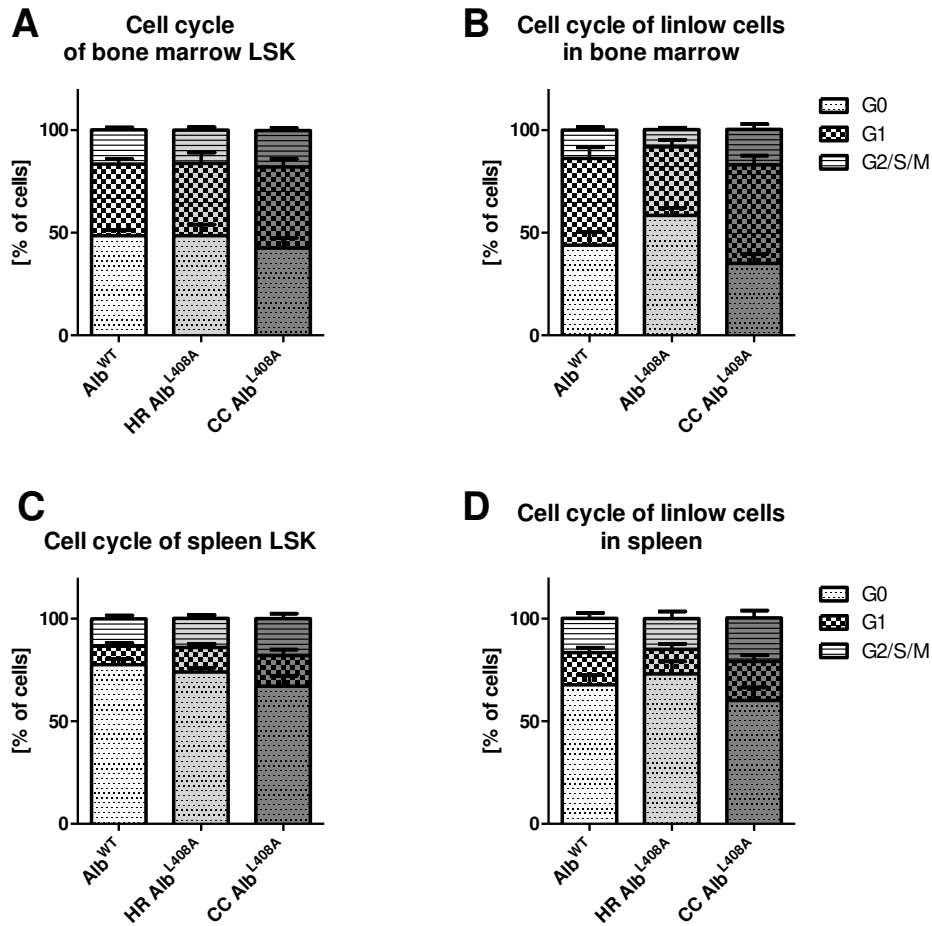


Figure 27: Cell cycle analysis of HSPC after sublethal irradiation. Immature LSK cells of BM (A) and more mature linlow cells (B) were analyzed regarding their cell cycle state via flow cytometric analysis while re-establishing hematopoiesis after sublethal irradiation. We distinguished between G0, G1 and G2/S/M phases using Ki67 and 7-AAD. The same was performed for splenic LSK (C) and linlow (D) cells. No differences in cell cycle states of neither cell type could be detected. $n \geq 10$ mice per group.

Endotoxin measurements were performed before irradiation and at ten days afterwards, showing no detectable endotoxin concentrations changes. All values measured were below the positive test limit of 4 EU/ml (data not shown). Also, 5-FU was administered to our mice and regeneration of hematopoietic cells was monitored. Recovery was comparable in all strains. Analysis of hematopoietic organs 14 days after injections revealed results similar to those after sublethal irradiation (data not shown).

3.7. Immune reaction to peritonitis is not dependent on EPI-X4

CXCR4 is not only the main retention signal for HSPC in the BM, it is also expressed on immune cells. Release of chemokines such as CXCL12 acting as an attraction signal guides these cells to sites of inflammation. EPI-X4, which could potentially be cleaved at those sites, could on one hand interfere with attracting signals and lead to diminished immune cell migrations. On the other hand, EPI-X4 itself could act as a chemoattractant inducing higher cell attraction. To test these hypotheses, a sterile inflammation of the peritoneal cavity was provoked by injection of thioglycolate medium. Immune reactions were monitored at indicated time points until 48 hours after injection. Characteristic migration of immune cells into the peritoneum was observed in all EPI-X4 variant mice. Eight hours after induction of peritonitis, high levels of granulocytes were found in the peritoneal cavity, as described [102]. Lymphocytes could be detected as well, reaching their maximum concentration at 24-48 hours after injection. At the same time the number of monocytes rose (Figure 29). Differentials were found to be similar in both Ala variants and in WT mice with equal migration kinetics. Total cell numbers, however, were significantly lower in CC Ala than in WT mice. Additionally, reactions in peripheral blood to the peritoneal inflammation were visible in terms of high neutrophil levels and elevated inflammatory cytokine levels in peripheral blood over 48 hours. No differences could be identified regarding peripheral blood leukocyte or inflammatory cytokine levels, as shown exemplarily for IL-1, IL-10 and IL-6 (Figure 28).

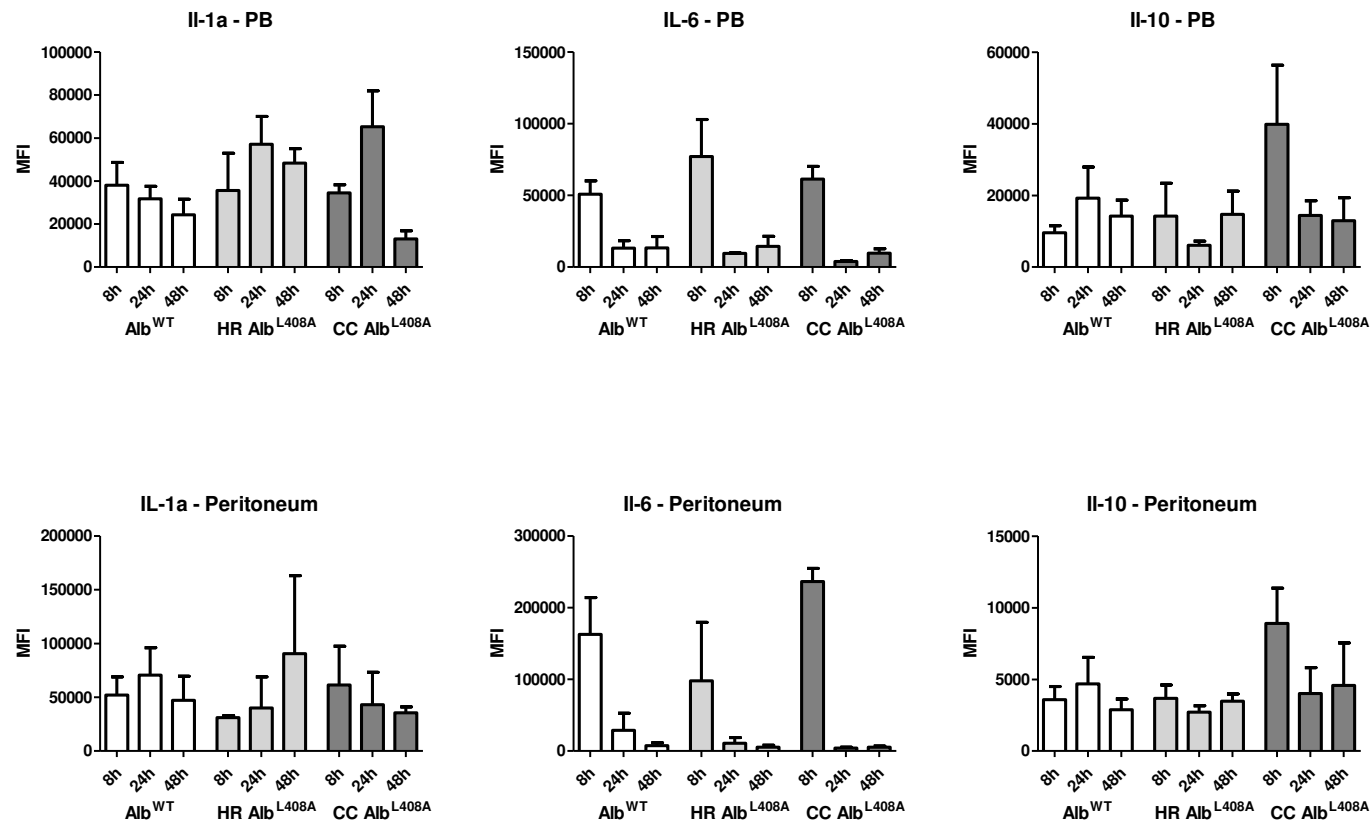


Figure 28: Inflammatory cytokine measurements after peritonitis induction. Levels of selected inflammatory cytokines were measured using a bead-based technology via flow cytometry. Markers of acute inflammation were elevated in all types of mice. IL-6 was markedly elevated after eight hours in all mice. CC Ala mice trended towards higher levels of IL-10 at the same time. $n \geq 10$ mice per group.

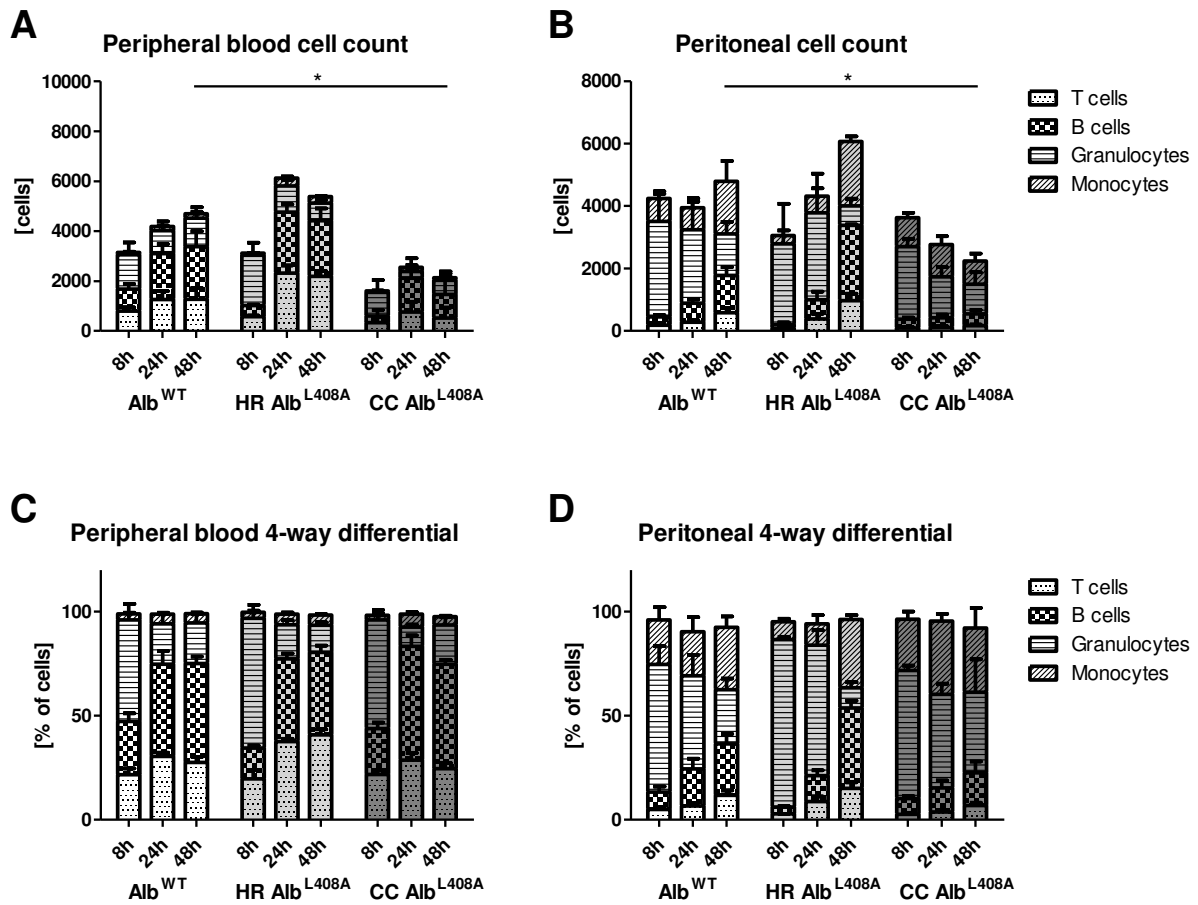


Figure 29: Cell counts in peripheral blood and peritoneal lavage after induction of peritonitis. Total numbers of mature hematopoietic cells were counted in peripheral blood (A) and in peritoneal lavage (B) via flow cytometry at the indicated time points. At all time points, peripheral blood cell counts were lower in CC Ala mice than in WT ones. Moreover, the number of peritoneal cells decreased over time in those mice while WT and HR Ala mice did barely change. Relative distribution of different cell types was altered neither in peripheral blood (C) nor in peritoneal lavage (D). $n \geq 3$ mice per group, $* p < 0.05$.

3.8. No role for EPI-X4 in DSS-induced colitis

A standard regimen of 3% DSS over seven days was used to induce an inflammation of the colon. DSS, a sulfated polysaccharide, penetrates the mucosal membrane of the intestine leading to physical lesions and subsequently inflammation of the colon. A seven-day treatment represents an acute colitis model with epithelial degeneration and severe diarrhea. Weight loss of all mice was monitored over time resulting in 10-20% minus at day 7. All mice lost weight ($p < 0.01$) without significant differences between strains. An untreated group of mice of all genotypes served as control.

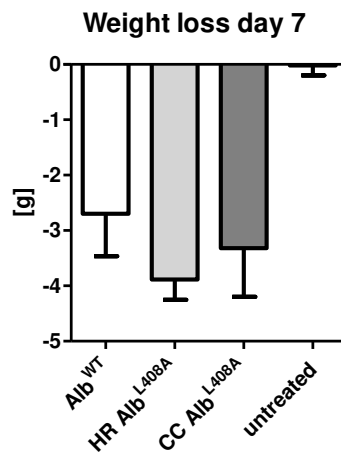


Figure 30: Weight loss during acute colitis. All DSS-treated mice lost up to 4 g bodyweight after one week of 3% DSS administration independently from their genotype. $n \geq 6$ mice per group.

EPI-X4 was previously shown to be generated in vaginal fluid and rectal mucosa [38], potentially serving as a blocker of CXCR4 to protect against X4-tropic HIV. However, EPI-X4 is evolutionarily much older than HIV, so that we speculated about overarching functions at the mucosal barrier. Relatively suppressed numbers of Treg and of IL-10 concentrations in the peritonitis model in mice deficient for EPI-X4 further strengthen the rationale. Cleavage of albumin at the mucosal barrier of the colon could lead to altered effects in this colitis model. We thus investigated our mice regarding infiltration of immune cells to affected sites and laboratory markers of systemic inflammation. Analysis of inflammatory markers in peripheral blood showed increased levels of IL-6 in all mice compared to untreated controls. Also, levels of IL-10, an anti-inflammatory cytokine, were slightly lower ($p = 0.07$) in CC Ala mice than in WT mice (although trending towards higher levels than WT in the HR Ala mice). Other cytokines measured included IL-23, IFN- γ , TNF- α , MCP-1, IL12-p70, IL-1 β , IL-27, IL-17A, IFN- β , GM-CSF; these were not significantly altered between genotypes.

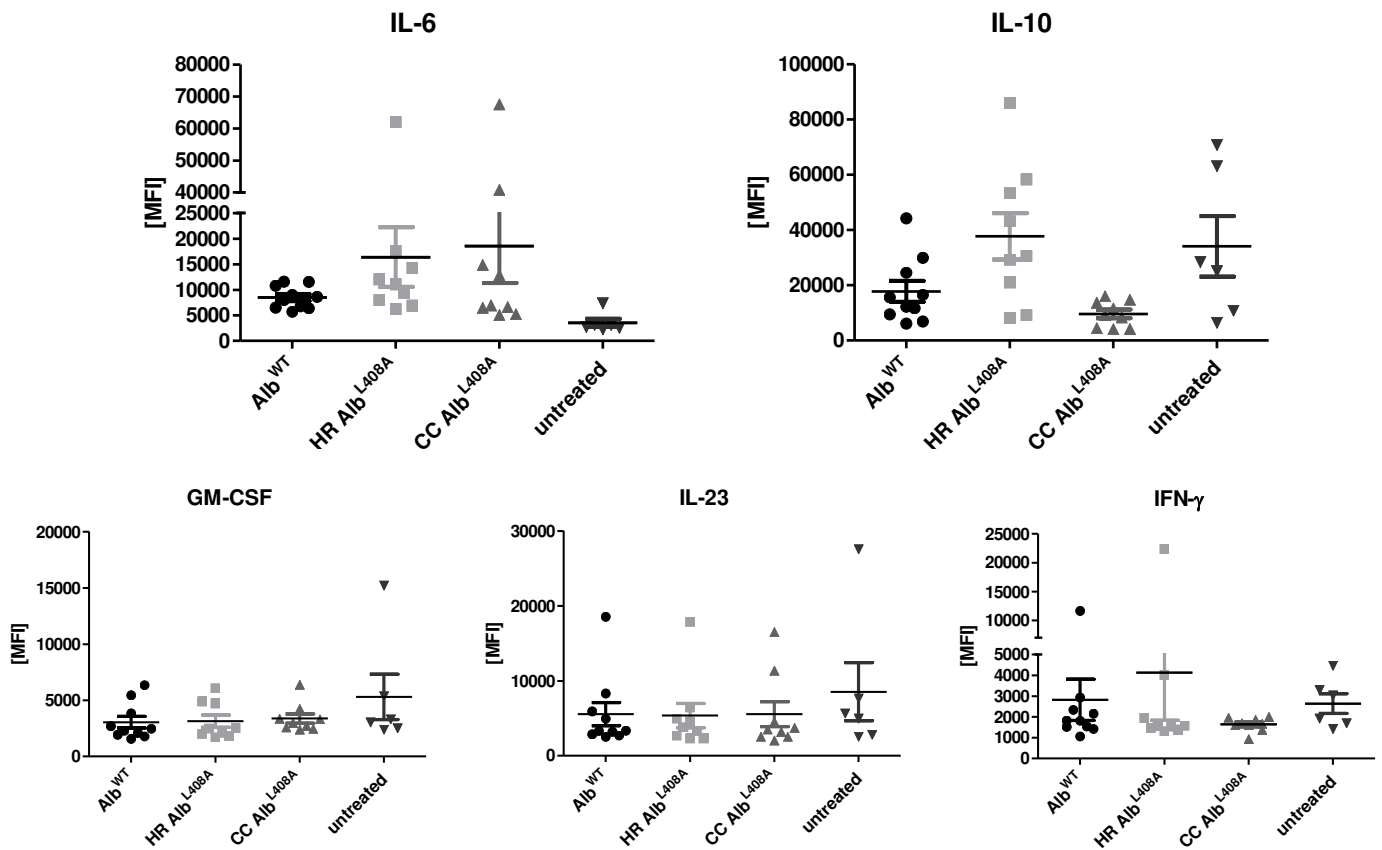


Figure 31: Inflammatory cytokine measurements in an acute colitis setting. Levels of selected inflammatory cytokines were measured using a bead-based technology via flow cytometry. Markers of acute inflammation were elevated in all types of mice. IL-10 was slightly lower in CC Ala mice ($p = 0.07$) while all other values did not differ between genotypes. $n \geq 6$ mice per group, * $p < 0.05$.

Mature hematopoietic cells in peripheral blood were analyzed in addition. In peripheral blood, significant changes in total cell numbers could be detected in CC Ala mice compared to untreated controls in terms of elevated WBC levels. No differences were found in BM cell numbers. However, we found a trend towards increased cell numbers in spleen of CC Ala mice after DSS-treatment, showing a potentially more pronounced response to inflammation than in WT mice as well as in HR Ala mice. Similar effects were found when counting immature hematopoietic cells: CFU-C counts were elevated after DSS-treatment in peripheral blood and spleen, reflecting the ongoing inflammation.

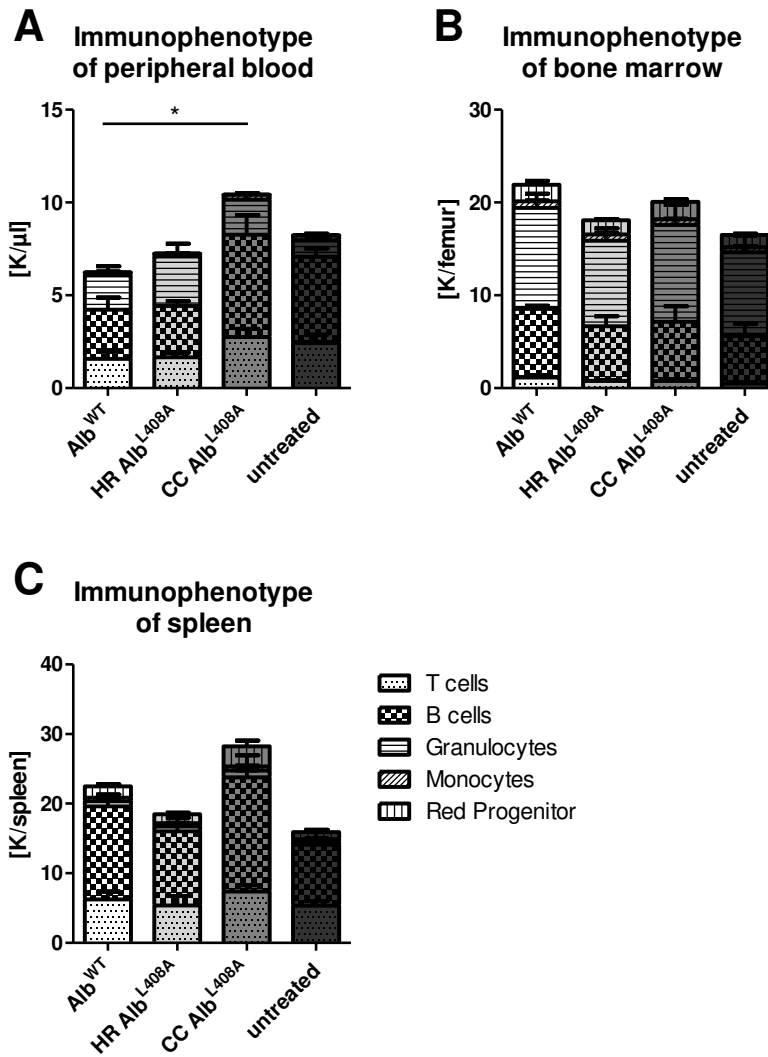


Figure 33: Mature hematopoietic cell count after DSS treatment. Mature cells from peripheral blood (A), BM (B) and spleen (C) were analyzed via flow cytometry. An increase in granulocytes was detected in peripheral blood of CC Ala mice. $n \geq 6$ mice per group, * $p < 0.05$.

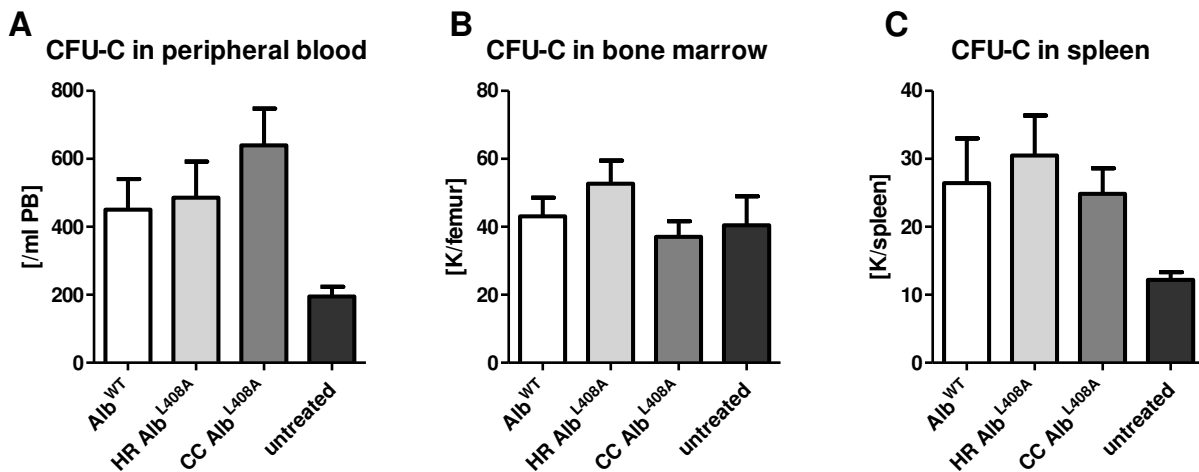


Figure 32: Functional analysis of HSPC after DSS treatment. HSPC were counted by CFU-C assays of peripheral blood (A), BM (B) and spleen (C). Higher numbers of progenitor cells were found in peripheral blood and spleen of mice of all genotypes compared to untreated controls, reflecting the acute inflammation. No changes were seen in BM, neither between genotypes nor to untreated control mice. $n \geq 6$ mice per group.

After sacrifice of the mice, colon was extracted, cleaned, measured and weighed before further histological examination. A significant decrease in weight of the colons of CC Ala mice as well as a significant shortening of colons of all types of mice compared to untreated controls was detected. Significant variations between Ala and WT mice were detected in terms of lower colon weights of CC Ala mice. They also trended towards a more pronounced shortening of colon.

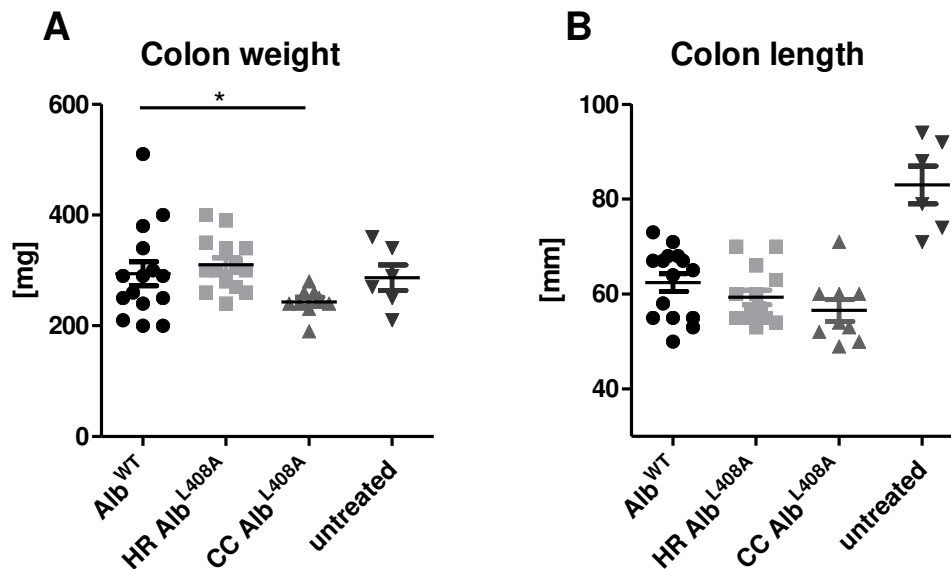


Figure 34: Colon analysis after DSS treatment. Acute colitic colons were weighted (A) and measured (B) after one week of DSS treatment. Colons of CC Ala mice were lighter and trended to be shorter than WT ones. All colons were shortened by ~ 40% independently from their genotypes. $n \geq 6$ mice per group, * $p < 0.05$.

In further investigations, the hypothesis of a more severe impact of DSS on CC Ala mice was resumed. Colons were opened longitudinally, rolled up from proximal to distal ends and fixed as so-called “swiss-rolls” for histological analyses. Subsequent slicing and staining allowed for objective semi-quantitative histological scoring of severity of the colon damage. For a general overview of colitis severity, three slices per mouse were analyzed for their damaged area. A colitis affected area was defined as a zone with visibly damaged mucosa and results were calculated as percentage affected of the whole colon. Results are presented in Figure 35. Lesions were seen in all mice at comparable levels. Also, the severity of damage to the mucosa was not altered nor could differences in crypt lesions of colons be detected. The number of mucus secreting goblet cells was also found diminished equally throughout all genotypes. In consequence, all mice were equally affected by an acute colitis.

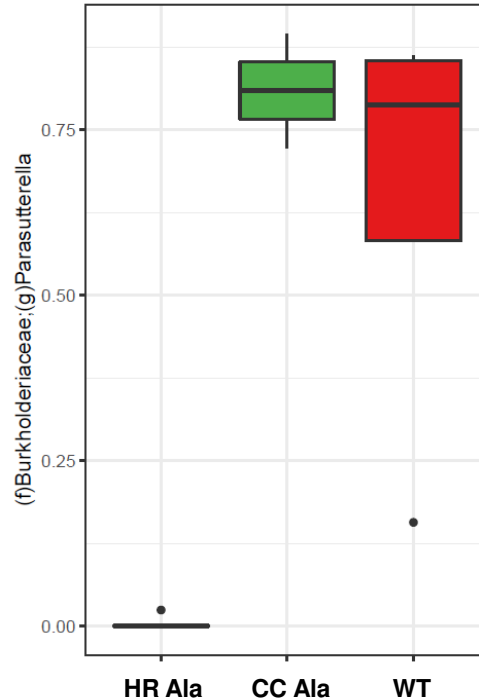


Figure 36: Abundance of Parasutterella in feces. Feces of mice that were housed together were analyzed regarding their microbiological composition. The taxon Parasutterella was found to be absent in male HR Ala mice. n ≥ 5 mice per group.

3.10. Pathogen defense is not influenced by EPI-X4

Lipopolysaccharides (LPS) derived from the outer membrane of Gram-negative bacteria act as the prototypical endotoxin as they bind the CD14/TLR/MD2 receptor complex in many cell types. Measuring endotoxin values or the concentration of LPS-binding proteins, a surrogate of LPS in plasma can thus give an impression of the ability of a host's pathogen defense. An impact of EPI-X4 that could potentially be created by proteolytic processes possibly influencing immune cells can be studied in our Ala mutants. Homeostatic endotoxin levels were measured in plasma of all genotypes as well as levels after sublethal irradiation when mice are more susceptible to pathogens and EPI-X4 is potentially generated in relevant amounts. Under steady-state conditions, LPS-binding protein levels were found similar in HR Ala mutants and WT littermates (Figure 37). Endotoxin levels of all mice were not altered either as already described in 3.6.

LPS-binding protein

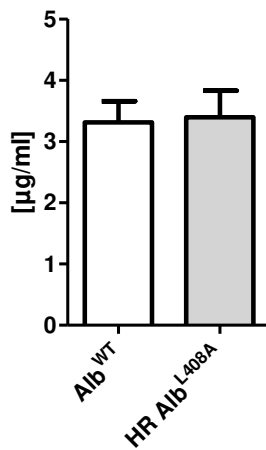


Figure 37: Measurement of LPS-binding protein in HR Ala plasma. Plasma samples of WT and HR Ala mice were analyzed regarding their LPS-binding protein content. No difference could be detected between genotypes. $n \geq 5$ mice per group.

3.11. Response to orally presented allergen might be influenced by EPI-X4

Correct B cell function in terms of cell activation, release of antibodies and antigen-presenting is crucial for antigen recognition and host defense. Chicken ovalbumin (OVA) is a foreign antigen to mice that has been successfully used for decades in allergen challenge investigations. Its well-known structure and broadly available detection reagents make it a suitable model for immunological studies in our mice. After sensitization with alum-adsorbed OVA, all mice were given OVA orally in order to induce an immunological response in the gut. In plasma samples, OVA-specific CD8⁺ T cells were counted additionally to measuring anti-OVA IgE levels. We counted higher numbers of T cells directed against OVA in CC Ala mice compared to WT mice and HR Ala mutants, which, however, did not reach statistical significance. IgE ELISA did not reveal any significant differences in antibody concentrations in plasma, but trended towards a stronger reaction of CC Ala mice towards OVA than WT and HR Ala ones.

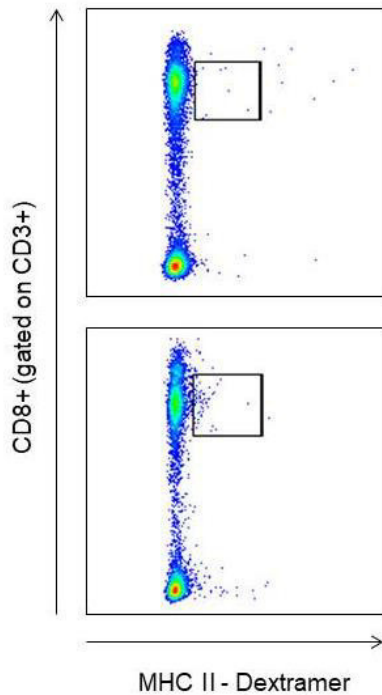


Figure 38: Detection of OVA-reactive CD8+ cells via flow cytometry. Lymphocytes from blood and spleen were analyzed via flow cytometry as described in 2.2.16.

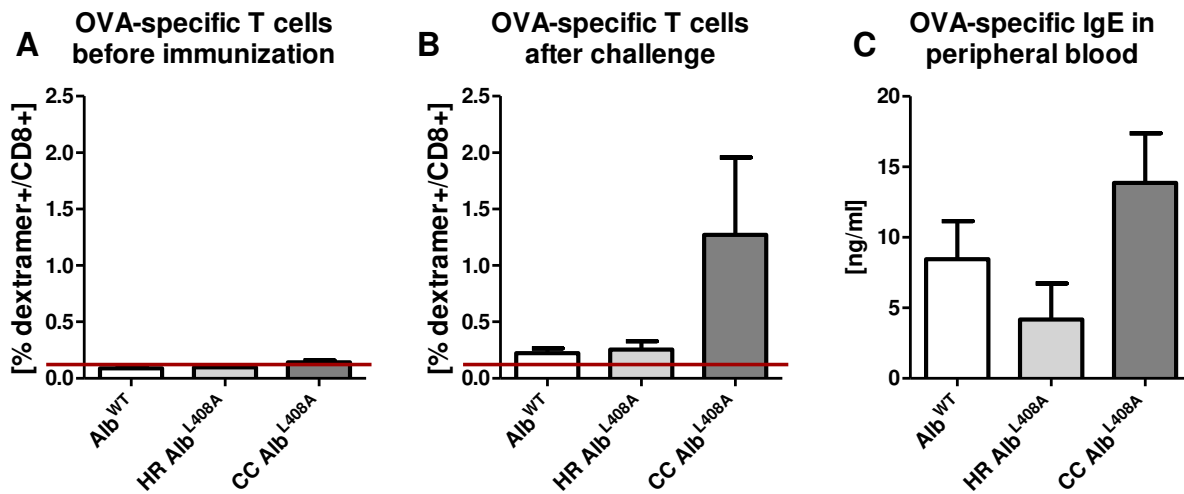


Figure 39: Analysis of OVA-specific reactions after immunization and subsequent oral challenge. OVA-reactive T cells in plasma were counted via flow cytometry before contact with OVA (A) and after immunization and challenge (B). An augmentation of OVA-specific CD8+ T cells was seen in all types of mice. However, CC Ala mutants trended towards higher numbers of OVA-reactive T cells in peripheral blood than their WT controls. IgE levels against OVA (C) were detected in all genotypes, but also trended towards higher levels in CC Ala mice. $n \geq 5$ mice per group, * $p < 0.05$.

4. Discussion

CXCR4 is one of the key players in both mature and immature hematopoiesis: Together with its main ligand CXCL12 it not only retains HSPC in their BM niches, it also controls multiple physiological processes where hematopoietic cells are involved. Additionally, it serves as an entry point for X4-tropic HI-viruses. The great interest in HIV fueled the development of CXCR4 targeting compounds. Many studies on CXCR4 ligands have been performed since its first description in 1996 [104]. Naturally occurring interaction partners as well as synthetically produced agonists and antagonists are highly interesting compounds for CXCR4 modulation. One recently discovered natural antagonist, termed EPI-X4, was found to be cleaved from serum albumin under acidic conditions. Due to its high conservational status through various mammals we posit that it serves an evolutionarily ancient physiological role. However, its physiological functions are entirely elusive. In the course of this study, we tried – largely in vain – to determine possible effects of EPI-X4 on normal and stress hematopoiesis as well as its immunological function at mucosal barriers. As EPI-X4 cannot be directly quantified *in situ* or even *ex vivo*, we sought to address the functional role or roles of EPI-X4 in an *in vivo* model of EPI-X4 deficiency, i.e. in mice where we had mutated the leading amino acid from leucine to alanine since, as structure-function analyses predicted and earlier studies with synthetic Ala-EPI-X4 confirmed, this variant is completely unable to interact with CXCR4.

For a number of years the creation of genetically modified mice for the purpose of systemic analyses has been a widely used experimental approach. Thereby, methods for gene modifications have improved from phenotype-driven mutagenesis with N-ethyl-N-nitrosourea (ENU) over gene modification by insertions of a selection cassette to directed single-point mutations in the DNA. The most widely used methods today are homologous recombination and CRISPR/Cas technology, where precisely targeted nucleotide exchange is possible. Reliability and possible side-effects of these technologies shall additionally be discussed in this work. With two presumably identical mouse models created with both methods, we compare possible off-target effects and identify important points to consider when evaluating data obtained from genetically modified mouse models.

4.1. Divergent findings in different Ala-EPI-X4 mouse models

Results derived from mouse models, especially when genetically modified, have to be examined carefully with respect to possible confounders. In the course of this study, we used two differentially engineered mouse strains, both on a C57Bl/6J background, to investigate the effect of a non-functional EPI-X4 variant in an *in vivo* setting. Formally, both models are based on a single point-mutation leading to an amino-acid exchange at position 408 of murine albumin.

Sanger sequencing of ± 500 bp around the locus confirmed the mutations as well as otherwise intactness of the reading frame; also both mice strains are normally albumin competent, arguing against relevant disruption of the albumin locus *per se*. Two different commonly used techniques have been applied for genetic modification: the principle of homologous recombination (HR) and the rather new CRISPR/Cas method. While for HR engineering mixed background ES cells were used, the CRISPR/Cas technique was applied directly to ES cells derived from C57Bl/6 mice. Therefore, HR Ala mice were backcrossed on a black background until all requested SNP markers, determining the principle benchmarks for a C57Bl/6 mouse [105], were verified. Although a SNP panel for background check covers all informative SNPs for the corresponding background strain, but indeed, it does not replace a whole genome screen. Undetected modifications, insertions or deletions of genes could have occurred outside the screening regions. The risk of an additional insertion of large parts of long homology arm in HR is low and its occurrence easy to detect. By contrast, off-target mutations using CC technology are more likely to occur and also more difficult to detect, while great effort has been made to minimize those side effects. A single point mutation could have happened in a genomic region that affects, for example, IL-10 production in a second place, maybe also in a region that has an impact on granulocyte development. To test for possible off-target effects, a screen of the genes of interest like transcription factors CBF and c-Myb [106] or cytokines, especially GM-CSF and IL-3 [107] might be useful. In order to analyze the subtle differences between our HR Ala and CC Ala strains, backcrossing over ten generations to the same strain could lead to a greater concordance of both mice in hematopoiesis. All assays performed would have to be repeated. Nevertheless, if the possible misintegration of a mutation or side-effects occurred in a genomic region near the Ala-mutation, only screen of the whole chromosome 5 is informative about possible differences.

In our case, the differences between both mouse models are modest, as far as we can currently tell restricted to immunological reactions to a foreign antigen and inflammation as well as microbiotic composition. The discrepancies could be explained by subtle strain differences although we cannot pinpoint these. Although both HR and CC Ala mice were on a C57Bl/6 background at the beginning of our studies, genetic drift could have happened over generations in colony breeding. Both strains were bred separately, increasing the risk of divergent genetics. Interestingly, all WT controls were found to be at similar levels in their homeostatic hematopoietic properties as well as after stress assays; this also applies for inflammation assays. In total, these observations do not support the occurrence of significant genetic drift within the distinct colonies. A possible explanation for similar results in all WT results regardless of the background strain is the use of harsh models, e.g. the acute colitis model that does not

allow detection of subtle differences. In contrast, the fact that CC Ala mice show a clear granulocyte retention phenotype, while their WT littermates and HR Ala mice do not express such a phenotype, would be quite compatible with a physiologic effect of EPI-X4, given the described non-redundant role of CXCR4 signals for mature granulocyte egress from marrow. The genetic background of the CC Ala strain may thus possibly be considered more susceptible for changes in CXCR4 signaling than the HR strain. What is observed in both strains of EPI-X4 deficient mice is a decrease in regulatory T cells in peripheral blood and spleen, quite strongly implicating EPI-X4 (and thus indirectly CXCR4) in Treg homeostasis. Until today, little is known about the effects of CXCR4 on these cells. However, roles of CXCR4 for Treg migration were previously suggested [108]. High CXCL12 levels in BM were shown to attract Tregs via CXCR4, generating a Treg reservoir in the latter [109]. A similar effect could potentially be driven by EPI-X4, its lack could thus account for a smaller number of Tregs in periphery. Decreased IL-10 production, distinctive for Tregs, was observed only in the CC variant which might again imply a higher sensitivity of the CC background towards disrupted CXCR4 signaling.

4.2. EPI-X4 in the context of immature hematopoiesis

The CXCR4/CXCL12 axis was proven critical for establishing definitive hematopoiesis. Knock-out models of mice on either side of the axis lead to early embryonic lethality, CXCR4/CXCL12 signaling is thus indispensable for development. In CXCR4^{-/-} mice a hypoplasia is described on day 15.5 of embryogenesis [4] which underlines the significant role of the signaling axis. Nevertheless, it is known from inducible knock-out models and transplant experiments that this signaling pathway is no longer crucial for survival once CXCR4-dependent organs have formed and bone marrow hematopoiesis has been established [4, 5, 110]. CXCR4^{-/-} fetal liver cells that are transplanted into lethally irradiated adult mice repopulated the BM and established functional hematopoiesis, albeit with a lack of B cells and pronounced leukocytosis [31, 111]. CXCL12-deficient BM cells were also able to sustain a normally performing hematopoiesis, without deficits, provided the stroma is CXCL12 competent [[111] and own, unpublished data]. HSPC-intrinsic CXCL12 is thus dispensable, its role, in fact, elusive. However, complete knock-out of CXCL12 in mice leads to early death of pups in utero due to defects of colonization of the BM by hematopoietic cells and defects in the development of heart, brain and large vessels [112, 113]. Very careful analyses of mice with CXCL12 deficiency in very narrow cellular lineages, albeit not completely conclusive, suggest that for immature hematopoiesis the critical source of CXCL12 is the BM endothelium [114, 115]. Wright and colleagues could show that fetal liver cells only migrate towards a CXCL12 induced gradient and do not react to other cytokines *in vitro* [116]. We deduce from these findings that the CXCR4/CXCL12 axis is critical for the primary formation

and localization of a stable hematopoiesis, but although still very functionally relevant its deficiency in adult mice is no longer lethal. Here, CXCR4-deficient hematopoiesis is characterized by copious, eventually (at least with additional stress) exhausting, proliferation of the normally overwhelmingly quiescent stem cells, as well as egress thereof from bone marrow (mobilization phenotype) [13] and B-cell deficiency [27]. So what could be the phenotype of mice lacking the natural endogenous CXCR4 antagonist EPI-X4 (provided the local conditions are conducive to EPI-X4 cleavage from its ubiquitous and highly abundant precursor)? Naturally occurring ligands like EPI-X4 could potentially lead to a modulation of the CXCR4/CXCL12 interaction in hematopoietic organs. Loss of EPI-X4, possibly leading to slightly larger response rates of CXCR4 to CXCL12, could thus yield initially higher numbers of HSPC in homeostasis in the BM. Alas, our data do not support this hypothesis. Indeed, we find equal numbers of HSPC in both Ala-EPI-X4 variants tested in here, comparable to WT mice. Moreover, egress and retention of immature cells out of the BM when regarding splenic and peripheral blood HSPC was not found to differ from mice expressing the WT-EPI-X4 variant. Modifications on homeostatic hematopoiesis after birth by EPI-X4 can thus be considered minimal (either because EPI-X4 is not generated or because it is generated but not noticeably involved in the observed functions), and in case it changes, it was not detectable with our methods.

An effect on hematopoiesis of EPI-X4 in homeostasis would presume the generation of the latter under (patho)physiological conditions. To this end, Zirafi *et al.* were able to detect the peptide in acidified human plasma as well as under non-physiological conditions in hemofiltrate, but more importantly in vaginal lavage, gastric juice and rectal mucosa [38]. These findings demonstrate that EPI-X4 needs an acidic environment to be cleaved – which is possibly normally not the case in healthy BM (although it has been argued that periosteal “niches” might be hypoxic and thus inherently somewhat acidic). Nevertheless, steady-state analysis of immature hematopoiesis in both Ala-models was performed to screen for abnormalities. Immature hematopoiesis in the EPI-X4 deficient animals was entirely normal for a C57Bl/6 mouse and indistinguishable from WT controls, so if we had detected defects in non-homeostatic settings, such as during mobilization, these could have been attributed to the loss of EPI-X4 (and would have indicated contributory roles thereof). Pharmacological disruption of the CXCR4/CXCL12 axis by antagonists, as performed in AMD3100 mobilization, leads to instant egress of HSPC into the periphery while providing acidic cleavage conditions for serum albumin. No detectable impact on mobilization efficacy after AMD3100 administration supports the independence of this type of mobilization from EPI-X4 production. An environment that with very high likelihood provides the conditions for EPI-X4 generation is produced by whole body irradiation or G-CSF administration [117]. Although the exact working mechanism of G-CSF is not entirely clear yet, it has been shown to

induce proliferation and at the same time egress of HSPC out of the BM [96]. Recent studies demonstrate a change of BM structure, leading to a down-regulation of CXCL12 production by osteoblasts. At the same time, cleavage of surface-bound chemokines (especially CXCL12), cytokines and receptors has been demonstrated [118]. Evidence has been provided [119], albeit not undisputed [120], that these effects are due to proteases, which are elaborated during G-CSF mobilization, together with down regulation of protease-inhibitors. Moreover, it has been suggested that prolonged administration of G-CSF induces a hypoxic (and hence, relatively acidic) milieu in the BM [117] which might lead to optimal conditions for serum albumin cleavage by cathepsins and neutrophil elastases. The expression of G-CSF receptor, G-CSFR, although lowly expressed on HSPC, is apparently dispensable for mobilization, pointing at a mechanism of passive mobilization [121]. However, high expression rates were detected on neutrophils [122] which are equally increased under G-CSF treatment and released into the periphery. Experimental data on G-CSFR^{-/-} mice show refractoriness to mobilization by G-CSF [121]. In contrast, in a mixed chimeric BM with G-CSFR competent and knock-out cells, both types of granulocytes and HSPC are mobilized equally after G-CSF treatment, albeit G-CSFR^{-/-} cells in reduced numbers, likely mostly for lack of G-CSF induced expansion [123]. These data point – at least in part – at indirect mobilization mechanisms. In any case, the rapid increase in neutrophils comes along with a large release of proteases that are able to cleave serum albumin. If, under these conditions, EPI-X4 contributes to mobilization with G-CSF, then in its absence mobilization should be attenuated. However, our findings do not corroborate this hypothesis: In CC Ala mutants, the number of granulocytes in the BM was elevated by ~25% compared to WT mice after the five-day mobilization course; progenitor cells in EPI-X4^{-/-} BM were also slightly increased relative to similarly treated WT controls (Figure 16 and Figure 17). We interpret these data to indicate that the cleavage of EPI-X4 could thus lead to an improvement of neutrophil proliferation and migration and thereby enhance HSPC egress out of the BM after G-CSF mobilization. With fewer neutrophils exiting the BM of CC Ala-EPI-X4 mice, the number of HSPC retained in there is accordingly higher. G-CSF was also shown to reduce CXCR4 surface expression [124], leading to fewer available binding sites for CXCL12 and other ligands. Competition is even higher in the presence of EPI-X4: The potentially generated antagonist could block retention induced by CXCL12, which is in accordance with our data and could account for the observed phenotype. When we see higher numbers of immature cells in BM under certain conditions, this observation could have several different, in fact, diametrically opposed causes. For once, we could be dealing with defective mobilization, second, with ineffective entry into lineage differentiation (during the course of which the immature phenotype would be lost although the progeny might remain in BM), as well as preferential self-renewing

differentiation of the most immature cells. These possibilities are difficult to explore experimentally, except that failure to detect differences in cell cycle status of LSK cells from WT and EPI-X4^{-/-} mice suggest that divergent cell cycling likely is not responsible. The discrete retention phenotype was restricted to the CC Ala-variant; the HR Ala-variant was indistinguishable from WT mice. We did not see the same phenotype, likely because of subtle differences in the genetic background of the mice.

A disturbed BM milieu cannot only be achieved by effects of proteases and elastases, it can also occur following irradiation damage. After sublethal irradiation, the BM milieu is disturbed in terms of an overall decrease in cell numbers [125] and occurrence of large acellular areas [126]. A decline in the number of HSPC leads to a defect in the mature leukocyte population necessary for a proper immune response [127]. Moreover, the HSPC environment, the possible BM niche, is altered: Damages on vascularization have been described [128, 129] as well as a loss of sinusoids is induced [130]. Additionally, CXCL12 producing osteoblasts and osteoclasts are damaged [131], leading to an imbalance of the CXCR4/CXCL12 axis. CXCL12 was shown to be important for neutrophil production in the BM [114, 132]. On top of that, a generally more acidic milieu is established, all favoring the cleavage of EPI-X4 from its precursor protein. Thus, an impact of EPI-X4 on leukocyte generation as well as on immunological defense seemed feasible. Contrary to our hypothesis, however, WBC as well as RBC engraftment was not impaired by the absence of a functional EPI-X4 variant. Even in the most acute phase of recovery (12 days after irradiation), an effect of EPI-X4 could not be detected with our methods. Moreover, a possible impact of EPI-X4 on barrier function in terms of a change in LPS-levels was not seen. The barrier function of Ala-EPI-X4 mice can thus be considered normal in our experimental setting. Higher LPS-levels in plasma could have accounted for a disturbed barrier function, which might not be detectable due to the relatively strong leakage that is induced by the irradiation. Then again, however, the, slightly lower levels of IL-10 detected in CC Ala mice in the acute recovery phase after sublethal irradiation could point to a subtle effect of EPI-X4 on immune function and can thus guide further experimentation. IL-10 is described as an anti-inflammatory cytokine [133] that predominantly inhibits LPS and bacterial product mediated induction of pro-inflammatory cytokine, i.e. TNF- α and IFN- γ [134, 135]. A lower release of IL-10 could thus reflect lower LPS concentrations in the blood stream which could eventually point at a less pronounced infection/inflammation. The fact that we only detect marginal changes in hematopoiesis shows that this experiment might not represent optimal conditions for the detection of these small differences. Repeated irradiation sessions could enhance the outcome and make the subtle influence of EPI-X4 in this setting visible.

Total body irradiation of 9.5 Gy leads to complete ablation of hematopoiesis followed by death of mice after 14 - 21 days [136]; to overcome BM failure, transplantation with functional HSPC is the standard treatment. The CXCR4 signaling pathway in this setting is important for re-establishment of functional hematopoiesis in lethally irradiated mice. More precisely, the immediate transplant functions – homing, engraftment, generation of radioprotecting numbers of mature blood cells of all lineages – are apparently preserved in the absence of CXCR4, whereas quite early after transplantation the CXCR4^{-/-} phenotype with, among other abnormalities, augmented numbers of HSPC in peripheral blood is established [137]. During the early phase of engraftment we believe the inflammatory conditions in the post-irradiation marrow filled with necrotic blood cells and disrupted vasculature override the anti-proliferative, quiescence-inducing signals of CXCL12 via CXCR4 on HSCs. So while we posit that EPI-X4 is likely created in the damaged BM after irradiation of the mice, as described above, we did not necessarily expect it to interfere in measurable ways with the CXCR4/CXCL12 signaling axis and thus have an impact on transplantation outcomes. However, subtle effects suggesting a contribution of EPI-X4 were observed, albeit non-overlapping in the two mutant strains. Higher HSPC counts in peripheral blood were not seen (such as after transplantation of CXCR4-deficient hematopoiesis), but we detected higher WBC counts in HR Ala mice, while CC Ala mice exhibited low proliferation rates in BM, accompanied by a lower cell count in spleen compared to WT mice. Moreover, HSPC in spleen were reduced relative to WT only in the CC Ala mice, but not in the HR Ala variant, as detected by flow cytometric analysis. In Ala variant mice, depending on their background, different experimental outcomes are detected, while WT mice behave equally. These incongruent findings might point at genetic background differences, which are not unmasked until the ablation of EPI-X4, indicating a significant role of the peptide on BM restoration.

4.3. Impact of EPI-X4 on lymphopoiesis

The critical role of CXCR4/CXCL12 on lymphopoiesis was what led to the erstwhile discovery of CXCL12: It enhanced growth of a murine preB-cell line [30] and was shown to be important for B cell development *in vivo* quickly thereafter. CXCR4 or CXCL12-deficiency leads to B cell aplasia in peripheral blood [4, 27]. Interestingly, the opposite, i.e. modification of the signal axis in terms of a hyperfunctional variant as it was shown for patients with certain CXCR4-mutations interfering with signal extinction (i.e. WHIM syndrome), similarly accounts for a marked deficiency of functional B cells [138, 139]. Minor changes in CXCR4/CXCL12 signaling thus likely modulate mature B cell numbers in peripheral blood. Modifications in B cell numbers were not detected in homeostatic WBC counts of CC Ala mice, but a higher number of B and T cells

was detected in the HR variant. Both direct effects (lack of the CXCR4 antagonist directly affecting lymphocyte expansion or distribution) and indirect effects (lack of the CXCR4 antagonist inducing some smoldering inflammatory situation which causes a very modest lymphocytosis) can be considered, neither currently be substantiated. Less activation of CXCR4 due to possibly generated EPI-X4 in the periphery could account for this phenomenon. Additionally, we know that T cells are also dependent on CXCR4/CXCL12 interactions, especially for the release of immature lymphocytes from the BM and the subsequent migration to the thymus [33], although the role of CXCR4/CXCL12 for subsequent T cell development is controversially discussed [140]. In CXCR4^{-/-} or CXCL12^{-/-} embryos, accumulation of T cell progenitors in the outer mesenchymal layer of the thymus anlage during initial colonization of the thymus was comparable to WT littermates [141]. Nevertheless, the subsequent maturation was impaired in terms of a diminished expansion of double-negative precursors, leading to lower numbers of CD4⁺ CD8⁺ thymocytes, followed by a reduction of mature T cells. Transplantation of CXCR4^{-/-} fetal liver cells into CXCR4 competent mice leads to reduced numbers of donor-derived lymphocytes even after correction for HSPC outgrowth effects [111, 142]. Thus, an impact of CXCR4/CXCL12 axis on homeostatic T cell counts has been shown. In Ala-variant mice, where no EPI-X4 is generated, less competition of CXCR4 ligands could lead to a better signal processing in T cell maturation, raising the number of mature T cells. This effect can indeed be observed in peripheral blood of HR Ala mice, but not in CC mutants. In the latter, lymphocytes trended to be elevated, but no statistical significance could be reached. Observation of a larger cohort of mice could improve the results to verify an impact of EPI-X4 on T cell numbers. Interestingly, we find similar T cell subset distributions in all Ala variants and WT mice, but consistently detect ~ 30% reduced regulatory T cell frequencies in Ala-EPI-X4 mutants (Figure 13) as one of the few observations that are reproduced by both genetic models and can thus confidently be considered systematic for EPI-X4 deficiency. Regulatory T cells are a subpopulation of T cells that were identified as a pivotal part for control of inflammatory processes [143] and are characterized by their expression of Foxp3 [144]. They are antigen-specific helper-type cells which, after contact with their cognate antigen, secrete not pro-inflammatory but tolerogenic mediators and thus suppress non-adaptive inflammatory responses such as to environmental non-pathogenic antigens. Studies by Sakaguchi and colleagues could show that Treg cell activity is regulated by numerous costimulatory interactions and cytokine microenvironment both in thymus and in tissues to maintain autotolerance [145]. Initial Treg generation can be induced from naïve T cells by repeated stimulation of their TCR in the presence of IL-10 [146], which will be of relevance in the following investigations. Up to 80% of Tregs express CXCR4 [108], possibly linking their number and function to EPI-X4. A tight

regulation of Treg numbers is important, as evidence was provided that low numbers of functional regulatory T cells may result in various autoimmune diseases, i.e. rheumatoid arthritis or multiple sclerosis [147]. Reduced numbers of Tregs in homeostasis could thus lead to a higher sensitivity to foreign antigens, as we examined by challenging Ala mice with OVA, which will be described in the following paragraph.

4.4. EPI-X4 in the context of inflammation

Inflammation is the protective response of an organism to stimulation by invading pathogens or endogenous signals such as damaged cells. It typically results in elimination of the initial cause of injury, clearance of necrotic cells, and tissue repair [148]. Self-limitation of inflammation is critical once the acute situation is under control, in order to protect against bystander effects on healthy tissues and autoimmunity. Cellular stimulation due to pathogen-associated molecular patterns or endogenous stress signals triggers inflammatory processes through the release of proinflammatory cytokines and chemokines. Cytokines activate endothelial cells, thus increasing vascular permeability and facilitating entrance of immune cells into tissues at the site of damage. CXCL12 is produced at sites of injury [149], leading to the assumption that recruiting of leukocytes to those sites is CXCR4/CXCL12 dependent [150]. Especially neutrophils that exert a crucial role in the phagocytosis and killing of pathogens are attracted [151], but also macrophages and lymphocytes react to that signal [152]. Activated monocytes and neutrophils will subsequently release cytokines themselves, leading to a broader response to the inflammation in the organism [153]. Additionally, non-specific anti-microbial mechanisms promote a tissue microenvironment, e.g. by generation of reactive oxygen species, that is presumably conducive to EPI-X4 cleavage [154]. Recent studies showed that CXCR4/CXCL12 axis is also involved in several inflammatory diseases, including rheumatoid arthritis and inflammatory bowel diseases [155]. Modifications in its signaling pathway could thus modulate inflammation outcome and cellular reactions on injury signals. Specifically pertinent to our experimental model for querying the role of EPI-X4 at the intestinal interface, Mikami and colleagues could show that blocking of CXCR4/CXCL12 axis was able to ameliorate colonic inflammation in experimental DSS-induced colitis models in mice [156]. They could prove that CXCL12 production in inflammatory colonic tissue was increased, leading to a higher influx of leukocytes. Additionally, CXCR4 expression was also upregulated on granulocytes and T cells, enhancing their attraction. We presume a generation of EPI-X4 after a seven-day treatment of DSS which could lead to a blockade of CXCR4/CXCL12 signaling. Thus, influx of leukocytes, especially neutrophils and lymphocytes, is expected to be diminished. Alas, as tempting as these hypotheses are, we were not able to detect such an impact directly in neither of our mouse

models. Slightly higher numbers of circulating leukocytes in peripheral blood could nevertheless give a hint on possible migration defects of those cells to the colon. If we presume EPI-X4 generation on the abluminal side of the colon, we expect it to block the entry of leukocytes into tissues. A trend towards smaller and lighter colons in CC Ala mice might also point into the same direction: We observe greater damage and thus a more severe reaction of the organism, where we would expect a large influx of lymphocytes correlating with the severity observed. In fact, fewer leukocytes are detected in the colon of CC Ala mice than in colons of their WT littermates. Even though our experiments did not yield convincing differences between WT and EPI-X4^{-/-} mice with respect to colonic damage, we continue to favor roles of EPI-X4 at the intestinal interface and presume that we may have selected a less suitable model and propose to next test a more subtle chronic colitis model. By lowering the DSS concentration (i.e. 1% instead of 3%), recovery phases and repeated treatments over weeks, subtle changes can more easily be unmasked. A chronic model is generally considered more sensitive for delicate parameters [157]. Another recurring observation points at a systematic defect in CC Ala mice: low IL-10 levels in plasma, similar to what we also detected after sublethal irradiation. IL-10 is considered one of the most important anti-inflammatory cytokines that is produced by B- and T-lymphocytes, macrophages, monocytes, dendritic cells and mast cells [158]. It can differentially modulate the function of various subsets of immune cells, affecting both the innate and the adaptive immune systems by inhibiting pro-inflammatory mediator production while increasing the production of anti-inflammatory mediators [159]. Mice deficient in IL-10 spontaneously develop enterocolitis, and the very same has been observed for infants with homozygous mutations in the IL-10 receptor genes [160, 161]. An impact of those low IL-10 levels in plasma of CC Ala mice on the outcome of DSS-induced colitis is thus conceivable.

Inflammation intensity of the colon can not only be modulated by cellular responses, but also by the composition of the intestinal microbiome, or inversely the integrity of the intestine can affect the microbiota. Evidence for alterations of the gut microbiota in inflammatory bowel diseases exist (reciprocal causality should not be assumed), as already described in 1.2, based on the observation that IL-10 deficient mice do not develop enterocolitis when housed under germ-free conditions [162]. Today, gut microbes are postulated to be an essential trigger for inflammation in genetically predisposed individuals. But if the presence of harmful microbes leads to disease or a beginning disease favors the presence of those bacteria is not clear yet. Studies on inflammatory bowel disease unsurprisingly show grossly altered microbiota in patients, but do not consider their microbiome composition before the onset of the inflammation. Furthermore, alterations in gene expression of genes like toll-like receptors (TLR) and C-type lectin or

peptidoglycans, which function as sensors for microbiota, are often present in those patients. Evidence has been provided that not only the host gets affected by its microbiome, but also that the microbiome is subject to change that adapts to specific host conditions. The absence of TLR5 for example is associated with changes in microbiota composition of mice [163]. Additionally, the impact of nutrition is the most obvious influencing factor of microbiome composition [164], leading to various disease-preventing, but also potentially harmful bacterial accumulations. Wiles et al. were able to link defects in host gut motility to abundance of particular gut microbes that would have been outcompeted in healthy organisms [165]. Their study proves a direct impact of host genetics to the gut microbiome. However, not only mechanical issues are responsible for microbiome divergences, but also the abundance of proteins produced at the barrier. O-linked oligosaccharides that contribute by about 80% to the total molecular weight of intestinal mucus [166] serve as an energy source for microbiota. As glycosylation profiles differ between species, the composition of bacteria varies as well [167]. A prominent example is the expression of 2- α -L-fucosyltransferase 2 that has been shown to affect the colonic mucosa-associated gut-microbiota composition [168]. A nonsense-mutation in the gene inactivates the enzyme and leads to a non-secretor phenotype that has been associated with Crohn's disease [169]. We figured that, if EPI-X4 plays a role in mucosal barrier integrity, then its absence could be reflected in disturbed integrity which might subsequently alter the microbiota, as was shown for a variety of inflammatory conditions [170]. We therefore examined microbiome composition of Ala-EPI-X4 mice by analysis of feces with respect to food intake and housing conditions and indeed, we found an alteration. The complete absence of the taxon *Parasutterella* in male CC Ala mice was the only difference detectable in Ala variants compared to WT littermates. *Parasutterella* are succinate-producing betaproteobacteria that are a natural, albeit low-abundance taxon in mouse feces. In humans, an effect on penetration with respect to proteobacteria is described: Penetrable mucus layers inhabit higher concentrations of proteobacteria than impenetrable ones [171]. HR Ala mice could thus be less susceptible for bacterial penetrations through the colon than their WT littermates. However, only about 1% of total bacteria belong to proteobacteria, and *Parasutterella* make less than 1% of the total amount, which points at a small impact of *Parasutterella* on the microbiome. Undetectable benefits in health, albeit not experimentally challenged, support the subtle impact of a possibly missing species in microbiome. Interestingly, the absence of *Parasutterella* was only discovered in male mice but not in females and overall microbiome composition was highly dependent on gender. Even though statistically significant, we propose not to over-interpret the absence of *Parasutterella* as indicative of some larger intestinal abnormality since this observation was strictly restricted to male CC Ala mice but not to female littermates nor EPI-X4-Ala mice of the

other strain. However, we see the observation as supporting our overarching hypothesis of EPI-X4 as a guardian of the sensitive equilibrium between inflammation and inertia at the mucosal interface. Larger numbers of analyses from independent sampling time points will be required to make more definitive and specific claims; a cohort of five mice might not be sufficient to state a systematic absence of the latter. Evidence has been provided that Parasutterella happen to be absent by chance in mice that were even housed together [172] so that upscaling cohort numbers must be considered. Additionally, differences between genders would have to be carefully examined.

5. Conclusion

In the course of this study, we assessed the role of the newly discovered highly specific CXCR4-antagonist EPI-X4. Two different knockout mouse models were used at this intention. We could show that steady-state hematopoiesis is barely affected by EPI-X4, the only effect detectable with our methods are lowered T cell counts. Involved in this observation are moderate modifications in cytokine levels in inflammation settings. Mucosal challenges show promising results, needing further, milder study models to detect for subtle effects of EPI-X4.

Literature

1. Bachelierie, F., et al., *International Union of Basic and Clinical Pharmacology. [corrected]. LXXXIX. Update on the extended family of chemokine receptors and introducing a new nomenclature for atypical chemokine receptors.* Pharmacol Rev, 2014. **66**(1): p. 1-79.
2. Zlotnik, A., O. Yoshie, and H. Nomiyama, *The chemokine and chemokine receptor superfamilies and their molecular evolution.* Genome Biol, 2006. **7**(12): p. 243.
3. Deng, H., et al., *Identification of a major co-receptor for primary isolates of HIV-1.* Nature, 1996. **381**(6584): p. 661-6.
4. Ma, Q., et al., *Impaired B-lymphopoiesis, myelopoiesis, and derailed cerebellar neuron migration in CXCR4- and SDF-1-deficient mice.* Proc Natl Acad Sci U S A, 1998. **95**(16): p. 9448-53.
5. Tachibana, K., et al., *The chemokine receptor CXCR4 is essential for vascularization of the gastrointestinal tract.* Nature, 1998. **393**(6685): p. 591-4.
6. Papayannopoulou, T., et al., *The role of G-protein signaling in hematopoietic stem/progenitor cell mobilization.* Blood, 2003. **101**(12): p. 4739-47.
7. Peled, A., et al., *Dependence of human stem cell engraftment and repopulation of NOD/SCID mice on CXCR4.* Science, 1999. **283**(5403): p. 845-8.
8. Bleul, C.C., et al., *The lymphocyte chemoattractant SDF-1 is a ligand for LESTR/fusin and blocks HIV-1 entry.* Nature, 1996. **382**(6594): p. 829-33.
9. Nagasawa, T., et al., *Molecular cloning and characterization of a murine pre-B-cell growth-stimulating factor/stromal cell-derived factor 1 receptor, a murine homolog of the human immunodeficiency virus 1 entry coreceptor fusin.* Proc Natl Acad Sci U S A, 1996. **93**(25): p. 14726-9.
10. Saini, V., A. Marchese, and M. Majetschak, *CXC chemokine receptor 4 is a cell surface receptor for extracellular ubiquitin.* J Biol Chem, 2010. **285**(20): p. 15566-76.
11. Schiraldi, M., et al., *HMGB1 promotes recruitment of inflammatory cells to damaged tissues by forming a complex with CXCL12 and signaling via CXCR4.* J Exp Med, 2012. **209**(3): p. 551-63.
12. Busillo, J.M. and J.L. Benovic, *Regulation of CXCR4 signaling.* Biochim Biophys Acta, 2007. **1768**(4): p. 952-63.
13. Foudi, A., et al., *Reduced retention of radioprotective hematopoietic cells within the bone marrow microenvironment in CXCR4-/- chimeric mice.* Blood, 2006. **107**(6): p. 2243-51.

14. Sugiyama, T., et al., *Maintenance of the hematopoietic stem cell pool by CXCL12-CXCR4 chemokine signaling in bone marrow stromal cell niches*. *Immunity*, 2006. **25**(6): p. 977-88.
15. Guo, Y., et al., *SDF-1/CXCL12 enhances survival and chemotaxis of murine embryonic stem cells and production of primitive and definitive hematopoietic progenitor cells*. *Stem Cells*, 2005. **23**(9): p. 1324-32.
16. Issaad, C., et al., *A murine stromal cell line allows the proliferation of very primitive human CD34⁺⁺/CD38⁻ progenitor cells in long-term cultures and semisolid assays*. *Blood*, 1993. **81**(11): p. 2916-24.
17. Liu, Q., et al., *CXCR4 antagonist AMD3100 redistributes leukocytes from primary immune organs to secondary immune organs, lung, and blood in mice*. *Eur J Immunol*, 2015. **45**(6): p. 1855-67.
18. Patterson, A.M. and L.M. Pelus, *G-CSF in stem cell mobilization: new insights, new questions*. *Ann Blood*, 2017. **2**.
19. To, L.B., et al., *The biology and clinical uses of blood stem cells*. *Blood*, 1997. **89**(7): p. 2233-58.
20. Flomenberg, N., et al., *The use of AMD3100 plus G-CSF for autologous hematopoietic progenitor cell mobilization is superior to G-CSF alone*. *Blood*, 2005. **106**(5): p. 1867-74.
21. Winkler, I.G., et al., *Hematopoietic stem cell mobilizing agents G-CSF, cyclophosphamide or AMD3100 have distinct mechanisms of action on bone marrow HSC niches and bone formation*. *Leukemia*, 2012. **26**(7): p. 1594-601.
22. Petit, I., et al., *G-CSF induces stem cell mobilization by decreasing bone marrow SDF-1 and up-regulating CXCR4*. *Nat Immunol*, 2002. **3**(7): p. 687-94.
23. Nervi, B., D.C. Link, and J.F. DiPersio, *Cytokines and hematopoietic stem cell mobilization*. *J Cell Biochem*, 2006. **99**(3): p. 690-705.
24. Winkler, I.G. and J.P. Levesque, *Mechanisms of hematopoietic stem cell mobilization: when innate immunity assails the cells that make blood and bone*. *Exp Hematol*, 2006. **34**(8): p. 996-1009.
25. Eash, K.J., et al., *CXCR4 is a key regulator of neutrophil release from the bone marrow under basal and stress granulopoiesis conditions*. *Blood*, 2009. **113**(19): p. 4711-9.
26. Christopher, M.J. and D.C. Link, *Regulation of neutrophil homeostasis*. *Curr Opin Hematol*, 2007. **14**(1): p. 3-8.
27. Nagasawa, T., et al., *Defects of B-cell lymphopoiesis and bone-marrow myelopoiesis in mice lacking the CXC chemokine PBSF/SDF-1*. *Nature*, 1996. **382**(6592): p. 635-8.

28. Gorlin, R.J., et al., *WHIM syndrome, an autosomal dominant disorder: clinical, hematological, and molecular studies*. Am J Med Genet, 2000. **91**(5): p. 368-76.
29. Diaz, G.A. and A.V. Gulino, *WHIM syndrome: a defect in CXCR4 signaling*. Curr Allergy Asthma Rep, 2005. **5**(5): p. 350-5.
30. Nagasawa, T., H. Kikutani, and T. Kishimoto, *Molecular cloning and structure of a pre-B-cell growth-stimulating factor*. Proc Natl Acad Sci U S A, 1994. **91**(6): p. 2305-9.
31. Ma, Q., D. Jones, and T.A. Springer, *The chemokine receptor CXCR4 is required for the retention of B lineage and granulocytic precursors within the bone marrow microenvironment*. Immunity, 1999. **10**(4): p. 463-71.
32. Beaussant Cohen, S., et al., *Description and outcome of a cohort of 8 patients with WHIM syndrome from the French Severe Chronic Neutropenia Registry*. Orphanet J Rare Dis, 2012. **7**: p. 71.
33. Plotkin, J., et al., *Critical role for CXCR4 signaling in progenitor localization and T cell differentiation in the postnatal thymus*. J Immunol, 2003. **171**(9): p. 4521-7.
34. Lucas, B., et al., *Progressive Changes in CXCR4 Expression That Define Thymocyte Positive Selection Are Dispensable For Both Innate and Conventional alphabetaT-cell Development*. Sci Rep, 2017. **7**(1): p. 5068.
35. Schabath, R., et al., *The murine chemokine receptor CXCR4 is tightly regulated during T cell development and activation*. J Leukoc Biol, 1999. **66**(6): p. 996-1004.
36. Bai, L., et al., *Upregulation of Chemokine CXCL12 in the Dorsal Root Ganglia and Spinal Cord Contributes to the Development and Maintenance of Neuropathic Pain Following Spared Nerve Injury in Rats*. Neurosci Bull, 2016. **32**(1): p. 27-40.
37. Gomperts, B.N., et al., *Circulating progenitor epithelial cells traffic via CXCR4/CXCL12 in response to airway injury*. J Immunol, 2006. **176**(3): p. 1916-27.
38. Zirafi, O., P.C. Hermann, and J. Munch, *Proteolytic processing of human serum albumin generates EPI-X4, an endogenous antagonist of CXCR4*. J Leukoc Biol, 2016. **99**(6): p. 863-8.
39. Ghuman, J., et al., *Structural basis of the drug-binding specificity of human serum albumin*. J Mol Biol, 2005. **353**(1): p. 38-52.
40. Fanali, G., et al., *Human serum albumin: from bench to bedside*. Mol Aspects Med, 2012. **33**(3): p. 209-90.
41. Tamamura, H., et al., *Pharmacophore identification of a chemokine receptor (CXCR4) antagonist, T22 ([Tyr(5,12),Lys7]-polyphemusin II), which specifically blocks T cell-line-tropic HIV-1 infection*. Bioorg Med Chem, 1998. **6**(7): p. 1033-41.

42. Majorek, K.A., et al., *Structural and immunologic characterization of bovine, horse, and rabbit serum albumins*. Mol Immunol, 2012. **52**(3-4): p. 174-82.
43. Vicenzi, E., P. Lio, and G. Poli, *The puzzling role of CXCR4 in human immunodeficiency virus infection*. Theranostics, 2013. **3**(1): p. 18-25.
44. Alkhatib, G., *The biology of CCR5 and CXCR4*. Curr Opin HIV AIDS, 2009. **4**(2): p. 96-103.
45. Flint, H.J., *The impact of nutrition on the human microbiome*. Nutr Rev, 2012. **70 Suppl 1**: p. S10-3.
46. Cani, P.D., *Human gut microbiome: hopes, threats and promises*. Gut, 2018. **67**(9): p. 1716-1725.
47. Cani, P.D., et al., *Metabolic endotoxemia initiates obesity and insulin resistance*. Diabetes, 2007. **56**(7): p. 1761-72.
48. Vich Vila, A., et al., *Gut microbiota composition and functional changes in inflammatory bowel disease and irritable bowel syndrome*. Sci Transl Med, 2018. **10**(472).
49. Strober, W., *Impact of the gut microbiome on mucosal inflammation*. Trends Immunol, 2013. **34**(9): p. 423-30.
50. Konig, J., et al., *Human Intestinal Barrier Function in Health and Disease*. Clin Transl Gastroenterol, 2016. **7**(10): p. e196.
51. McKenzie, C., et al., *The nutrition-gut microbiome-physiology axis and allergic diseases*. Immunol Rev, 2017. **278**(1): p. 277-295.
52. Perlman, R.L., *Mouse models of human disease: An evolutionary perspective*. Evol Med Public Health, 2016. **2016**(1): p. 170-6.
53. Yoshiki, A. and K. Moriwaki, *Mouse phenome research: implications of genetic background*. ILAR J, 2006. **47**(2): p. 94-102.
54. Heyer, W.D., *Biochemistry of eukaryotic homologous recombination*. Top Curr Genet, 2007. **17**: p. 95-133.
55. Fung-Leung, W.P. and T.W. Mak, *Embryonic stem cells and homologous recombination*. Curr Opin Immunol, 1992. **4**(2): p. 189-94.
56. Garneau, J.E., et al., *The CRISPR/Cas bacterial immune system cleaves bacteriophage and plasmid DNA*. Nature, 2010. **468**(7320): p. 67-71.
57. Cong, L., et al., *Multiplex genome engineering using CRISPR/Cas systems*. Science, 2013. **339**(6121): p. 819-23.
58. Babinet, C. and M. Cohen-Tannoudji, *Genome engineering via homologous recombination in mouse embryonic stem (ES) cells: an amazingly versatile tool for the study of mammalian biology*. An Acad Bras Cienc, 2001. **73**(3): p. 365-83.

59. Kunkel, T.A., *Rapid and efficient site-specific mutagenesis without phenotypic selection*. Proc Natl Acad Sci U S A, 1985. **82**(2): p. 488-92.
60. Limaye, A., B. Hall, and A.B. Kulkarni, *Manipulation of mouse embryonic stem cells for knockout mouse production*. Curr Protoc Cell Biol, 2009. **Chapter 19**: p. Unit 19 13 19 13 1-24.
61. Bouabe, H., M. Moser, and J. Heesemann, *Enhanced selection for homologous-recombinant embryonic stem cell clones by Cre recombinase-mediated deletion of the positive selection marker*. Transgenic Res, 2012. **21**(1): p. 227-9.
62. Harms, D.W., et al., *Mouse Genome Editing Using the CRISPR/Cas System*. Curr Protoc Hum Genet, 2014. **83**: p. 15 7 1-27.
63. Sanger, F., S. Nicklen, and A.R. Coulson, *DNA sequencing with chain-terminating inhibitors*. Proc Natl Acad Sci U S A, 1977. **74**(12): p. 5463-7.
64. Markel, P., et al., *Theoretical and empirical issues for marker-assisted breeding of congenic mouse strains*. Nat Genet, 1997. **17**(3): p. 280-4.
65. Danner, E., et al., *Modest and non-essential roles of the endocannabinoid system in immature hematopoiesis of mice*. Exp Hematol, 2019.
66. Shyamala, V. and G. Ferro-Luzzi Ames, *Single Specific Primer-Polymerase Chain Reaction (SSP-PCR) and Genome Walking*. Methods Mol Biol, 1993. **15**: p. 339-48.
67. Karpova, D., et al., *Targeting VLA4 integrin and CXCR2 mobilizes serially repopulating hematopoietic stem cells*. J Clin Invest, 2019. **129**(7): p. 2745-2759.
68. Karpova, D., et al., *The novel CXCR4 antagonist POL5551 mobilizes hematopoietic stem and progenitor cells with greater efficiency than Plerixafor*. Leukemia, 2013. **27**(12): p. 2322-31.
69. Yu, V.W.C., et al., *Epigenetic Memory Underlies Cell-Autonomous Heterogeneous Behavior of Hematopoietic Stem Cells*. Cell, 2016. **167**(5): p. 1310-1322 e17.
70. Kojima, E. and A. Tsuboi, *Effects of 5-fluorouracil on hematopoietic stem cells in normal and irradiated mice*. J Radiat Res, 1992. **33**(3): p. 218-26.
71. Chernyshev, A.V., et al., *Erythrocyte lysis in isotonic solution of ammonium chloride: theoretical modeling and experimental verification*. J Theor Biol, 2008. **251**(1): p. 93-107.
72. Bonig, H., et al., *PTX-sensitive signals in bone marrow homing of fetal and adult hematopoietic progenitor cells*. Blood, 2004. **104**(8): p. 2299-306.
73. Ray, A. and B.N. Dittel, *Isolation of mouse peritoneal cavity cells*. J Vis Exp, 2010(35).
74. Chassaing, B., et al., *Dextran sulfate sodium (DSS)-induced colitis in mice*. Curr Protoc Immunol, 2014. **104**: p. Unit 15 25.
75. Fox, C.H., et al., *Formaldehyde fixation*. J Histochem Cytochem, 1985. **33**(8): p. 845-53.

76. Yoo, J., et al., *Systemic sensitization with the protein allergen ovalbumin augments local sensitization in atopic dermatitis*. J Inflamm Res, 2014. **7**: p. 29-38.
77. Batard, P., et al., *Dextramers: new generation of fluorescent MHC class I/peptide multimers for visualization of antigen-specific CD8+ T cells*. J Immunol Methods, 2006. **310**(1-2): p. 136-48.
78. Randall, T.D. and I.L. Weissman, *Phenotypic and functional changes induced at the clonal level in hematopoietic stem cells after 5-fluorouracil treatment*. Blood, 1997. **89**(10): p. 3596-606.
79. Chen, X. and J.J. Oppenheim, *Resolving the identity myth: key markers of functional CD4+FoxP3+ regulatory T cells*. Int Immunopharmacol, 2011. **11**(10): p. 1489-96.
80. Sambrook, J., E.F. Fritsch, and T. Maniatis, *Molecular cloning a laboratory manual*. 2nd ed ed. 1989: Cold Spring Harbor, N.Y Cold Spring Harbor Laboratory.
81. Fischer, A.H., et al., *Hematoxylin and eosin staining of tissue and cell sections*. CSH Protoc, 2008. **2008**: p. pdb prot4986.
82. Adams, G.G. and P.N. Dilly, *Differential staining of ocular goblet cells*. Eye (Lond), 1989. **3 (Pt 6)**: p. 840-4.
83. Dieleman, L.A., et al., *Chronic experimental colitis induced by dextran sulphate sodium (DSS) is characterized by Th1 and Th2 cytokines*. Clin Exp Immunol, 1998. **114**(3): p. 385-91.
84. Shin, J., et al., *Analysis of the mouse gut microbiome using full-length 16S rRNA amplicon sequencing*. Sci Rep, 2016. **6**: p. 29681.
85. Callahan, B.J., et al., *DADA2: High-resolution sample inference from Illumina amplicon data*. Nat Methods, 2016. **13**(7): p. 581-3.
86. Katoh, K. and D.M. Standley, *MAFFT multiple sequence alignment software version 7: improvements in performance and usability*. Mol Biol Evol, 2013. **30**(4): p. 772-80.
87. Price, M.N., P.S. Dehal, and A.P. Arkin, *FastTree 2--approximately maximum-likelihood trees for large alignments*. PLoS One, 2010. **5**(3): p. e9490.
88. Quast, C., et al., *The SILVA ribosomal RNA gene database project: improved data processing and web-based tools*. Nucleic Acids Res, 2013. **41**(Database issue): p. D590-6.
89. Lozupone, C., et al., *UniFrac: an effective distance metric for microbial community comparison*. ISME J, 2011. **5**(2): p. 169-72.
90. Hernandez-Lopez, C., et al., *Stromal cell-derived factor 1/CXCR4 signaling is critical for early human T-cell development*. Blood, 2002. **99**(2): p. 546-54.

91. Dinkel, B.A., et al., *GRK2 mediates TCR-induced transactivation of CXCR4 and TCR-CXCR4 complex formation that drives PI3Kgamma/PREX1 signaling and T cell cytokine secretion*. J Biol Chem, 2018. **293**(36): p. 14022-14039.
92. Gerlach, L.O., et al., *Molecular interactions of cyclam and bicyclam non-peptide antagonists with the CXCR4 chemokine receptor*. J Biol Chem, 2001. **276**(17): p. 14153-60.
93. Broxmeyer, H.E., et al., *Rapid mobilization of murine and human hematopoietic stem and progenitor cells with AMD3100, a CXCR4 antagonist*. J Exp Med, 2005. **201**(8): p. 1307-18.
94. Mueller, M.M., et al., *Safety and efficacy of healthy volunteer stem cell mobilization with filgrastim G-CSF and mobilized stem cell apheresis: results of a prospective longitudinal 5-year follow-up study*. Vox Sang, 2013. **104**(1): p. 46-54.
95. Bonig, H., et al., *Biosimilar granulocyte-colony-stimulating factor for healthy donor stem cell mobilization: need we be afraid?* Transfusion, 2015. **55**(2): p. 430-9.
96. Bonig, H. and T. Papayannopoulou, *Hematopoietic stem cell mobilization: updated conceptual renditions*. Leukemia, 2013. **27**(1): p. 24-31.
97. Molineux, G., Z. Pojda, and T.M. Dexter, *A comparison of hematopoiesis in normal and splenectomized mice treated with granulocyte colony-stimulating factor*. Blood, 1990. **75**(3): p. 563-9.
98. Abadir, E., et al., *Targeting the niche: depleting haemopoietic stem cells with targeted therapy*. Bone Marrow Transplant, 2019. **54**(7): p. 961-968.
99. Bonig, H., G.V. Priestley, and T. Papayannopoulou, *Hierarchy of molecular-pathway usage in bone marrow homing and its shift by cytokines*. Blood, 2006. **107**(1): p. 79-86.
100. Karpova, D. and H. Bonig, *Concise Review: CXCR4/CXCL12 Signaling in Immature Hematopoiesis--Lessons From Pharmacological and Genetic Models*. Stem Cells, 2015. **33**(8): p. 2391-9.
101. Billings, P.C., A.L. Romero-Weaver, and A.R. Kennedy, *Effect of Gender on the Radiation Sensitivity of Murine Blood Cells*. Gravit Space Res, 2014. **2**(1): p. 25-31.
102. Hermida, M.D.R., et al., *Selecting the right gate to identify relevant cells for your assay: a study of thioglycollate-elicited peritoneal exudate cells in mice*. BMC Res Notes, 2017. **10**(1): p. 695.
103. Dieterich, W., M. Schink, and Y. Zopf, *Microbiota in the Gastrointestinal Tract*. Med Sci (Basel), 2018. **6**(4).
104. Feng, Y., et al., *HIV-1 entry cofactor: functional cDNA cloning of a seven-transmembrane, G protein-coupled receptor*. Science, 1996. **272**(5263): p. 872-7.

105. Mekada, K., et al., *Genetic differences among C57BL/6 substrains*. Exp Anim, 2009. **58**(2): p. 141-9.
106. Ward, A.C., et al., *Regulation of granulopoiesis by transcription factors and cytokine signals*. Leukemia, 2000. **14**(6): p. 973-90.
107. Okuda, K., R. Foster, and J.D. Griffin, *Signaling domains of the beta c chain of the GM-CSF/IL-3/IL-5 receptor*. Ann N Y Acad Sci, 1999. **872**: p. 305-12; discussion 312-3.
108. Lim, H.W., H.E. Broxmeyer, and C.H. Kim, *Regulation of trafficking receptor expression in human forkhead box P3+ regulatory T cells*. J Immunol, 2006. **177**(2): p. 840-51.
109. Zou, L., et al., *Bone marrow is a reservoir for CD4+CD25+ regulatory T cells that traffic through CXCL12/CXCR4 signals*. Cancer Res, 2004. **64**(22): p. 8451-5.
110. Lapidot, T. and O. Kollet, *The essential roles of the chemokine SDF-1 and its receptor CXCR4 in human stem cell homing and repopulation of transplanted immune-deficient NOD/SCID and NOD/SCID/B2m(null) mice*. Leukemia, 2002. **16**(10): p. 1992-2003.
111. Kawabata, K., et al., *A cell-autonomous requirement for CXCR4 in long-term lymphoid and myeloid reconstitution*. Proc Natl Acad Sci U S A, 1999. **96**(10): p. 5663-7.
112. Lazarini, F., et al., *Role of the alpha-chemokine stromal cell-derived factor (SDF-1) in the developing and mature central nervous system*. Glia, 2003. **42**(2): p. 139-48.
113. Zou, Y.R., et al., *Function of the chemokine receptor CXCR4 in haematopoiesis and in cerebellar development*. Nature, 1998. **393**(6685): p. 595-9.
114. Ding, L. and S.J. Morrison, *Haematopoietic stem cells and early lymphoid progenitors occupy distinct bone marrow niches*. Nature, 2013. **495**(7440): p. 231-5.
115. Greenbaum, A., et al., *CXCL12 in early mesenchymal progenitors is required for haematopoietic stem-cell maintenance*. Nature, 2013. **495**(7440): p. 227-30.
116. Wright, D.E., et al., *Hematopoietic stem cells are uniquely selective in their migratory response to chemokines*. J Exp Med, 2002. **195**(9): p. 1145-54.
117. Levesque, J.P., et al., *Hematopoietic progenitor cell mobilization results in hypoxia with increased hypoxia-inducible transcription factor-1 alpha and vascular endothelial growth factor A in bone marrow*. Stem Cells, 2007. **25**(8): p. 1954-65.
118. Bonig, H. and T. Papayannopoulou, *Mobilization of hematopoietic stem/progenitor cells: general principles and molecular mechanisms*. Methods Mol Biol, 2012. **904**: p. 1-14.
119. Heissig, B., et al., *Recruitment of stem and progenitor cells from the bone marrow niche requires MMP-9 mediated release of kit-ligand*. Cell, 2002. **109**(5): p. 625-37.
120. Levesque, J.P., et al., *Characterization of hematopoietic progenitor mobilization in protease-deficient mice*. Blood, 2004. **104**(1): p. 65-72.

121. Liu, F., J. Poursine-Laurent, and D.C. Link, *Expression of the G-CSF receptor on hematopoietic progenitor cells is not required for their mobilization by G-CSF*. *Blood*, 2000. **95**(10): p. 3025-31.
122. Christopher, M.J., et al., *Expression of the G-CSF receptor in monocytic cells is sufficient to mediate hematopoietic progenitor mobilization by G-CSF in mice*. *J Exp Med*, 2011. **208**(2): p. 251-60.
123. Greenbaum, A.M. and D.C. Link, *Mechanisms of G-CSF-mediated hematopoietic stem and progenitor mobilization*. *Leukemia*, 2011. **25**(2): p. 211-7.
124. Kim, H.K., et al., *G-CSF down-regulation of CXCR4 expression identified as a mechanism for mobilization of myeloid cells*. *Blood*, 2006. **108**(3): p. 812-20.
125. Green, D.E. and C.T. Rubin, *Consequences of irradiation on bone and marrow phenotypes, and its relation to disruption of hematopoietic precursors*. *Bone*, 2014. **63**: p. 87-94.
126. Jiang, Y., et al., *On the adaptation of endosteal stem cell niche function in response to stress*. *Blood*, 2009. **114**(18): p. 3773-82.
127. Trigg, M.E., *Hematopoietic stem cells*. *Pediatrics*, 2004. **113**(4 Suppl): p. 1051-7.
128. Mauch, P., et al., *Hematopoietic stem cell compartment: acute and late effects of radiation therapy and chemotherapy*. *Int J Radiat Oncol Biol Phys*, 1995. **31**(5): p. 1319-39.
129. Lo Celso, C., et al., *Live-animal tracking of individual haematopoietic stem/progenitor cells in their niche*. *Nature*, 2009. **457**(7225): p. 92-6.
130. Garrett, R.W. and S.G. Emerson, *Bone and blood vessels: the hard and the soft of hematopoietic stem cell niches*. *Cell Stem Cell*, 2009. **4**(6): p. 503-6.
131. Cao, X., et al., *Irradiation induces bone injury by damaging bone marrow microenvironment for stem cells*. *Proc Natl Acad Sci U S A*, 2011. **108**(4): p. 1609-14.
132. Tokoyoda, K., et al., *Cellular niches controlling B lymphocyte behavior within bone marrow during development*. *Immunity*, 2004. **20**(6): p. 707-18.
133. Couper, K.N., D.G. Blount, and E.M. Riley, *IL-10: the master regulator of immunity to infection*. *J Immunol*, 2008. **180**(9): p. 5771-7.
134. Opp, M.R., E.M. Smith, and T.K. Hughes, Jr., *Interleukin-10 (cytokine synthesis inhibitory factor) acts in the central nervous system of rats to reduce sleep*. *J Neuroimmunol*, 1995. **60**(1-2): p. 165-8.
135. Varma, T.K., et al., *Cellular mechanisms that cause suppressed gamma interferon secretion in endotoxin-tolerant mice*. *Infect Immun*, 2001. **69**(9): p. 5249-63.

136. Kallman, R.F. and H.I. Kohn, *The influence of strain on acute x-ray lethality in the mouse. I. LD50 and death rate studies*. Radiat Res, 1956. **5**(4): p. 309-17.
137. Nie, Y., Y.C. Han, and Y.R. Zou, *CXCR4 is required for the quiescence of primitive hematopoietic cells*. J Exp Med, 2008. **205**(4): p. 777-83.
138. Badolato, R., J. Donadieu, and W.R. Group, *How I treat warts, hypogammaglobulinemia, infections, and myelokathexis syndrome*. Blood, 2017. **130**(23): p. 2491-2498.
139. Kawai, T., et al., *Enhanced function with decreased internalization of carboxy-terminus truncated CXCR4 responsible for WHIM syndrome*. Exp Hematol, 2005. **33**(4): p. 460-8.
140. Campbell, J.J., J. Pan, and E.C. Butcher, *Cutting edge: developmental switches in chemokine responses during T cell maturation*. J Immunol, 1999. **163**(5): p. 2353-7.
141. Ara, T., et al., *A role of CXC chemokine ligand 12/stromal cell-derived factor-1/pre-B cell growth stimulating factor and its receptor CXCR4 in fetal and adult T cell development in vivo*. J Immunol, 2003. **170**(9): p. 4649-55.
142. Onai, N., et al., *Impairment of lymphopoiesis and myelopoiesis in mice reconstituted with bone marrow-hematopoietic progenitor cells expressing SDF-1-intrakine*. Blood, 2000. **96**(6): p. 2074-80.
143. Hori, S., T. Nomura, and S. Sakaguchi, *Control of regulatory T cell development by the transcription factor Foxp3*. Science, 2003. **299**(5609): p. 1057-61.
144. Fontenot, J.D., et al., *Regulatory T cell lineage specification by the forkhead transcription factor foxp3*. Immunity, 2005. **22**(3): p. 329-41.
145. Sakaguchi, S., et al., *Immunologic self-tolerance maintained by activated T cells expressing IL-2 receptor alpha-chains (CD25). Breakdown of a single mechanism of self-tolerance causes various autoimmune diseases*. J Immunol, 1995. **155**(3): p. 1151-64.
146. Battaglia, M., et al., *Tr1 cells: from discovery to their clinical application*. Semin Immunol, 2006. **18**(2): p. 120-7.
147. Vojdani, A. and J. Erde, *Regulatory T cells, a potent immunoregulatory target for CAM researchers: modulating tumor immunity, autoimmunity and allereactive immunity (III)*. Evid Based Complement Alternat Med, 2006. **3**(3): p. 309-16.
148. Netea, M.G., et al., *A guiding map for inflammation*. Nat Immunol, 2017. **18**(8): p. 826-831.
149. Yamada, M., et al., *The increase in surface CXCR4 expression on lung extravascular neutrophils and its effects on neutrophils during endotoxin-induced lung injury*. Cell Mol Immunol, 2011. **8**(4): p. 305-14.

150. Hummel, S., H. Van Aken, and A. Zarbock, *Inhibitors of CXC chemokine receptor type 4: putative therapeutic approaches in inflammatory diseases*. *Curr Opin Hematol*, 2014. **21**(1): p. 29-36.
151. Bonecchi, R., et al., *Chemokines and chemokine receptors: an overview*. *Front Biosci (Landmark Ed)*, 2009. **14**: p. 540-51.
152. Oo, Y.H., S. Shetty, and D.H. Adams, *The role of chemokines in the recruitment of lymphocytes to the liver*. *Dig Dis*, 2010. **28**(1): p. 31-44.
153. Shattuck, E.C. and M.P. Muehlenbein, *Human sickness behavior: Ultimate and proximate explanations*. *Am J Phys Anthropol*, 2015. **157**(1): p. 1-18.
154. Summers, C., et al., *Neutrophil kinetics in health and disease*. *Trends Immunol*, 2010. **31**(8): p. 318-24.
155. Gijsbers, K., K. Geboes, and J. Van Damme, *Chemokines in gastrointestinal disorders*. *Curr Drug Targets*, 2006. **7**(1): p. 47-64.
156. Mikami, S., et al., *Blockade of CXCL12/CXCR4 axis ameliorates murine experimental colitis*. *J Pharmacol Exp Ther*, 2008. **327**(2): p. 383-92.
157. Wirtz, S., et al., *Chemically induced mouse models of acute and chronic intestinal inflammation*. *Nat Protoc*, 2017. **12**(7): p. 1295-1309.
158. Mosmann, T.R., *Properties and functions of interleukin-10*. *Adv Immunol*, 1994. **56**: p. 1-26.
159. de Moreno de Leblanc, A., et al., *Importance of IL-10 modulation by probiotic microorganisms in gastrointestinal inflammatory diseases*. *ISRN Gastroenterol*, 2011. **2011**: p. 892971.
160. Glocker, E.O., et al., *Inflammatory bowel disease and mutations affecting the interleukin-10 receptor*. *N Engl J Med*, 2009. **361**(21): p. 2033-45.
161. Kuhn, R., et al., *Interleukin-10-deficient mice develop chronic enterocolitis*. *Cell*, 1993. **75**(2): p. 263-74.
162. Sellon, R.K., et al., *Resident enteric bacteria are necessary for development of spontaneous colitis and immune system activation in interleukin-10-deficient mice*. *Infect Immun*, 1998. **66**(11): p. 5224-31.
163. Vijay-Kumar, M., et al., *Metabolic syndrome and altered gut microbiota in mice lacking Toll-like receptor 5*. *Science*, 2010. **328**(5975): p. 228-31.
164. Chassaing, B., et al., *Dietary emulsifiers directly alter human microbiota composition and gene expression ex vivo potentiating intestinal inflammation*. *Gut*, 2017. **66**(8): p. 1414-1427.

165. Wiles, T.J., et al., *Host Gut Motility Promotes Competitive Exclusion within a Model Intestinal Microbiota*. PLoS Biol, 2016. **14**(7): p. e1002517.
166. Johansson, M.E., et al., *Composition and functional role of the mucus layers in the intestine*. Cell Mol Life Sci, 2011. **68**(22): p. 3635-41.
167. Marcobal, A., et al., *A metabolomic view of how the human gut microbiota impacts the host metabolome using humanized and gnotobiotic mice*. ISME J, 2013. **7**(10): p. 1933-43.
168. Rausch, P., et al., *Colonic mucosa-associated microbiota is influenced by an interaction of Crohn disease and FUT2 (Secretor) genotype*. Proc Natl Acad Sci U S A, 2011. **108**(47): p. 19030-5.
169. McGovern, D.P., et al., *Fucosyltransferase 2 (FUT2) non-secretor status is associated with Crohn's disease*. Hum Mol Genet, 2010. **19**(17): p. 3468-76.
170. Ferreira, C.M., et al., *The central role of the gut microbiota in chronic inflammatory diseases*. J Immunol Res, 2014. **2014**: p. 689492.
171. Jakobsson, H.E., et al., *The composition of the gut microbiota shapes the colon mucus barrier*. EMBO Rep, 2015. **16**(2): p. 164-77.
172. Ju, T., et al., *Defining the role of Parasutterella, a previously uncharacterized member of the core gut microbiota*. ISME J, 2019. **13**(6): p. 1520-1534.

Abbreviations

5-FU	Fluorouracil
7-AAD	7-aminoactinomycin D
APC	Allophycocyanin
BM	Bone marrow
BSA	Bovine serum albumin
CBC	Complete blood count
CC	CRISPR/Cas
CCR5	C-C chemokine receptor type 5
CD	Cluster of differentiation
CFU-C	Colony-forming unit cell
CRISPR	Clustered regularly interspaced short palindromic repeats
CXCL12	C-X-C motif chemokine 12
CXCR4	C-X-C chemokine receptor type 4
DAMP	Damage-associated molecular pattern
DMEM	Dulbecco's Modified Eagle Medium
DNA	Deoxyribonucleic acid
DSS	Dextran Sulfate Sodium Salt
EDTA	Ethylenediaminetetraacetic acid
ELISA	Enzyme-linked immunosorbent assay
EPI-X4	Endogenous peptide inhibitor of CXCR4
EPO	Erythropoietin
ES cell	Embryonic stem cell
EU	Endotoxin units
FACS	Fluorescence-activated cell sorting
FCS	Fetal calf serum
FITC	Fluorescein isothiocyanate
Foxp3	Forkhead box P3
G-CSF	Granulocyte-colony stimulating factor
G-CSFR	G-CSF receptor
GM-CSF	Granulocyte-macrophage colony-stimulating factor
GPCR	G-protein coupled receptor

HCT	Haematocrit
HIF-1	Hypoxia inducible factor-1
HiV	Human immunodeficiency virus
HMGB1	High mobility group box 1 protein
HR	Homologous recombination
HSPC	Hematopoietic stem and progenitor cells
i.p.	Intraperitoneal
i.v.	Intravenous
IFN	Interferon
IL	Interleukin
KO	Knock-out
lin	Lineage marker
LPS	Lipopolysaccharides
LSK	lin- sca-1+ c-kit+ cells
LSK-SLAM	lin- sca-1+ c-kit+ CD150+ CD 48- cells
MCP	Monocyte chemoattractant protein
MD2	Lymphocyte antigen 96
MFI	Mean fluorescence intensity
MHC	Major histocompatibility complex
NHEJ	Non-homologous end joining
OVA	Ovalbumin
PAM	Protospacer adjacent motif
PAMP	Pathogen-associated molecular pattern
PBS	Phosphate buffered saline
PCR	Polymerase chain reaction
PE	Phycoerythrin
RBC	Red blood cells
RNA	Ribonucleic acid
RPMI medium	Roswell Park Memorial Institute Medium
RT	Room temperature
SCF	Stem cell factor
SNP	Single nucleotide polymorphisms
SPF	Specific-pathogen-free

TAE	Tris, acetic acid, EDTA buffer
TCR	T cell receptor
TFA	Trifluoroacetic acid
TLR	Toll-like receptor
TNF	Tumor necrosis factor
Treg	Regulatory T cell
WBC	White blood cells
WHIM	Warts, Hypogammaglobulinemia, Infections, and Myelokathexis
WT	Wildtype

Table of Figures

Figure 1: Model of EPI-X4 and its binding to CXCR4 receptor.....	11
Figure 2: Sequence alignment of albumin proteins of the indicated species	13
Figure 3: Schematic representation of CRISPR/Cas induced genome editing	15
Figure 4: Sanger sequencing of Ala-mutants.....	21
Figure 5: Schematic representation of the SSP-PCR used for mouse genotyping	22
Figure 6: Genotyping of HR Ala and CC Ala mutant strains.....	23
Figure 7: Schematic representation of OVA immunization and challenge regimen	27
Figure 8: Relative amounts of mEPI-X4 peptides in acidified mouse plasma.....	32
Figure 9: Phenotypical analysis of progenitor cells in BM and spleen under steady-state conditions	33
Figure 10: Functional analysis of hematopoietic progenitor cells under steady-state conditions	34
Figure 11: Phenotypical analysis of mature hematopoietic cells under steady-state conditions.	35
Figure 12: Cell cycle analysis of hematopoietic cells in BM and spleen under steady-state conditions	36
Figure 13: Regulatory T cell counts in peripheral blood under steady-state conditions	37
Figure 14: Mobilization outcome after AMD3100 administration	38
Figure 15: Mature hematopoietic cell count after G-CSF induced mobilization	39
Figure 16: Functional analysis of hematopoietic progenitor cells after G-CSF-induced mobilization	40
Figure 17: Phenotypical analysis of immature hematopoietic cells after G-CSF-induced mobilization	41
Figure 18: Cell cycle analysis after G-CSF-induced mobilization	42
Figure 19: Engraftment analysis after transplantation regimen	43
Figure 20: Mature hematopoietic cell count after transplantation	44
Figure 21: Phenotypical and functional analysis of HSPC after transplantation	45
Figure 22: Cell cycle analysis after transplantation	46
Figure 23: Engraftment analysis after sublethal irradiation	47
Figure 24: Functional analysis of HSPC after sublethal irradiation.....	48
Figure 25: Inflammatory cytokine measurements after sublethal irradiation.....	49
Figure 26: Phenotypical analysis of immature hematopoietic cells after sublethal irradiation	50
Figure 27: Cell cycle analysis of HSPC after sublethal irradiation.....	51
Figure 28: Inflammatory cytokine measurements after peritonitis induction	53

Figure 29: Cell counts in peripheral blood and peritoneal lavage after induction of peritonitis....	54
Figure 30: Weight loss during acute colitis.....	55
Figure 31: Inflammatory cytokine measurements in an acute colitis setting	56
Figure 32: Mature hematopoietic cell count after DSS treatment	57
Figure 33: Functional analysis of HSPC after DSS treatment	57
Figure 34: Colon analysis after DSS treatment.....	58
Figure 35: Scoring results of colon damage.....	59
Figure 36: Abundance of Parasutterella in feces	60
Figure 37: Measurement of LPS-binding protein in HR Ala plasma	61
Figure 38: Detection of OVA-reactive CD8+ cells via flow cytometry	62
Figure 39: Analysis of OVA-specific reactions after immunization and subsequent oral challenge.....	62

Tables

Table 1: Antibodies used for flow cytometry stainings..... 17
Table 2: Histopathology scoring system for DSS-induced colitis model 30


Appendix

Danner, E., Bönig, H., Wiercinska, E. 2019: Albumin Modifies Responses to Hematopoietic Stem Cell Mobilizing Agents in Mice. *Cells*. 2019 Dec 18;9(1). pii: E4. doi: 10.3390/cells9010004

Danner, E., Hoffmann, F., Lee, S.-Y. *et al.* 2019: Modest and non-essential roles of the endocannabinoid system in immature hematopoiesis of mice. *Exp Hematol*. 2019 Sep 25. pii: S0301-472X(19)31020-3. doi: 10.1016/j.exphem.2019.09.022.

Article

Albumin Modifies Responses to Hematopoietic Stem Cell Mobilizing Agents in Mice

Eva Danner^{1,2}, Halvard Bonig^{1,3} and Eliza Wiercinska^{1,3,*} 

¹ German Red Cross Blood Donor Service Baden-Wuerttemberg-Hesse, 60528 Frankfurt, Germany; e.danner@blutspende.de (E.D.); h.boenig@blutspende.de (H.B.)

² Faculty of Biological Sciences, Goethe University, 60438 Frankfurt, Germany

³ Goethe University Medical School, Institute for Transfusion Medicine and Immunohematology, 60528 Frankfurt, Germany

* Correspondence: e.wiercinska@blutspende.de; Tel.: +49-69-6782-4922

Received: 19 November 2019; Accepted: 15 December 2019; Published: 18 December 2019



Abstract: Albumin, the most abundant plasma protein, not only controls osmotic blood pressure, but also serves as a carrier for various small molecules, including pharmaceuticals. Its impact on pharmacological properties of many drugs has been extensively studied over decades. Here, we focus on its interaction with the following mobilizing agents: Granulocyte-colony stimulating factor (G-CSF) and AMD3100, where such analyses are lacking. These compounds are widely used for hematopoietic stem cell mobilization of healthy donors or patients. Using albumin-deficient (Alb^{-/-}) mice, we studied the contribution of albumin to mobilization outcomes. Mobilization with the bicyclam CXCR4 antagonist AMD3100 was attenuated in Alb^{-/-} mice compared to wild-type littermates. By contrast, mobilization with recombinant human G-CSF (rhG-CSF), administered twice daily over a five-day course, was significantly increased in Alb^{-/-} mice. In terms of a mechanism, we show that rhG-CSF bioavailability in the bone marrow is significantly improved in Alb^{-/-} mice, compared to wild-type (WT) littermates, where rhG-CSF levels dramatically drop within a few hours of the injection. These observations likely explain the favorable mobilization outcomes with split-dose versus single-dose administration of rhG-CSF to healthy donors.

Keywords: hematopoietic stem cell mobilization; hematopoietic stem cell transplantation; granulocyte-colony stimulating factor; serum albumin deficiency; pharmacodynamics; AMD3100; Plerixafor

1. Introduction

Albumin is, by a wide margin, the most abundant plasma protein of all higher species, including man, typically at concentrations of 30–50 g/L. It not only controls colloid osmotic pressure [1–3] but also serves as a depot and a carrier for both endogenous small molecules and medicinal substances [4]. Its structure was described in the 1970s [5] and binding pockets were characterized shortly after [6]. Due to its high binding potential for a broad range of substances, serum albumin is an obvious frequent focus of pharmacokinetic studies [6–8]. Until recently, the lack of animal models for studying pharmaceutical properties of albumin-binding drugs restricted experiments to in vitro models, which, however, were inadequately predictive. In 2015, the group of Michael Wiles developed a mouse model that lacked endogenous albumin [9]. The model was intended to facilitate substitution of mice with human serum albumin, which increases albumin half-life, from 2.6 to 4.2 days, thus allowing for the study of drug binding to human albumin in mice. Albumin deficient (Alb^{-/-}) mice are viable and healthy; they compensate for the lack of serum albumin by increasing plasma levels of triglycerides, cholesterol, and aspartate aminotransferase. Nevertheless, the total serum protein level is still significantly lower than in wild-type mice and comparable to hypoalbuminemic patients [9,10].

Hematopoiesis is the continuous, life-long process of generating short-lived mature blood cells that originate from hematopoietic stem and progenitor cells (HSPC). The process of proliferation and cell differentiation is tightly controlled. Individual HSPC will undergo asymmetric cell divisions, whereby progenitors arise. Under the influence of their environment in the bone marrow (BM), they will give rise to increasingly more differentiated precursors and mature blood cells, which are ultimately released into the circulation [11]. The near-quantitative retention of HSPC in the BM is significantly, albeit not exclusively, controlled by the interaction of stroma-derived C-X-C motif chemokine ligand 12 (CXCL12), with C-X-C chemokine receptor type 4 (CXCR4), which is expressed on the surface of HSPC [12,13].

Our interest in HSPC is significantly driven by translational aspects. In particular, the enforced egress of HSPC, so called mobilization, for graft manufacturing, remains a focus of our studies. HSPC are routinely collected from the peripheral blood of healthy donors after a 5-day course of mobilization with recombinant human granulocyte-colony stimulating factor (rhG-CSF) [14,15]. As a small glycoprotein, rhG-CSF could potentially bind to albumin, and thus be either stabilized and transported through the blood stream, or functionally neutralized. The exact mechanism of action of G-CSF in the BM during mobilization is still not completely understood, but evidence was presented that, at first, HSPC are forced by G-CSF to proliferate [16–20]. Later on, a proteolytic milieu, possibly established by G-CSF-activated neutrophils, cleaves retention factors, allowing for HSPC egress [11,21]. Moreover, a plethora of other cellular G-CSF targets within the BM niche was suggested (osteoblasts [22], osteocytes [23], CXCL12-abundant reticular cells [24], nestin-positive mesenchymal stromal cells [25], or osteo-macs [26] to name a few). Thus, it is conceivable that the need for orchestrated activation of multiple niche components contributes to the rather slow kinetics of G-CSF mobilization. In contrast, AMD3100 can be used as a bolus injection to mobilize HSPC. It is a direct CXCR4 antagonist, disrupting the CXCR4–CXCL12 axis and activating proteases; thus, leading to a more rapid (within hours), albeit much less efficient mobilization than G-CSF [27]. AMD3100 is approved for use in combination with G-CSF in G-CSF refractory patients. Pharmacokinetic studies showed a half-life of 4–5 h for AMD3100 [28] and 4–22 h for G-CSF in human blood [29,30], but how these relate to the biological half-life is entirely unclear, as pharmacodynamics effects are, by comparison, much protracted. Development of rhG-CSF and AMD3100 preceding the Wiles' mouse, studies in the absence of albumin, were not previously performed.

Serum albumin plays a crucial role in the transport of small molecules and drugs through the blood stream, and as such is a potential carrier of both AMD3100 and rhG-CSF. As was shown, up to 58% of administered AMD3100 directly binds to plasma proteins [31] including albumin. A potential impact of albumin on rhG-CSF bioavailability was not previously studied. Albumin null mice gave us the opportunity to test for responsiveness of HSPC to mobilizing agents in the absence of albumin, and to test specificity of the observations by substituting albumin prior to mobilization. In the course of this study, we demonstrate a negative impact of human serum albumin on the tissue distribution of rhG-CSF. Inversely, analbuminemia strongly enhances the mobilization efficiency.

2. Materials and Methods

2.1. Mice

For all experiments, young adult mice (8–12 weeks, male or female) were used. C57BL/6J-Alb^{em8Mvw}/MvwJ (Alb^{-/-}) mice were described previously [9], albeit not with respect to their hematopoietic phenotype, and were purchased from Jackson Laboratory (JAX stock #025200, Sulzfeld, Germany). Albumin-competent wild-type (WT) littermates of the corresponding strain were used as controls. All experiments were performed in agreement with the German Animal Welfare Act and approved by the municipal government (F27/1004, Regierungspraesidium Darmstadt, Darmstadt, Germany).

2.2. Hematopoietic Cells

Peripheral blood was drawn from the facial vein into EDTA tubes using a 23G needle. Total cell counts were analyzed by Hemavet 950SF+ (Drew Scientific, Dallas, TX, USA). BM cells were harvested by aseptically flushing femurs and/or tibiae using Phosphate-Buffered Saline (PBS) + 0.5% Bovine Serum Albumin (BSA). Splenic cells were obtained by aseptic blunt extrusion of the capsule.

2.3. Enumeration of Hematopoietic Cells

Hematopoietic cells in blood, BM, and spleen were enumerated using multi-parametric flow cytometry for informative markers, for mature and immature subsets, as well as in vitro clonogenic assays [32–34]. Antibodies used are listed in Supplemental Table S1; acquisition was done with FACS LSR Fortessa (Becton-Dickinson, Heidelberg, Germany) and analysis with FACSDiva 7 (Becton-Dickinson, Heidelberg, Germany). Clonogenic assays were performed with cytokine-replete semisolid culture media (Methocult GF M3434, Stem Cell Technologies, Cologne, Germany). A defined aliquot of white blood cells (WBCs) from the different tissues (after hypotonic red blood cell lysis for peripheral blood) was plated in duplicate, and colony growth was scored after 7 days using an inverted 2.5× microscope (Olympus, Hamburg, Germany). Cell cycle analysis was performed using Ki67 as a marker for cell proliferation. 7-AAD was added to distinguish between G1 and G2/S/M phases.

2.4. Mobilization

Progenitor cells were mobilized into peripheral blood using either AMD3100 (5 mg/kg bolus, i.p., Sigma-Aldrich, Darmstadt, Germany) or rhG-CSF (nine doses of 100 µg/kg q12h i.p., Sandoz-Hexal, Holzkirchen, Germany) either in 0.9% NaCl (BBraun, Melsungen, Germany) or 20% human albumin solution (Baxter, Deerfield, IL, USA). Blood was drawn 1 h, 2 h, and 4 h after administration of AMD3100 or 1 h after the last administration of rhG-CSF (unless otherwise stated), followed by colony-forming unit culture (CFU-C) enumeration in blood, as well as, where indicated, in BM and spleen. WBC were counted at every time point. LSK, LSK-SLAM, and cell cycle analysis were performed in BM and spleen cell suspensions using flow cytometry.

2.5. Albumin Quantification

Human serum albumin in mouse serum was detected and quantified using human albumin ELISA (Merck, Darmstadt, Germany) according to the manufacturer's recommendations.

2.6. rhG-CSF Quantification

Human G-CSF Flex Set (BD Biosciences, Franklin Lakes, NJ, USA) was used to quantify levels of rhG-CSF in murine plasma or BM-fluid samples.

2.7. Statistics

Descriptive statistics and students' *t*-tests were calculated using Excel (Microsoft, Redmond, WA, USA); twoway ANOVA with Bonferroni post-test was calculated using GraphPad Prism 5 (GraphPad Software, Inc., La Jolla, CA, USA); for non-normally distributed data, the nonparametric Mann-Whitney U test was calculated using SPSS (IBM, Armonk, NY, USA). Unless stated otherwise, results are presented as mean ± standard error of the mean (SEM), ns $p \geq 0.05$, * $p < 0.05$, ** $p < 0.01$, *** $p < 0.001$.

3. Results

3.1. Homeostatic Hematopoiesis is Unaffected by Albumin Deficiency

In order to assess the effect of albumin deficiency on hematopoietic stem cell mobilization, we first enumerated phenotypically and functionally mature and immature hematopoietic cells in all hematopoietic organs of untreated young adult Alb^{-/-} mice, or wild-type littermates as baseline values.

The numbers of mature leukocytes in all compartments (peripheral blood, including differentials, BM, and spleen) were normal in *Alb*^{-/-} mice (Figure 1A and Figure S1A). Moreover, the number of functional HSPC (CFU-C) in all hematopoietic compartments was unaffected by albumin deficiency (Figure 1B and Figure S1B), whereas the number of phenotypic HSPC (lineage-Sca1+ c-kit+; LSK) was modestly increased in spleens of *Alb*^{-/-} mice (Figure S1C). Complementing the assessment of overwhelming similarity of homeostatic hematopoiesis of *Alb*^{-/-} mice, cell cycle analysis of HSPC (example Figure 1C) did not reveal any differences in HSPC-cycling, neither in BM (Figure 1D), nor in spleen (Figure 1E). In summary, we conclude that homeostatic hematopoiesis is normal in *Alb*^{-/-} mice.

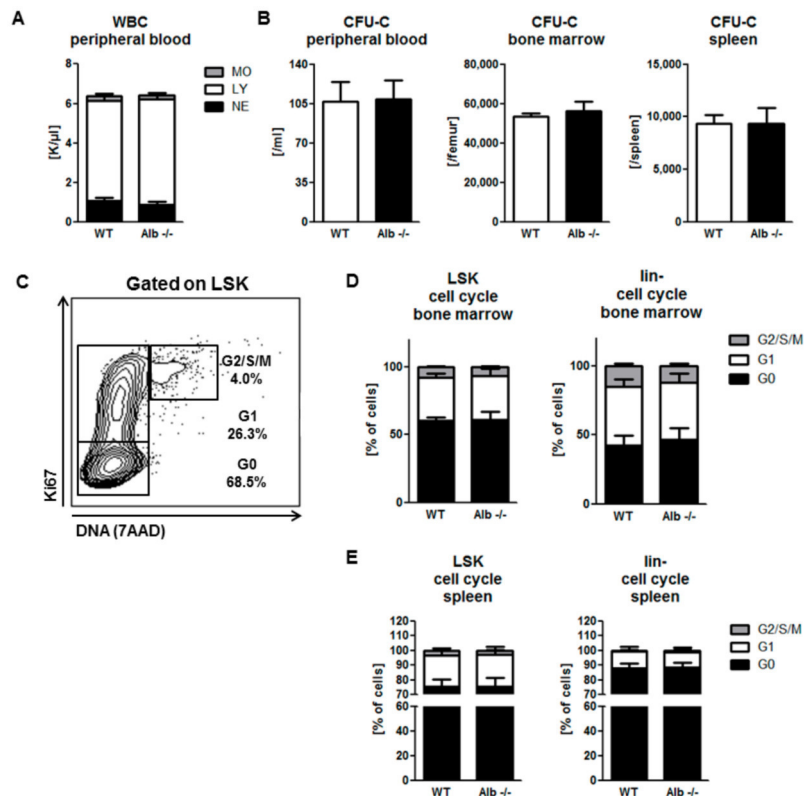


Figure 1. Adult hematopoiesis is unaffected by albumin deficiency. Peripheral blood leukocyte counts and three-way differential were no different in young adult albumin deficient (*Alb*^{-/-}) mice vs. wild-type (WT) littermates (A) MO, monocytes; LY, lymphocytes; NE, neutrophils. Indistinguishable colony-forming unit culture (CFU-C) counts in peripheral blood, bone marrow (BM), and spleen (B) FACS-based cell cycle analysis (C) Highly similar cell cycle distribution of LSK and lin-cells in BM (D) and spleen between the genotypes (E) Data from three individual experiments, $n \geq 10$ mice per group.

3.2. Role of Albumin in the Pharmacodynamics of the Small-Molecule CXCR4 Antagonist AMD3100

Mice received a single i.p. bolus injection of AMD3100. WBC egress and accumulation in peripheral blood could be detected as early as 1 h after administration, with a maximum at 2 h in both *Alb*^{-/-} and WT mice (Figure 2A) irrespective of genotype. Peripheral blood WBC returned to baseline values within 4 h of AMD3100 administration. In contrast to these observations for mature leukocyte species, *Alb*^{-/-} mice were abnormal with respect to HSPC mobilization. They were characterized by one-third diminished peak values in *Alb*^{-/-} mice, despite similar pharmacodynamics in both settings (Figure 2B). Accordingly, the area under the curve (AUC) value for total mobilization efficiency was 30% lower in *Alb*^{-/-} mice. Remarkably, i.p. substitution of human albumin (hAlb), co-injected together with the AMD3100 bolus did not rescue the effect (data not shown). By contrast, when intravenous hAlb substitution at the same dose preceded the i.p. AMD3100 bolus by as little as 30 min, HSPC mobilization in *Alb*^{-/-} mice normalized to WT level (Figure 2C,D). Taken together, the presence of human serum

albumin facilitates AMD3100 mobilization efficiency, likely by virtue of altering bioavailability and/or pharmacological half-life.

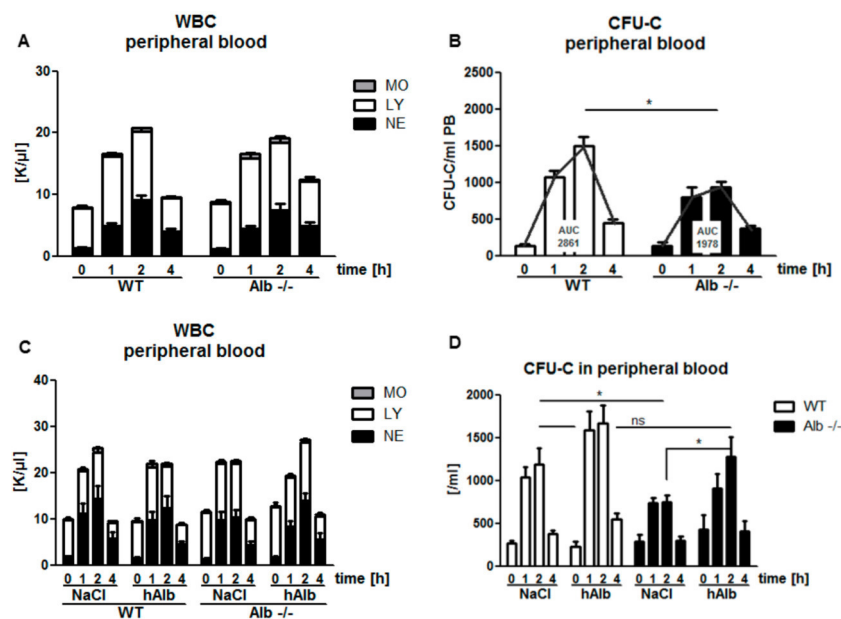


Figure 2. Attenuated hematopoietic stem and progenitor cells (HSPC) mobilization by AMD3100 in *Alb*^{-/-} mice: Normal mature cell mobilization in *Alb*^{-/-} mice after AMD3100 treatment (A) MO, monocytes; LY, lymphocytes; NE, neutrophils; whereas attenuated HSPC mobilization (CFU-C assay), albeit without affecting pharmacodynamics (B) i.v. supplementation with human albumin (hAlb) did not affect white blood cell (WBC) counts in neither genotype (C) and largely normalized responsiveness of immature cells (D). Data from two to five individual experiments with $n \geq 5$ mice per group. ns $p \geq 0.05$, * $p < 0.05$.

3.3. Role of Albumin in G-CSF-Induced Mobilization

Similarly, modeling clinical mobilization with the more slowly acting cytokine G-CSF, mice received a total of nine, 12-hourly i.p. injections of rhG-CSF, followed by mature and immature leukocyte enumeration in blood, BM, and spleen. Interestingly, albumin-deficient mice showed a 2-fold higher WBC and HSPC mobilization into the circulation, when compared to WT controls (Figure 3A,B and Figure S2A), but the mature cell numbers in the spleen and BM were not affected (Figure S2B). Moreover neither BM progenitor cells (LSK) nor hematopoietic stem cells (HSC: LSK CD48-CD150+, LSK-SLAM) numbers were affected by albumin deficiency (Figure 3C,D). However, HSPC proliferation in the BM of *Alb*^{-/-} mice upon rhG-CSF treatment was more strongly induced compared to WT littermates (Figure 3E), possibly contributing to the enhanced mobilization. Moreover, splenic HSPC accumulation and HSPC cell cycle activity, after rhG-CSF-treatment of *Alb*^{-/-} or WT controls, were also indistinguishable (Figure S2C,D).

We hypothesized that local rhG-CSF concentrations might be affected by albumin, and by that mechanism, lead to differences in mobilization efficiency. To test that, we studied the pharmacokinetics of rhG-CSF in plasma and BM fluids of *Alb*^{-/-} and WT mice. In plasma, we observed the same high (15 ng/mL) and only slowly (over 8 h) decreasing levels of rhG-CSF in both *Alb*^{-/-} and WT mice (Figure 3F). On the other hand, rhG-CSF peak concentrations in BM were much lower than in blood, and levels were much less sustained: In WT mice, peak levels were 1 ng/mL and 4 h after administration dropped by 70%. In contrast, rhG-CSF BM concentrations in *Alb*^{-/-} mice reached about 3 ng/mL and were sustained, so that they were 8-fold higher than in WT mice at the four-hour time point (Figure 3G). Thus, albumin impedes accumulation of rhG-CSF in BM, hence resulting in diminished mobilization efficiency.

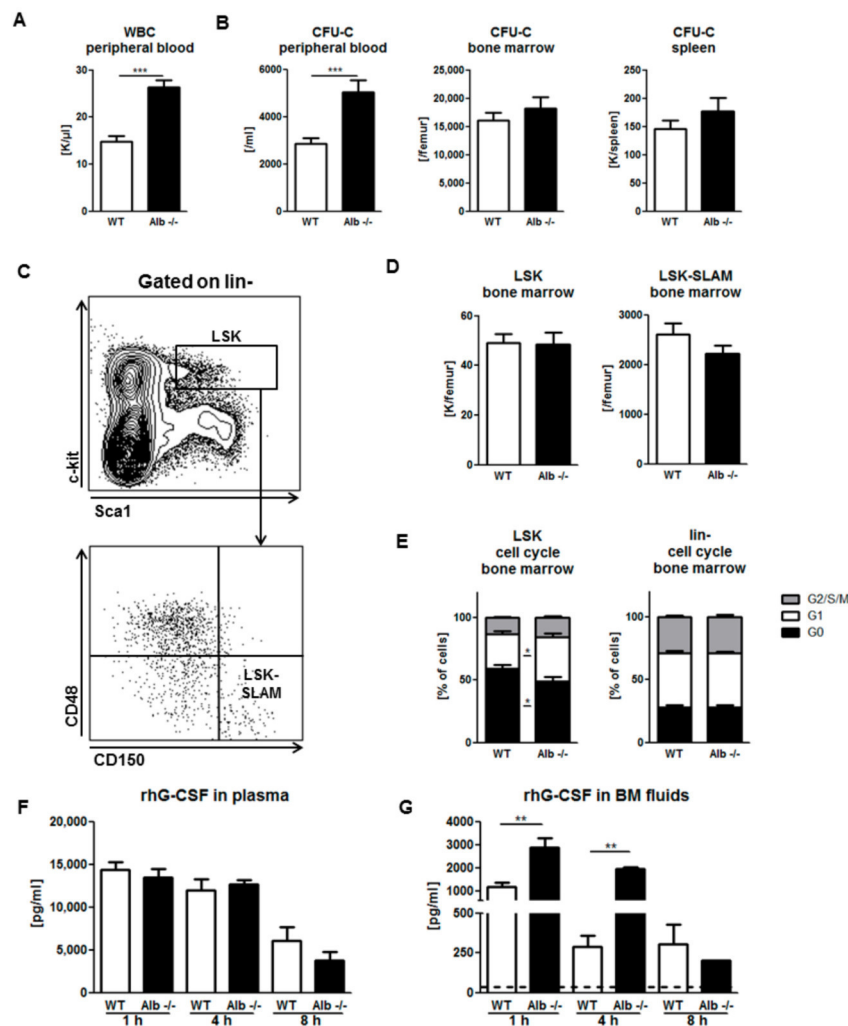


Figure 3. Albumin deficiency enhances Granulocyte-colony stimulating factor (G-CSF)-induced HSPC mobilization: both mature (A) and immature (B) cell numbers were markedly increased after rhG-CSF treatment in Alb^{-/-} mice compared to WT littermates. Gating strategy for LSK and LSK-SLAM cells (C) Number of immature cells in BM and spleen (B,D) of Alb^{-/-} mice was similar to WT littermates. Significantly, more Alb^{-/-} HSPC were proliferating compared to WT cells (E) whereas the effect was gone in the more mature compartment. Data from three individual experiments with $n \geq 12$ mice per group. Steep gradient of rhG-CSF concentrations between plasma (F) and BM fluids (G) as well as markedly enhanced and prolonged rhG-CSF accumulation in BM fluids of Alb^{-/-} mice (G) Dotted line marks the background (murine plasma without rhG-CSF substitution). Data from two independent experiments with $n \geq 3$ mice per group and time point. * $p < 0.05$, ** $p < 0.01$, *** $p < 0.001$.

3.4. Human Albumin Substitution in the G-CSF Mobilization Setting

To ascertain that the observed mobilization phenotype of the Alb^{-/-} mouse is directly attributable to lack of albumin, as opposed to some complex compensatory mechanism, we also tested rhG-CSF in hAlb-substituted mice of both genotypes, Alb^{-/-} and WT. Bioavailability of hAlb was independent of genotype, so that hAlb substitution raised albumin in Alb^{-/-} mice to near-normal levels (Figure 4A). Endogenous murine, plus substituted human albumin in the WT mice, induced some degree of hyperalbuminemia in the latter (Figure 4A). Thus, in hAlb-substituted mice, HSPC mobilization efficiency was analyzed after a five-day course of rhG-CSF, as described before. Mobilization efficiency in Alb^{-/-} mice was corrected to levels reached by normal WT littermates (Figure 4B,C). Consistent with the impact of albumin substitution on the mobilization in Alb^{-/-} mice, albumin over-supplementation in WT mice also slightly reduced the levels of mobilized WBC and HSPC in the circulation (Figure 4B,C).

HSPC counts in BM (Figure 4D) and spleen (Figure S3A) remained unchanged. Cell cycle analysis of BM LSK cells showed a decreased fraction of cells in G1 phase in hAlb-substituted Alb^{-/-} mice (Figure 4E), without similar changes in the more mature lin⁻ compartment. Cell cycle states of LSK cells in spleen were not altered; here, the more mature cells (lin⁻) were relatively more quiescent after albumin substitution of Alb^{-/-} mice (Figure S3B). Human serum albumin injection markedly reduced plasma rhG-CSF levels in WT mice, while barely affecting those in Alb^{-/-} mice (Figure 4F). In the functionally presumably most relevant compartment for mobilization, however, in BM, after human albumin supplementation, the very low concentrations of rhG-CSF in WT mice were increased, whereas the rather high rhG-CSF concentrations in the Alb^{-/-} mice decreased to essentially similar values in both groups (Figure 4G), albeit the decrease did not reach statistical significance. Thus, we conclude that albumin affects the bioavailability of rhG-CSF in the BM with severe consequences for G-CSF mobilization efficiency.

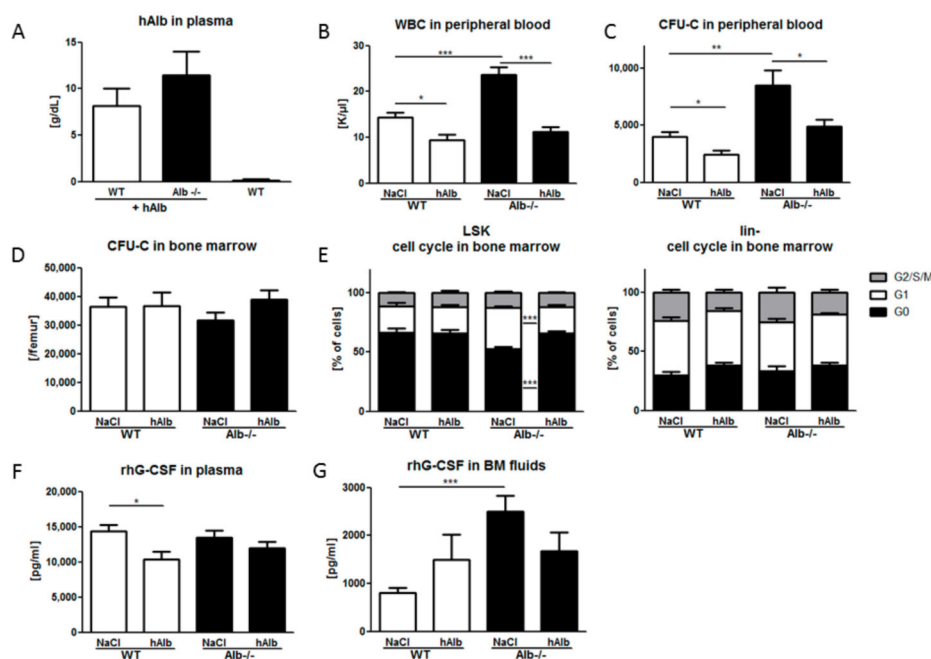


Figure 4. Substitution with hAlb corrects responsiveness to rhG-CSF in Alb^{-/-} mice. Human albumin concentrations were measured one hour after last injection (A) showing slightly supra-physiological levels without differences between the genotypes. The hAlb substitution of Alb^{-/-} mice reduced G-CSF-induced mobilization of WBC (B) and HSPC (C) to WT level. Total CFU-C content in BM was not significantly different between the four groups (D) LSK cell cycle activity, slightly increased in the rhG-CSF + NaCl treated Alb^{-/-} mice, was normalized in rhG-CSF + hAlb treated mice (E) No such changes were observed in the lin⁻ cell proliferation. The rhG-CSF plasma levels were reduced in WT mice treated with rhG-CSF + hAlb compared to rhG-CSF + NaCl controls (F) while rhG-CSF levels in BM fluids after hAlb substitution were comparable between the genotypes (G) Data from three individual experiments with $n \geq 6$ mice per group. * $p < 0.05$, ** $p < 0.01$, *** $p < 0.001$.

4. Discussion

Albumin is the most abundant serum protein, controlling osmotic pressure and acting as a cargo carrier [1–3]. In the course of this study, we attempted to reveal its role in the context of pharmacological mobilization of HSPC, a complex process with many interacting partners, which cannot be adequately modeled in vitro. Albumin knockout mice provided the opportunity to address this topic in an in vivo model. Alb^{-/-} mice are healthy; homeostatic hematopoiesis, both immature and mature, is comparable to their WT littermates. Thus, we conclude that albumin has no apparent effect on mature and immature hematopoiesis under physiological conditions. From these observations, specifically

normal neutrophil counts, we conclude that endogenous G-CSF, which almost exclusively drives neutrophil production and maturation in the BM, clearly acts independently from serum albumin levels, likely because it is generated within BM (i.e., directly at its site of function). However, neither the role of albumin deficiency during hematopoietic aging, nor on the function of HSC niche in transplantation models, nor radiation protection, were addressed in our study. Thus, possible long-term effects of albumin deficiency on stress hematopoiesis cannot be excluded. In contrast, we show a high impact of albumin in settings of transport of G-CSF, or similar substances, when albumin works as a drug carrier. The two compounds used for clinical stem cell mobilization seem to be strongly influenced by serum albumin concentrations, albeit in opposite directions. AMD3100 mobilizes HSPC by directly targeting CXCR4 [35]. AMD3100 was previously shown to bind to plasma proteins in healthy individuals [31]; up to 60% of circulating AMD3100 is captured. Apparently, the interaction with albumin stabilizes AMD3100, since we could show that in the absence of albumin, 30% of its mobilizing activity is lost. Human serum albumin substitution to physiological levels rescued AMD3100-induced mobilization in *Alb*^{-/-} mice. rhG-CSF-induced HSPC mobilization, on the other hand, showed a very unique picture in *Alb*^{-/-} mice. The five-day course of rhG-CSF administration led to a 2-fold higher mobilization efficiency in *Alb*^{-/-} mice compared to WT littermates. The much elevated rhG-CSF levels in the BM of *Alb*^{-/-} mice, and the induced proliferation, presumably account for this phenomenon. rhG-CSF not only accumulated more efficiently in the BM of *Alb*^{-/-} mice after i.p. administration, but its clearance was also delayed in albumin deficient hosts (8-fold more rhG-CSF 4 h after administration in *Alb*^{-/-} BM). Interestingly, rhG-CSF plasma levels were independent of albumin levels. Thus, in *Alb*^{-/-} mice, BM resident HPSCs are specifically exposed to higher rhG-CSF levels and the exposure is significantly prolonged compared to WT mice. This, in aggregate, presumably caused enhanced proliferation and higher mobilization efficiency in albumin-deficient mice. This effect is strictly albumin-dependent, as substitution of *Alb*^{-/-} mice with human serum albumin reduced BM HSPC proliferation, and the number of circulating HSPC after rhG-CSF treatment to normal levels. Regarding the fact that rhG-CSF is used clinically for the mobilization of HSPC in healthy volunteers and in hematologic patients, who typically have largely physiological amounts of serum albumin, we assume fast clearance of rhG-CSF from their BM. Standard regimen is 10 µg/kg/day as a single or split dose (q12h) [14]. Here, we provide evidence supporting the twice-daily injection regimen: Plasma levels of rhG-CSF were already assessed in various studies after a single or multiple injections [36–39]. However, our data demonstrate that plasma rhG-CSF concentration poorly correlates with rhG-CSF levels in BM (i.e., pharmacologically effective rhG-CSF levels) and thus with mobilization efficacy. We show that rhG-CSF was already barely detectable in the BM of WT mice 4 h after rhG-CSF administration, even though plasma levels remained constant over that time. Seemingly, the prolonged exposure of HSPC to rhG-CSF in the BM of the *Alb*^{-/-} mice is causal for the observed increase of circulating HSPC, while plasma rhG-CSF concentrations are independent of albumin. Thus, we conclude that BM rhG-CSF concentration more reliably predicts HSPC mobilization efficiency than rhG-CSF plasma levels. Moreover, the prompt drop of rhG-CSF concentration in the BM of WT mice suggests that split-dose rhG-CSF regimen leads to prolonged, essentially continuous rhG-CSF exposure of BM resident HSPC, and thus could explain the observed higher mobilization efficiencies [40]. Efforts have been made to prolong the half-life of rhG-CSF by PEGylation [41]. Studies have shown that single injections of PEG-rhG-CSF were at least as potent as multiple injections of rhG-CSF in treating neutropenia [42]. Fusion of rhG-CSF to an Fc receptor [43] or serum albumin [44,45] was effective in increasing half-life of rhG-CSF and thus mobilization efficiency. In all of these studies, plasma levels of rhG-CSF were considered to be a marker for effectiveness of the modification. Based on our data, we conclude that comparison of the accumulation of those variants in the BM after injection over time would likely lead to a better understanding of rhG-CSF mobilization outcomes.

In the course of this study, we have addressed the impact of serum albumin on homeostatic hematopoiesis and pharmacological mobilization of HSPC. We have shown that homeostatic mature and immature hematopoiesis is independent from albumin. However, when it comes to drug delivery

and drug efficacy of clinically relevant mobilizing agents, albumin has marked impact on hematopoietic outcomes, as similarly already shown for many other pharmaceuticals [46–48]. Here, we specifically addressed the interactions between albumin and the mobilization drugs AMD3100 and rhG-CSF, showing the dependence of both substances on albumin. In the presence of albumin, rhG-CSF was rapidly cleared out of the BM. Thus, multiple injections per day of rhG-CSF in clinics can be considered reasonable.

Supplementary Materials: The following are available online at <http://www.mdpi.com/2073-4409/9/1/4/s1>, Table S1: FACS antibodies used in the study; Figure S1: Immunological 5-lineage differentials reveal no difference between WT and Alb^{-/-} mice; Figure S2: No effect of albumin on cellularity and cell cycle in spleen of rhG-CSF treated mice; Figure S3: Normalization of rhG-CSF induced cell cycle activity of lin⁻ cells in spleens of Alb^{-/-} mice after substitution with hAlb.

Author Contributions: E.D., H.B., and E.W. designed the experiments. E.D. and E.W. performed the experiments. E.D., H.B., and E.W. wrote and approved the paper. All authors have read and agreed to the published version of the manuscript

Funding: This research received no external funding.

Conflicts of Interest: H.B. has received research support from and served on the speakers' bureau of Sandoz-Hexal and Chugai, makers of rhG-CSF. E.D. and E.W. have no declarations.

References

1. Fanali, G.; di Masi, A.; Trezza, V.; Marino, M.; Fasano, M.; Ascenzi, P. Human serum albumin: From bench to bedside. *Mol. Aspects Med.* **2012**, *33*, 209–290. [[CrossRef](#)] [[PubMed](#)]
2. Evans, T.W. Review article: Albumin as a drug—Biological effects of albumin unrelated to oncotic pressure. *Aliment Pharmacol. Ther.* **2002**, *16*, 6–11. [[CrossRef](#)] [[PubMed](#)]
3. Peters, J.T. *All about Albumin: Biochemistry, Genetics, and Medical Applications*; Academic press: San Diego, CA, USA, 1995.
4. Ghuman, J.; Zunszain, P.A.; Petitpas, I.; Bhattacharya, A.A.; Otagiri, M.; Curry, S. Structural basis of the drug-binding specificity of human serum albumin. *J. Mol. Biol.* **2005**, *353*, 38–52. [[CrossRef](#)] [[PubMed](#)]
5. Meloun, B.; Moravek, L.; Kostka, V. Complete amino acid sequence of human serum albumin. *FEBS Lett.* **1975**, *58*, 134–137. [[CrossRef](#)]
6. Sudlow, G.; Birkett, D.J.; Wade, D.N. The characterization of two specific drug binding sites on human serum albumin. *Mol. Pharmacol.* **1975**, *11*, 824–832.
7. Bern, M.; Sand, K.M.; Nilsen, J.; Sandlie, I.; Andersen, J.T. The role of albumin receptors in regulation of albumin homeostasis: Implications for drug delivery. *J. Control. Release.* **2015**, *211*, 144–162. [[CrossRef](#)]
8. Zhivkova, Z.D. Studies on drug-human serum albumin binding: The current state of the matter. *Curr Pharm. Des.* **2015**, *21*, 1817–1830. [[CrossRef](#)]
9. Roopenian, D.C.; Low, B.E.; Christianson, G.J.; Proetzel, G.; Sproule, T.J.; Wiles, M.V. Albumin-deficient mouse models for studying metabolism of human albumin and pharmacokinetics of albumin-based drugs. *MAbs* **2015**, *7*, 344–351. [[CrossRef](#)]
10. Koot, B.G.; Houwen, R.; Pot, D.J.; Nauta, J. Congenital analbuminaemia: Biochemical and clinical implications. A case report and literature review. *Eur. J. Pediatr.* **2004**, *163*, 664–670. [[CrossRef](#)]
11. Bonig, H.; Papayannopoulou, T. Mobilization of hematopoietic stem/progenitor cells: General principles and molecular mechanisms. *Methods Mol. Biol.* **2012**, *904*, 1–14.
12. Bonig, H.; Watts, K.L.; Chang, K.H.; Kiem, H.P.; Papayannopoulou, T. Concurrent blockade of alpha4-integrin and CXCR4 in hematopoietic stem/progenitor cell mobilization. *Stem Cells* **2009**, *27*, 836–837. [[CrossRef](#)] [[PubMed](#)]
13. Karpova, D.; Bonig, H. Concise Review: CXCR4/CXCL12 Signaling in Immature Hematopoiesis—Lessons From Pharmacological and Genetic Models. *Stem Cells* **2015**, *33*, 2391–2399. [[CrossRef](#)] [[PubMed](#)]
14. Holig, K. G-CSF in Healthy Allogeneic Stem Cell Donors. *Transfus. Med. Hemother.* **2013**, *40*, 225–235. [[CrossRef](#)] [[PubMed](#)]
15. Aapro, M.S.; Cameron, D.A.; Pettengell, R.; Bohlius, J.; Crawford, J.; Ellis, M.; Kearney, N.; Lyman, G.H.; Tjan-Heijnen, V.C.; Walewski, J.; et al. EORTC guidelines for the use of granulocyte-colony stimulating factor to reduce the incidence of chemotherapy-induced febrile neutropenia in adult patients with lymphomas and solid tumours. *Eur. J. Cancer* **2006**, *42*, 2433–2453. [[CrossRef](#)] [[PubMed](#)]

16. Metcalf, D.; Nicola, N.A. Proliferative effects of purified granulocyte colony-stimulating factor (G-CSF) on normal mouse hemopoietic cells. *J. Cell Physiol.* **1983**, *116*, 198–206. [[CrossRef](#)]
17. Morrison, S.J.; Wright, D.E.; Weissman, I.L. Cyclophosphamide/granulocyte colony-stimulating factor induces hematopoietic stem cells to proliferate prior to mobilization. *Proc. Natl. Acad. Sci. USA* **1997**, *94*, 1908–1913. [[CrossRef](#)]
18. Wright, D.E.; Cheshier, S.H.; Wagers, A.J.; Randall, T.D.; Christensen, J.L.; Weissman, I.L. Cyclophosphamide/granulocyte colony-stimulating factor causes selective mobilization of bone marrow hematopoietic stem cells into the blood after M phase of the cell cycle. *Blood* **2001**, *97*, 2278–2285. [[CrossRef](#)]
19. Lapid, K.; Glait-Santar, C.; Gur-Cohen, S.; Canaani, J.; Kollet, O.; Lapidot, T. Egress and Mobilization of Hematopoietic Stem and Progenitor Cells: A Dynamic Multi-facet Process. Available online: <https://www.stembook.org> (accessed on 16 December 2019).
20. Bonig, H.; Papayannopoulou, T. Hematopoietic stem cell mobilization: Updated conceptual renditions. *Leukemia* **2013**, *27*, 24–31. [[CrossRef](#)]
21. Klein, G.; Schmal, O.; Aicher, W.K. Matrix metalloproteinases in stem cell mobilization. *Matrix Biol.* **2015**, *44–46*, 175–183. [[CrossRef](#)]
22. Christopher, M.J.; Liu, F.; Hilton, M.J.; Long, F.; Link, D.C. Suppression of CXCL12 production by bone marrow osteoblasts is a common and critical pathway for cytokine-induced mobilization. *Blood* **2009**, *114*, 1331–1339. [[CrossRef](#)]
23. Sugiyama, T.; Kohara, H.; Noda, M.; Nagasawa, T. Maintenance of the hematopoietic stem cell pool by CXCL12-CXCR4 chemokine signaling in bone marrow stromal cell niches. *Immunity* **2006**, *25*, 977–988. [[CrossRef](#)] [[PubMed](#)]
24. Mendez-Ferrer, S.; Michurina, T.V.; Ferraro, F.; Mazloom, A.R.; Macarthur, B.D.; Lira, S.A.; David, T.S.; Avi, M.; Grigori, N.; Grigori, N.E.; et al. Mesenchymal and haematopoietic stem cells form a unique bone marrow niche. *Nature* **2010**, *466*, 829–834. [[CrossRef](#)] [[PubMed](#)]
25. Winkler, I.G.; Levesque, J.P. Mechanisms of hematopoietic stem cell mobilization: When innate immunity assails the cells that make blood and bone. *Exp. Hematol.* **2006**, *34*, 996–1009. [[CrossRef](#)] [[PubMed](#)]
26. Liu, F.; Poursine-Laurent, J.; Link, D.C. The granulocyte colony-stimulating factor receptor is required for the mobilization of murine hematopoietic progenitors into peripheral blood by cyclophosphamide or interleukin-8 but not flt-3 ligand. *Blood* **1997**, *90*, 2522–2528. [[CrossRef](#)] [[PubMed](#)]
27. Broxmeyer, H.E.; Orschell, C.M.; Clapp, D.W.; Hangoc, G.; Cooper, S.; Plett, P.A.; Liles, W.C.; Li, X.; Graham-Evans, B.; Timothy, B.C.; et al. Rapid mobilization of murine and human hematopoietic stem and progenitor cells with AMD3100, a CXCR4 antagonist. *J. Exp. Med.* **2005**, *201*, 1307–1318. [[CrossRef](#)] [[PubMed](#)]
28. Hendrix, C.W.; Flexner, C.; MacFarland, R.T.; Giandomenico, C.; Fuchs, E.J.; Redpath, E.; Bridger, G.; Henson, G.W. Pharmacokinetics and safety of AMD-3100, a novel antagonist of the CXCR-4 chemokine receptor, in human volunteers. *Antimicrob. Agents Chemother.* **2000**, *44*, 1667–1673. [[CrossRef](#)]
29. Stute, N.; Santana, V.M.; Rodman, J.H.; Schell, M.J.; Ihle, J.N.; Evans, W.E. Pharmacokinetics of subcutaneous recombinant human granulocyte colony-stimulating factor in children. *Blood* **1992**, *79*, 2849–2854. [[CrossRef](#)] [[PubMed](#)]
30. Sturgill, M.G.; Huhn, R.D.; Drachtman, R.A.; Ettinger, A.G.; Ettinger, L.J. Pharmacokinetics of intravenous recombinant human granulocyte colony-stimulating factor (rhG-CSF) in children receiving myelosuppressive cancer chemotherapy: Clearance increases in relation to absolute neutrophil count with repeated dosing. *Am. J. Hematol.* **1997**, *54*, 124–130. [[CrossRef](#)]
31. EMEA. CHMP Assessment Report for Mozobil 2009. Available online: https://www.ema.europa.eu/en/documents/assessment-report/mozobil-epar-public-assessment-report_en.pdf (accessed on 16 December 2019).
32. Bonig, H.; Priestley, G.V.; Oehler, V.; Papayannopoulou, T. Hematopoietic progenitor cells (HPC) from mobilized peripheral blood display enhanced migration and marrow homing compared to steady-state bone marrow HPC. *Exp. Hematol.* **2007**, *35*, 326–334. [[CrossRef](#)]
33. Winkler, I.G.; Wiercinska, E.; Barbier, V.; Nowlan, B.; Bonig, H.; Levesque, J.P. Mobilization of hematopoietic stem cells with highest self-renewal by G-CSF precedes clonogenic cell mobilization peak. *Exp. Hematol.* **2016**, *44*, 303–314. [[CrossRef](#)]
34. Bonig, H.; Priestley, G.V.; Nilsson, L.M.; Jiang, Y.; Papayannopoulou, T. PTX-sensitive signals in bone marrow homing of fetal and adult hematopoietic progenitor cells. *Blood* **2004**, *104*, 2299–2306. [[CrossRef](#)]

35. Rosenkilde, M.M.; Gerlach, L.O.; Jakobsen, J.S.; Skerlj, R.T.; Bridger, G.J.; Schwartz, T.W. Molecular mechanism of AMD3100 antagonism in the CXCR4 receptor: Transfer of binding site to the CXCR3 receptor. *J. Biol. Chem.* **2004**, *279*, 3033–3041. [[CrossRef](#)]
36. Merlin, E.; Piguet, C.; Auvrignon, A.; Rubie, H.; Demeocq, F.; Kanold, J. The pros and cons of split-dose granulocyte colony-stimulating factor alone rather than a single high dose for hematopoietic progenitor cell mobilization in small children (<15 kg) with solid tumors. *Haematologica* **2006**, *91*, 1004–1005.
37. Carrion, R.; Serrano, D.; Gomez-Pineda, A.; Diez-Martin, J.L. A randomised study of 10 microg/kg/day (single dose) vs 2 x 5 microg/kg/day (split dose) G-CSF as stem cell mobilisation regimen in high-risk breast cancer patients. *Bone Marrow Transplant.* **2003**, *32*, 563–567. [[CrossRef](#)]
38. Van Der Auwera, P.; Platzer, E.; Xu, Z.X.; Schulz, R.; Feugeas, O.; Capdeville, R.; David, J.E. Pharmacodynamics and pharmacokinetics of single doses of subcutaneous pegylated human G-CSF mutant (Ro 25-8315) in healthy volunteers: Comparison with single and multiple daily doses of filgrastim. *Am. J. Hematol.* **2001**, *66*, 245–251. [[CrossRef](#)] [[PubMed](#)]
39. Tanaka, H.; Kaneko, T. Pharmacokinetics of recombinant human granulocyte colony-stimulating factor in the rat. Single and multiple dosing studies. *Drug Metab. Dispos.* **1991**, *19*, 200–204. [[PubMed](#)]
40. Kroger, N.; Renges, H.; Kruger, W.; Gutensohn, K.; Loliger, C.; Carrero, I.; Lourdes, C.; Axel, R.Z. A randomized comparison of once versus twice daily recombinant human granulocyte colony-stimulating factor (filgrastim) for stem cell mobilization in healthy donors for allogeneic transplantation. *Br. J. Haematol.* **2000**, *111*, 761–765. [[PubMed](#)]
41. Tanaka, H.; Satake-Ishikawa, R.; Ishikawa, M.; Matsuki, S.; Asano, K. Pharmacokinetics of recombinant human granulocyte colony-stimulating factor conjugated to polyethylene glycol in rats. *Cancer Res.* **1991**, *51*, 3710–3714.
42. Kim, M.G.; Han, N.; Lee, E.K.; Kim, T. Pegfilgrastim vs filgrastim in PBSC mobilization for autologous hematopoietic SCT: A systematic review and meta-analysis. *Bone Marrow Transplant.* **2015**, *50*, 523–530. [[CrossRef](#)]
43. Do, B.H.; Kang, H.J.; Song, J.A.; Nguyen, M.T.; Park, S.; Yoo, J.; Do, B.H.; Kang, H.J.; Song, J.A.; Nguyen, M.T.; et al. Granulocyte colony-stimulating factor (GCSF) fused with Fc Domain produced from E. coli is less effective than Polyethylene Glycol-conjugated GCSF. *Sci Rep.* **2017**, *7*, 6480. [[CrossRef](#)]
44. Zhao, S.; Zhang, Y.; Tian, H.; Chen, X.; Cai, D.; Yao, W.; Gao, X. Extending the serum half-life of G-CSF via fusion with the domain III of human serum albumin. *Biomed. Res. Int.* **2013**, *2013*, 107238. [[CrossRef](#)] [[PubMed](#)]
45. Huang, Y.S.; Wen, X.F.; Yang, Z.Y.; Wu, Y.L.; Lu, Y.; Zhou, L.F. Development and characterization of a novel fusion protein of a mutated granulocyte colony-stimulating factor and human serum albumin in *Pichia pastoris*. *PLoS ONE* **2014**, *9*, e115840. [[CrossRef](#)] [[PubMed](#)]
46. Meyer, M.C.; Guttman, D.E. The binding of drugs by plasma proteins. *J. Pharm. Sci.* **1968**, *57*, 895–918. [[CrossRef](#)] [[PubMed](#)]
47. Vallner, J.J. Binding of drugs by albumin and plasma protein. *J. Pharm. Sci.* **1977**, *66*, 447–465. [[CrossRef](#)] [[PubMed](#)]
48. Schmidt, S.; Gonzalez, D.; Derendorf, H. Significance of protein binding in pharmacokinetics and pharmacodynamics. *J. Pharm. Sci.* **2010**, *99*, 1107–1122. [[CrossRef](#)]



REGULAR SUBMISSION

Modest and nonessential roles of the endocannabinoid system in immature hematopoiesis of mice

Eva Danner^{a,b}, Frauke Hoffmann^a, Seo-Youn Lee^a, Fabian Cordes^a, Sabine Orban^a, Katrin Dauber^a, Doreen Chudziak^a, Gabriele Spohn^a, Eliza Wiercinska^a, Benjamin Tast^a, Darja Karpova^a, and Halvard Bonig^{a,c}

^aGerman Red Cross Blood Donor Service Baden-Wuerttemberg-Hessen, Frankfurt, Germany; ^bGoethe University Frankfurt, Faculty of Biological Sciences, Frankfurt, Germany; ^cGoethe University Medical School, Institute for Transfusion Medicine and Immunohematology, Frankfurt, Germany

(Received 22 March 2019; revised 13 September 2019; accepted 14 September 2019)

Endocannabinoids are lipid mediators that signal via several seven-transmembrane domain G protein-coupled receptors. The endocannabinoid receptor CB2 is expressed on blood cells, including stem cells, and mediates the effects of cannabinoids on the immune system. The role of the endocannabinoid system in immature hematopoiesis is largely elusive. Both direct effects of endocannabinoids on stem cells and indirect effects through endocannabinoid-responsive niche cells like macrophages have been reported. Using two different CB2-deficient mouse models, we studied the role of the endocannabinoid system in immature hematopoiesis. Moreover, we utilized both models to assess the specificity of putative CB2 agonists. As heterodimerization of CB2 and CXCR4, which is highly expressed on hematopoietic stem cells, has already been described, we also assessed potential consequences of CB2 loss for CXCR4/CXCL12 signaling. Overall, no differential effects were observed with any of the compounds tested; the compounds barely induced signaling by themselves, whereas they attenuated CXCL12-induced signals in both CB2-competent and CB2-deficient cells. In vivo experiments were therefore by necessity restricted to loss-of-function studies in knockout (CB2^{-/-}) mice: Except for mild lymphocytosis and slightly elevated circulating progenitor cells, homeostatic hematopoiesis in CB2^{-/-} mice appears to be entirely normal. Mobilization in response to pharmacological stimuli, Plerixafor or G-CSF, was equally potent in wild-type and CB2^{-/-} mice. CB2^{-/-} bone marrow cells reconstituted hematopoiesis in lethally irradiated recipients with engraftment kinetics indistinguishable from those of wild-type grafts. In summary, we found the endocannabinoid system to be largely dispensable for normal murine hematopoiesis. © 2019 ISEH – Society for Hematology and Stem Cells. Published by Elsevier Inc. All rights reserved.

Hematopoiesis, that is, the continuous, lifelong process of generating short-lived mature blood cells, originates from hematopoietic stem and progenitor cells (HSPCs) [1], the proliferation of which is tightly controlled. The

hematopoietic organ is physically located in the bone marrow (BM), where HSPCs interact in an intricate fashion with their environment, the niche [2]. Under the influence of the latter, HSPCs give rise to increasingly more differentiated precursors and mature blood cells, which are ultimately released into the peripheral blood [3]. The niche consists of bone-forming cells, the osteoblasts, cells of mesenchymal origin such as CXCL12-abundant reticular cells, as well as mature hematopoietic cells

Offprint requests to: Halvard Bönig, Sandhofstrasse 1, 60528 Frankfurt, Germany; E-mail: h.bonig@blutspende.de

Supplementary material associated with this article can be found in the online version at <https://doi.org/10.1016/j.exphem.2019.09.022>.

including “osteomacs” and osteoclasts. Moreover, a tight association of the niche with sympathetic nerve fibers has been demonstrated [4]. Together with extracellular matrix components, niche-derived chemokines and cytokines control HSPC survival, proliferation, and retention [5]. The interaction between the C-X-C chemokine receptor type 4 (CXCR4) expressed on the HSPC surface with its chief ligand, the chemokine CXCL12, is a key axis facilitating HSPC retention in BM. However, although the vast majority of HSPCs are retained in BM, a small number regularly circulate in the blood [6–8].

The endocannabinoid system consists of short-lived lipid mediators, the endocannabinoids, which are generated through enzymatic processing of the cell membrane phospholipid phosphatidylethanolamine, and their receptors, the G-protein-coupled receptors CB1 and CB2. It is a well-described neurotransmitter pathway [9]. However, expression of CB2 on lymphocytes and immunosuppressive effects of cannabinoid receptor agonists on lymphocytes clearly link endocannabinoid and immune systems. Anti-inflammatory effects of pharmacological endocannabinoid receptor agonists have been exploited clinically [10,11]. Integration of endocannabinoid signals by cells is complex and likely cell specific; of possible relevance within the hematopoietic system, CB2 was described to heterodimerize with CXCR4 [12] and thereby modulate CXCR4 agonist-induced signaling. Definitive evidence of direct or indirect modulation of HSPC function by endocannabinoids has thus far not been provided. Importantly, as previously shown and here confirmed, CB2 is expressed on immature hematopoietic cells in addition to mature blood cells [13].

To study endocannabinoid receptor function, both additive (pharmacological agonists) and subtractive (pharmacological antagonists) approaches have been employed, with characteristic limitations. AM1241, JWH133, and CP55940 have been utilized as selective agonists, and AM630 as a selective antagonist [14]. However, apparent cell- and species-specific differences in signaling readout after exposure to these small-molecule compounds complicated interpretation of results [15]. Availability of receptor-deficient mice gave us the opportunity to study organismic effects of lack of CB2 signaling on immature hematopoiesis for the first time. Moreover, the specificity of CB2-targeting compounds, along with their effects on the hematopoietic system, could be assessed with CB2^{-/-} cells as the perfect negative controls. As we describe here, the four compounds were associated with virtually identical intracellular signaling events in CB2-competent and ⁻deficient cells and are thus not suitable for exploration of CB2-mediated effects on hematopoietic cells *in vitro* or *in vivo*. CB2-deficient mice exhibit very subtle perturbations of the hematopoietic system: a mild lymphocytosis was observed in line with previous reports. Furthermore,

increased numbers of homeostatically circulating HSPCs were detected. Both observations were corroborated in two different CB2-deficient mouse strains.

Methods

Mice

For all experiments, young adult mice (8–12 weeks, either sex) were used. B6.129P2-Cnr2^{tm1Dgen/J} (CB2^{-/-}) mice, described previously [16], were purchased from Jackson Laboratory (JAX stock No. 005786). Buckley CB2^{-/-} mice [17] were a generous gift from Anne Zimmer (Haus für Experimentelle Therapie, Bonn, Germany). From CB2^{+/-} heterozygote breedings, CB2-competent wild-type (WT) littermates of the corresponding strains were used as controls. For transplantation experiments, B6.SJL-*Ptprc*^a*Pep3*^b/BoyJ (JAX stock No. 002014; CD45.1) were used as recipients. Experiments were performed in accordance with the agreement on national animal protection and were approved by the municipal government (F27/24 and F27/1010, Darmstadt, Germany).

Hematopoietic cells

Peripheral blood was drawn from the facial vein into EDTA tubes using a 23G needle. Total cell counts were analyzed with Hemavet 950SF+ (Drew Scientific, Dallas, TX). BM cells were harvested by flushing femurs and/or tibias using phosphate-buffered saline + 0.5% bovine serum albumin. Splenic cells were obtained by blunt extrusion of the capsule.

Enumeration of hematopoietic cells

Hematopoietic cells in blood, BM, and spleen were enumerated using multiparametric flow cytometry for informative markers for mature (CD45, CD3, B220, Ter-119, CD11b, Gr-1) and immature (lineage, c-kit, sca-1, CD48, CD150) subsets, as were clonogenic assays. Antibodies used are listed in [Supplementary Table E1](#) (online only, available at www.exphem.org); acquisition was done with FACS LSR Fortessa (Becton-Dickinson, Heidelberg, Germany) and analysis with FACS Diva 7 (BD Biosciences). Clonogenic assays were performed with cytokine-replete semisolid culture media (Methocult GF M3434, Stem Cell Technologies). A defined aliquot of white blood cells (WBCs) (50,000 BM WBCs, 200,000 spleen WBCs, and 70 μ L of peripheral blood after hypotonic red blood cell [RBC] lysis) from the different tissues was plated in duplicate. Colony growth, including differentiation of colony-forming units granulocytes–macrophages (CFU-GM), blast-forming units erythroid (BFU-E), and colony-forming units granulocytes, erythrocytes, monocytes/macrophages, megakaryocytes (CFU-GEMM), was scored after 7 days using an inverted 2.5 \times microscope. Cell cycle analysis was performed using Ki67 as a marker for cell proliferation. 7-Aminoactinomycin D (7-AAD) was added to distinguish between G1 and G2/S/M phases.

Isolation of mRNA and RT-PCR

Whole BM cell or immunomagnetically enriched BM c-kit⁺ cell mRNA was isolated using the RNeasy kit (Qiagen, Vanlo, Netherlands) according to the manufacturer's instructions. For CB2 detection on HSPC subtypes, LSK, MPP,

CMP, and HSC progenitor cells were sorted via fluorescence-activated cell sorting (FACS) as described [18], and mRNA was isolated. One microgram of RNA was reverse transcribed using the iScript cDNA synthesis kit (Bio-Rad, Irvine, CA) and diluted 1:10 for the use in real-time reverse transcriptase polymerase chain reaction (RT-PCR). We used the primers for murine transcripts (CB2-fw1—TCA TTG CCA TCC TCT TTT CC, CB2-rev1—GAA CCA GCA TAT GAG CAG CA, CB2-fw2—GGA GTT CAA CCC CAT GAA GGA GTA C, CB2-rev2—GAC TAG AGC TTT GTA GGT AGG CGG G) to generate a PCR product 188 bp (1) or 385 bp (2) in length. No-reverse transcriptase samples were used as controls to exclude contamination with gDNA. Sequencing of the resulting fragments was done with Microsynth (Balgach, Switzerland).

CB2 antibody staining

BM and spleen cells were harvested as described. One million unmanipulated cells were prepared for FACS analysis and stained with two different CB2 antibodies (Davis Biotechnology, Regensburg, Germany, and Cayman Chemical, Ann Arbor, MI). Twenty micrograms of antibody was conjugated using the Alexa Fluor 488 antibody labeling kit (Thermo Fisher, Darmstadt, Germany). CB2^{-/-} cells were used as a negative control. Data acquisition and analysis were performed as described earlier.

Signaling

Lysis-resistant BM leukocytes were starved for 2 hours at 37°C in RPMI+0.5 % fetal calf serum. Stimulation was started by adding 10 μmol/L CXCL12, 10 μmol/L CB2 agonist (2.5 μmol/L for CP55940), or both. AM1241, CP55940, and JWH133 as agonists, as well as AM630 as an antagonist, were assessed. Phosphorylation of ERK1/2, MEK, and AKT was analyzed via FACS staining.

Mobilization

Progenitor cells were mobilized into peripheral blood using either AMD3100 (5 mg/kg once, intraperitoneally; Sigma-Aldrich, Darmstadt, Germany) or rhG-CSF (9 doses of 100 μg/kg every 12 hours, intraperitoneally; Hexal, Holzkirchen, Germany). Blood was drawn 1, 2, and 4 hours after administration of AMD3100 or 1 hour after the last administration of G-CSF, followed by CFU-C enumeration of colony-forming units cells (CFU-C) in blood as well as, where indicated, in BM and spleen. WBCs were counted at every time point. LSK, LSK-SLAM, and cell cycle analysis was performed in BM and spleen cell suspensions using flow cytometry.

Transplantation

Donor mice were sacrificed by cervical dislocation; femurs and tibias were harvested. BM cells were obtained as described above and resuspended in 0.9% NaCl at a concentration of 1 mol/mL. Recipient mice were irradiated with 9.5 Gy using a cesium source with a dose rate of 0.75 Gy/min (Biobeam 2000, Gamma-Service Medical, Leipzig, Germany). Mice then received intravenous transplants of unmanipulated (not HSPC-enriched) BM cell suspensions of wild-type or CB2^{-/-} mice (200,000 cells/mouse) into the lateral tail vein. Engraftment

kinetics were analyzed by drawing blood twice weekly. Mice were sacrificed for final analysis 14 weeks after transplantation.

Statistics

Descriptive statistics and Student *t* tests were calculated using Excel (Microsoft, Redmond, WA); two-way analysis of variance (ANOVA) with the Bonferroni posttest was calculated using GraphPad Prism 5 (GraphPad Software, Inc., La Jolla, CA); for non-normally distributed data, the nonparametric Mann–Whitney *U* test was calculated using SPSS (IBM, Armonk, NY). Unless stated differently, results are presented as the mean ± SEM nonsignificant [n.s.] $p \geq 0.05$, * $p < 0.05$, ** $p < 0.01$, *** $p < 0.001$.

Results

Expression of endocannabinoid receptors on HSPCs

Expression of CB2 mRNA in BM and spleen cells, including the immature hematopoietic fraction, had been described by Lattin et al. [19], and was confirmed here for murine c-kit⁺ BM cells (Fig. 1A), whole BM cells (Fig. 1B), and HSPC subtypes (Fig. 1C). However, direct demonstration of CB2 surface expression turned out to be challenging. Thus, the polyclonal antibody from Davis Biotechnology (Regensburg, Germany), designed to be CB2 specific, stained CB2-competent and CB2-deficient BM and spleen cells with equal efficiency (Fig. 1D). Our attempt to generate a novel antibody against one of the CB2 extracellular loops was unsuccessful. For lack of suitable reagents, CB2 presence versus deficiency was therefore inferred from CB2 gene expression as well as from sequencing of the CB2 locus. The inserted stop codons were confirmed, and in silico translation predicted expression of a truncated receptor in the Buckley strain (Supplementary Figure E1, online only, available at www.exphem.org). Even if mRNA transcripts could partially be detected by Zhang et al. [16], complete loss of CB2 protein in the Deltagen strain is assumed (Supplementary Figure E2, online only, available at www.exphem.org). We excluded a possible compensatory upregulation of alternative cannabinoid receptor CB1 or GPR55 (Fig. 1A, C) in hematopoietic cells. Both CB2^{-/-} strains are thus completely endocannabinoid receptor deficient in their hematopoietic system.

The inverse agonist AM1241 fails to modulate CB2-specific signals in hematopoietic cells.

Availability of CB2-deficient BM leukocytes allowed us to investigate potential changes in intracellular signaling responses. Presence of CB2 mRNA in a variety of hematopoietic lineages in the BM has been reported [19,20] and confirmed here by us (Fig. 1). After short serum starvation, lysis-resistant whole BM cells were stimulated using CXCL12. We assessed stimulation kinetics, expecting similar responsiveness irrespective of CB2 expression. Indeed peak activation of ERK, MEK, and AKT occurred 60 s after stimulation and returned to basal levels by 10 min

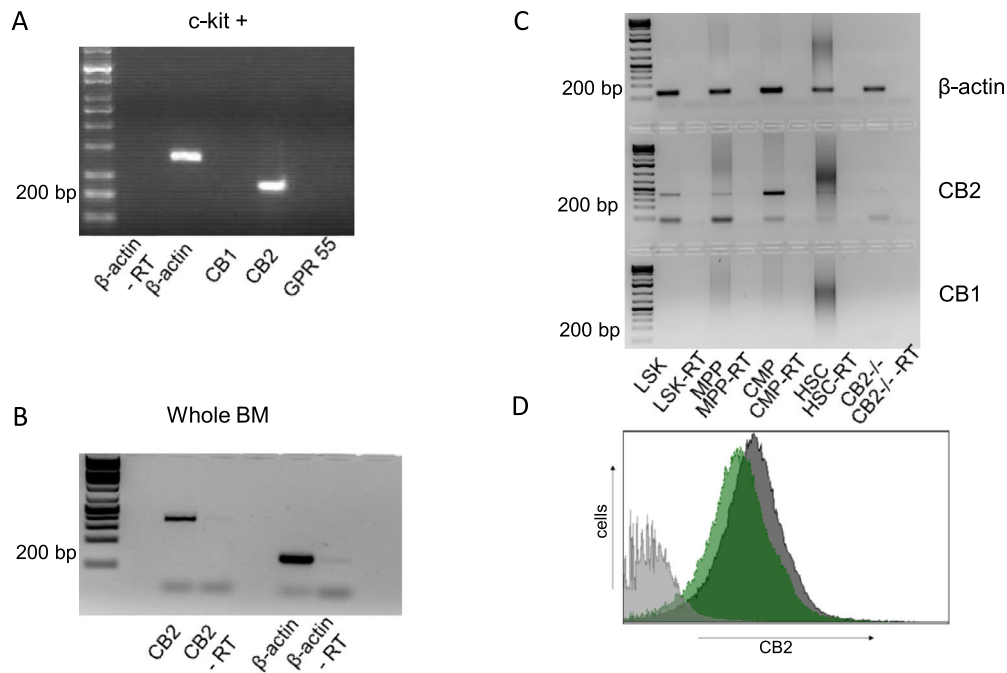


Figure 1. CB2 gene expression in BM cells. BM cells were isolated from C57Bl/6 WT mice, and mRNA was extracted and reverse transcribed into cDNA. RT-PCR verified CB2 expression, but not CB1 and GPR55 expression, in c-kit enriched (A) and CB2 expression in whole BM (B) WT cells. The negative control was performed simultaneously using a no-RT control. LSK, MPP, CMP, and HSC progenitor cells were sorted via FACS. After mRNA isolation and cDNA transcription, PCR for CB1, CB2, and β -actin transcripts was performed (C). CB2 was expressed only in WT cells irrespective of maturational stage; CB1 was expressed in cells of neither genotype. Representative flow cytometry histogram of a staining of WT (dark gray) and CB2 $^{-/-}$ (green) BM cells with anti-CB2-antibody (Davis Biotechnology) indicating lack of CB2 specificity. Isotype staining was used as negative control (light gray) (D).

(Fig. 2A). Signals were very similar in magnitude and duration in CB2-deficient and CB2-competent cells. Cooperative signaling between chemokines, specifically CXCL12, and endocannabinoid receptor ligands has been reported [12]. We therefore further analyzed signaling in response to co-stimulation with the putative CB2 agonist AM1241 and CXCL12 (Fig. 2B). AM1241 partly suppressed CXCL12-induced signaling irrespective of the genetic background of the cells. On its own, AM124 modestly activated MAPK signaling 1 min after stimulation in both CB2-competent and knockout BM cells (data not shown). Similar observations were made with the agonists JWH133 and CP55940 (Supplementary Figure E3), as well as the antagonist AM630. From these results we conclude that the compounds tested here cannot be used to decipher roles of CB2 *in vitro* or *in vivo*, restricting our further experiments to comparative studies, that is, in CB2-deficient mice and littermates.

Steady-state hematopoiesis of CB2 $^{-/-}$ mice is largely unperturbed

Mature and immature blood cells were enumerated in BM, spleen, and peripheral blood of CB2 $^{-/-}$ or CB2-competent wild-type littermates. Immature cells were evaluated phenotypically (LSK, LSK-SLAM) as well as functionally (CFU-C as well as transplantation–reconstitution assays,

see below). The only notable difference in the immature hematopoietic compartment between CB2 $^{-/-}$ and WT mice was a 50% elevation of steady-state circulating CFU-C numbers in CB2 $^{-/-}$ compared with WT mice (Fig. 3A). The relative distribution of different colony types was the same in both genotypes (data not shown). Mature blood cell counts were normal in BM and spleen (data not shown), whereas in blood, a 30% increase in leukocyte counts, entirely attributable to lymphocytes, was detected in CB2 $^{-/-}$ mice (Fig. 3B), in line with previous observations [21,22]. Similar frequencies and total numbers of immature cells were detected in BM and spleen (Fig. 3C). Cell cycle analyses of the variably immature populations in spleen and marrow revealed no difference between the strains (Fig. 3D).

CB2 deficiency does not affect mobilization of HSPCs

As a mild hematopoietic stress model, we investigated mobilization kinetics in CB2 $^{-/-}$ versus WT mice. Mice received intraperitoneal injections of the small-molecule CXCR4 antagonist AMD3100, a low-potency but rapid inducer of leukocyte (including HSPC) mobilization. In both, CB2 $^{-/-}$ and WT mice, circulating WBCs (Fig. 4A) and CFU-C (Fig. 4B) increased to expected levels in response to AMD3100 with no difference between genotypes. As next, mice received a 5-day course of twice-daily

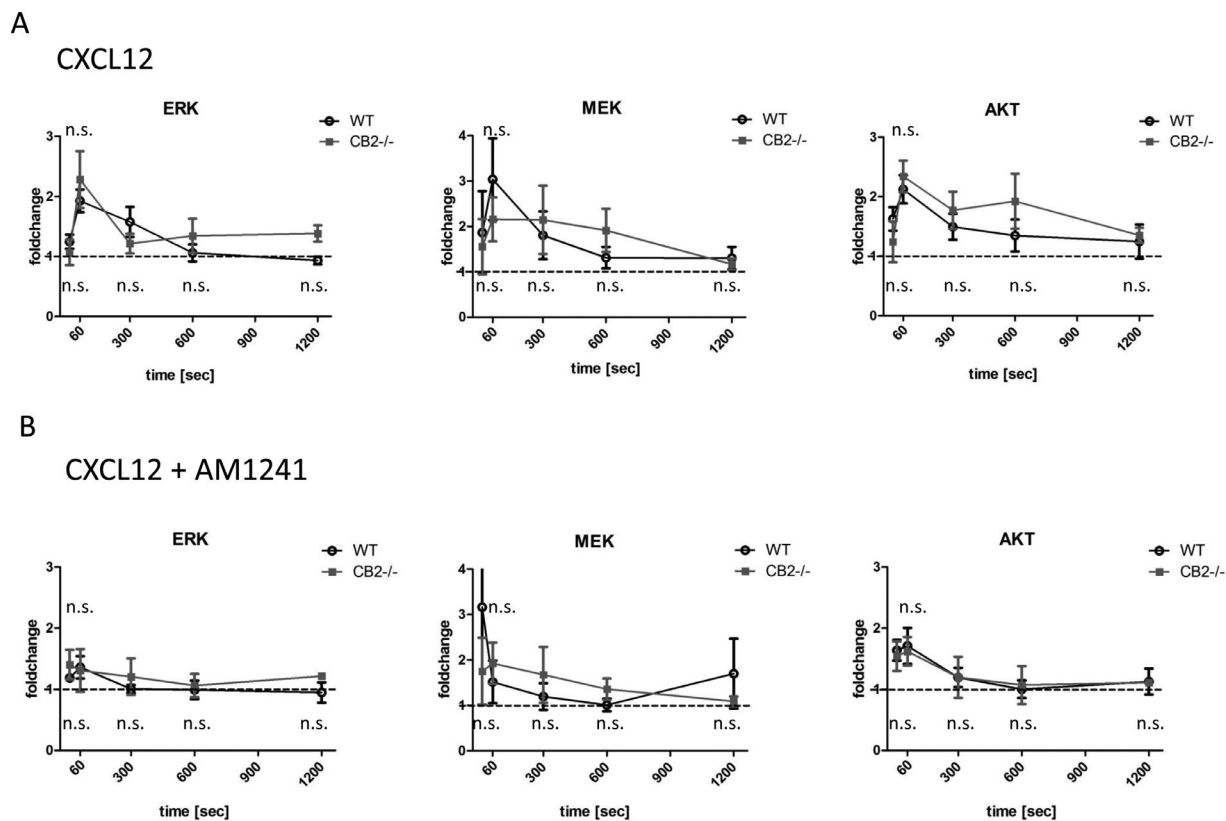


Figure 2. MAPK and AKT signaling after AM1241 stimulation. BM cells from CB2^{-/-} and WT mice were isolated and serum starved. Stimulation of 100,000 cells of either group was performed using 10 $\mu\text{mol/L}$ CXCL12 alone (A) or in combination with a 10 $\mu\text{mol/L}$ concentration of the putative CB2 agonist AM1241 (B). Phosphorylation of ERK, MEK, and AKT kinases was assessed via flow cytometry staining. Genotype-specific responses were not observed, indicating lack of CB2 specificity of the compounds. Measurements were performed in duplicate in at least five independent experiments; $n \geq 5$ per time point.

G-CSF injections. One hour after the last injection, mice were sacrificed to study mature and immature hematopoietic cells in the hematopoietic compartments. In blood, WBCs and CFU-C were increased to the same level in CB2^{-/-} versus WT mice. Progenitor cells in BM and spleen were enumerated and analyzed functionally (CFU-C) (Fig. 4C) as well as immunophenotypically (Fig. 4D). Remarkably, the characteristic depletion (approx 50%) of CFU-C content in the BM after a 5-day course of G-CSF was observed in WT but not CB2^{-/-} mice. Although our data suggest that this effect is not due to differential cell cycle activity in immature cells (Fig. 4E), our assay may lack sensitivity to detect subtle changes.

CB2 deficiency-associated lymphocytosis is hematopoietic-intrinsic

The ability to reconstitute long-term multilineage hematopoiesis is a hallmark of the hematopoietic stem cell. To assess this property, we transplanted the low dose of 200,000 CB2^{-/-} or WT BM cells into lethally irradiated wild-type recipients. Fourteen days after transplantation, we started monitoring engraftment kinetics. Serial differential blood count analysis, twice weekly for 8 weeks,

revealed no differences between CB2^{-/-} and WT mice except for lymphocyte counts (Fig. 5A). Fourteen weeks after transplantation, when hematopoiesis is considered to be fully established [23], significantly increased peripheral blood WBC and lymphocyte counts were detected in WT recipients repopulated with CB2^{-/-} HSCs, similar to homeostatic CB2^{-/-} mice, thus indicating the hematopoietic-intrinsic nature of the observed lymphocytosis. Furthermore, analysis of the immature cell compartments in BM and spleen as described before revealed no differences between both recipient groups (Fig. 5B). Neither LSK nor LSK-SLAM numbers, nor CFU-C counts (Fig. 5C), differed in WT mice reconstituted with CB2^{-/-} versus WT cells. These results confirm that CB2-deficient HSPCs exhibit no major functional deficiencies.

Discussion

Within the hematopoietic system, expression of CB2 receptor was first described in splenic cells [24]. Shortly thereafter, CB2 was found to be expressed on immune cells in blood [20] and also shown to modulate immunologic responses in mice [9,25]. Reports of expression of CB2 receptors on HSPCs and a potential

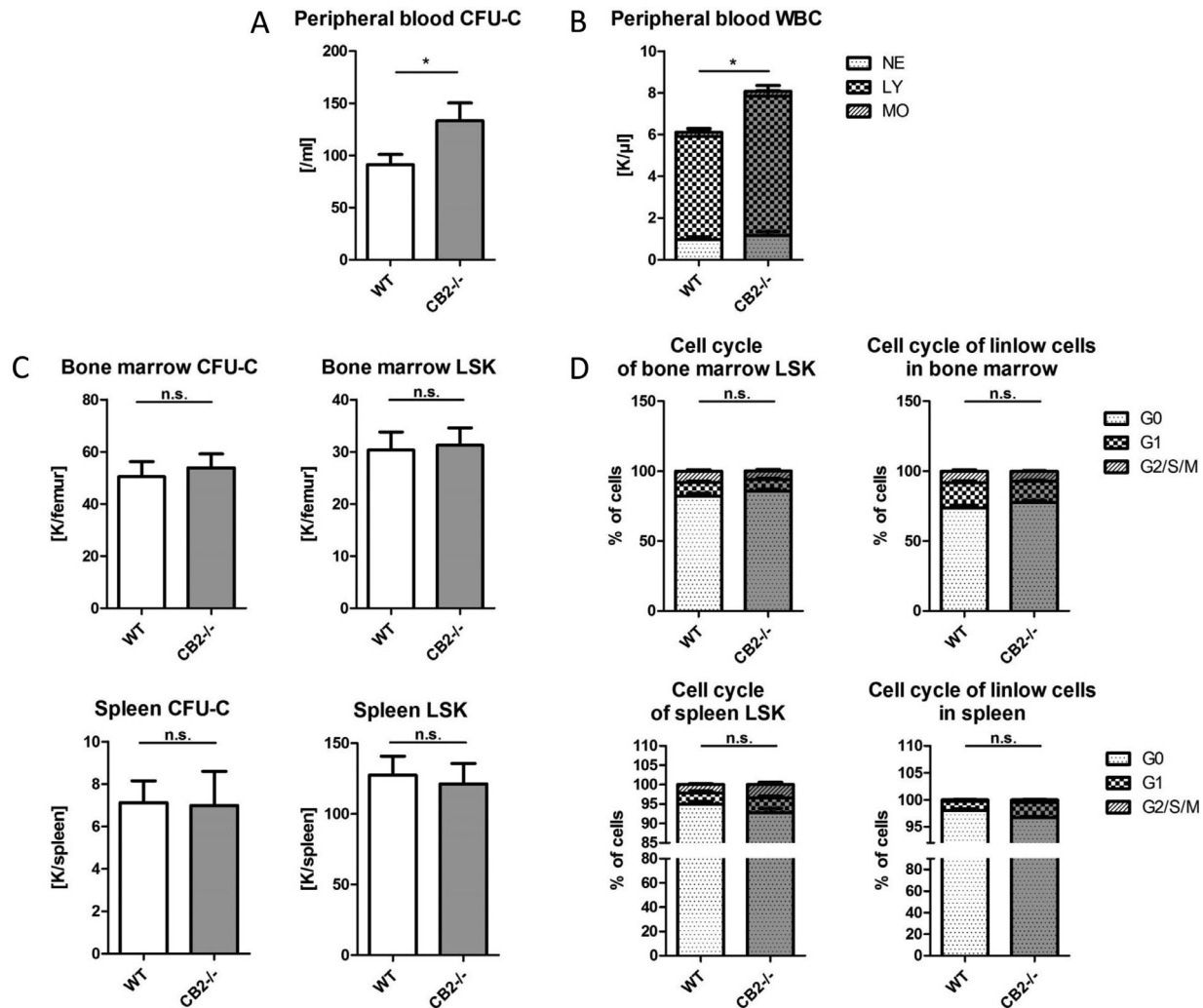


Figure 3. Steady-state analysis of CB2^{-/-} and WT hematopoiesis. (A) CFU-C content in peripheral blood. (B) Differential blood counts in peripheral blood. (C) Hematopoietic progenitor cells in BM (top row) and spleen (bottom row), enumerated functionally as CFU-C (left) or phenotypically as LSK cells (right). (D) Cell cycle activity of LSK (left) and lineage-low (right) in bone marrow (top row) or spleen (bottom row) cells. No significant changes were observed between genotypes in BM and spleen. Except for mild lymphocytosis and elevated circulating CFU-C in CB2^{-/-} mice, blood counts were normal throughout. $n \geq 9$ mice per group in two independent experiments.

dimerization with CXCR4 led us to the assumption that cannabinoid receptors might not only affect mature blood cells, but also be relevant for immature hematopoiesis [12]. Under steady-state conditions the individual HSPC needs to undergo only infrequent self-renewing divisions in contrast to stress hematopoiesis, where rapid HSPC expansion and generation and egress of mature blood cells are necessary. More than two decades ago, Valk et al. [26] proposed an influence of CB2 on HSPC proliferation, but the influence of CB2 on hematopoiesis has never been directly addressed. In this study, we aimed to clarify its role in steady-state and stress hematopoiesis using CB2^{-/-} mice. As no reliably staining/performing CB2 antibodies were available, we had to rely on the knockout mouse models.

Given the fact that lack of CB2 could be verified by PCR, these mice represent a suitable model for studying the role of CB2 in hematopoiesis.

In the course of this study, we first tried to distinguish CB2 knockout and CB2-competent cells using various antibodies: All antibodies tested also stained cells from CB2^{-/-} mice, which, when tested using PCR, did not express CB2 receptor mRNA. In line with our observations, Cécyre et al. [27] had previously reported the lack of specificity of several commercial CB2 antibodies. We were able to confirm expression of CB2 in HSPCs in all studied HSPC subpopulations (LSK, MPP, CMP, and HSC) by PCR, yet could not specifically assess its function using small-molecule compounds in vitro. AM1241 and JWH133 are

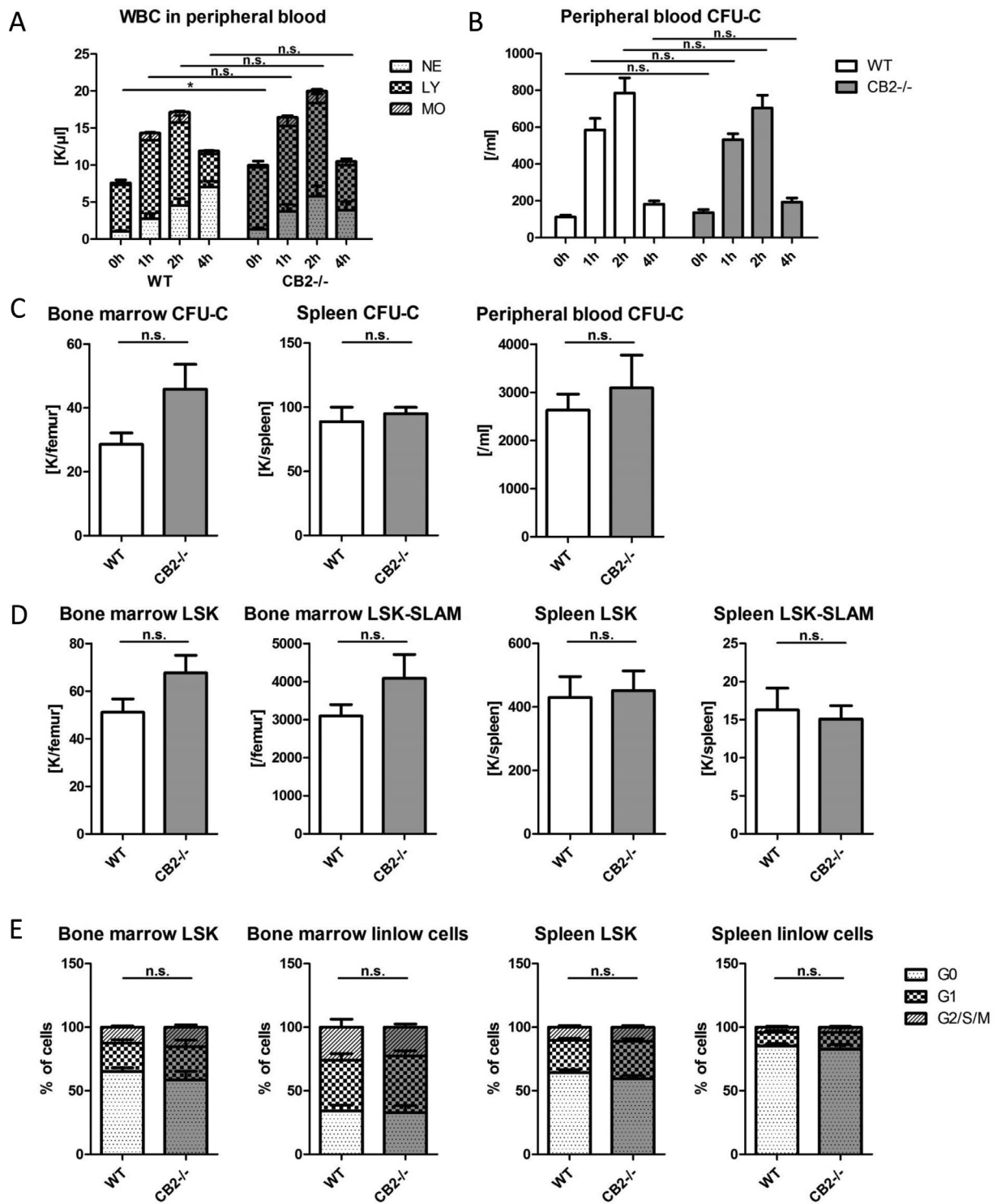
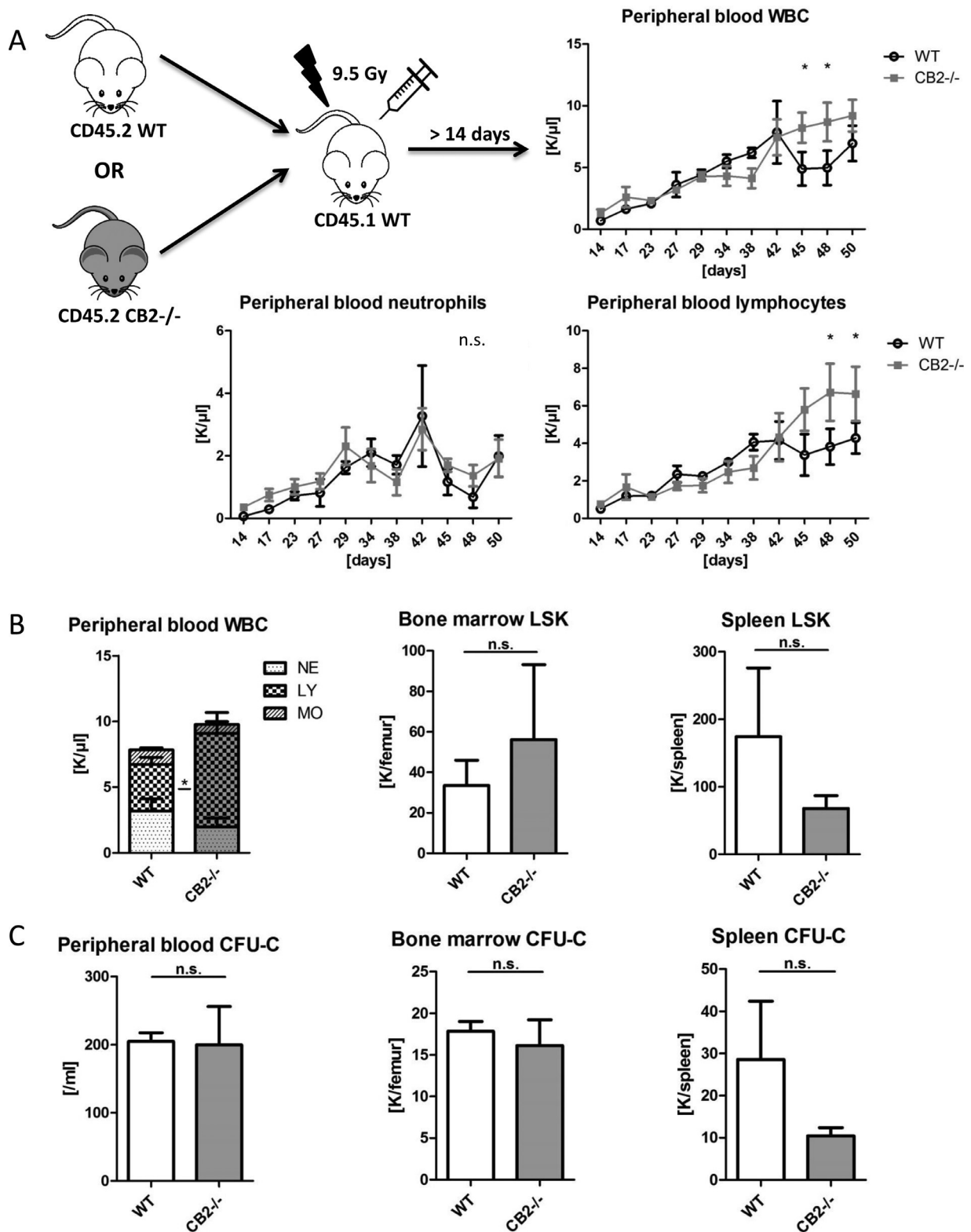


Figure 4. Blood cell mobilization in response to Plerixafor and G-CSF. (A, B) A single Plerixafor injection was administered intraperitoneally, and peripheral blood WBCs (A) and CFU-C (B) were enumerated at the indicated times. (C–E) Nine doses every 12 h of G-CSF were administered. CFU-C (C) and LSK (D) cells in bone marrow and spleen were enumerated. Cell cycle status of immature cells in BM and spleen was determined (E). Mobilization was normal except for lack of the characteristic post-mobilization depletion of HSPCs in CB2^{-/-} mice. $n \geq 9$ mice per group in two independent experiments with at least 14 days of recovery between AMD3100 and G-CSF administration.



commonly used as specific CB2 agonists, whereas AM630 is considered a specific antagonist. Yet, none of the compounds has been tested in CB2^{-/-} versus WT hematopoietic cells. Ibrahim et al. [28] found that pretreatment with AM630 blocked the binding of AM1241 by CB2 in rat brain cells, while the exposure to a presumably specific CB1 agonist did not. As a valid negative control was not included, off-target effects of AM630 cannot be excluded, and CB2 specificity was not definitively established in that study. A functional test for AM1241 was performed by Coke et al. [12]. The authors reported reduced migration of breast cells toward a CXCL12 gradient when adding AM1241 to wild-type cells, an observation that they inferred to be CB2 mediated. Here, CB2^{-/-} control cells were also not included. Given our results regarding the lack of specificity of CB2 agonists we can conclude that the reported effects are likely not or not solely CB2 mediated. We observed activation of ERK signaling after stimulation of BM cells with CXCL12 along with a reduction of ERK phosphorylation when the chemokine was combined with AM1241, both consistent with findings by Coke et al. [12]. However, this reduction of CXCL12-induced phosphorylation of MAP-kinases did not appear to be CB2 mediated, as it was observed in both CB2^{-/-} and CB2-competent cells. Similarly to AM1241, the agonist CP44930 also did not show specificity for CB2. In both CB2^{-/-} and WT cells, it induced modest prolongation of CXCL12 signaling *in vitro* at a concentration of 2.5 $\mu\text{mol/L}$. Higher doses were cytotoxic for both WT and CB2-deficient cells. *In vivo*, no pharmacologic effect on WBC counts or circulating HSPCs was discernible at doses between 0.1 and 1 mg/kg; a dose of 10 mg/kg, as previously used [29], was immediately lethal for both CB2^{-/-} and WT mice. Absence of expression of the alternative endocannabinoid receptors CB1 and GPR55 on hematopoietic cells exclude the hypothetical possibility of compensation for CB2 deletion. Thus, the dampening effect of the small-molecule compounds tested by us either may be mediated by a different receptor or represent a ubiquitous, unspecific, non-receptor-mediated effect. Alternatively, as the knockout could only be verified by RT-PCR and based on *in silico* protein structure/length predictions, it is possible that a truncated protein could be present on the surface membrane, which in fact was proposed for the Buckley mouse model [16]. However, in the second, the Delta-gen CB2^{-/-} mouse model tested here, the deleted region is located close to the C-terminus and predicted to result in complete loss of CB2 [30]. Compensatory effects by alternative cannabinoid receptors could be excluded because we are showing lack of expression of CB1 and GPR55 by PCR, but the possibility of non-CB-receptor-mediated compensation cannot be ruled

out. In summary, our data indicate that the supposedly CB2-targeting agonists tested here affect CB2-expressing and -deleted hematopoietic cells alike, that is, do not possess CB2 specificity in the context of (immature) hematopoietic cells.

Jiang et al. [31] proposed an effect of the cannabinoid system on regulation of the HSPC compartment. Similarly, given CB2 expression in HSPCs, we expected to find a role for CB2 receptor signaling in immature hematopoiesis. However, enumeration and characterization of progenitor cells in BM, spleen, and peripheral blood revealed only minor differences between CB2-deficient and healthy WT mice. Consistent with published data, we observed a mild lymphocytosis in both CB2^{-/-} strains. With respect to the modest mobilization phenotype observed in homeostatic CB2^{-/-} mice, we propose that this effect is likely an indication of endocannabinoids favoring HSPC retention. Although cooperative signaling of CXCL12 and cannabinoid agonists has been reported, we lacked the tools to reproduce this, and hence, the co-opted signaling pathway may be distinct from CXCL12/CXCR4. An alternative hypothesis would be that the HSPCs are being passively mobilized with the excessive lymphocyte numbers trafficking out of the bone marrow, as all reported HSPC mobilization is accompanied by a leukocytosis, often very pronounced. Of possible relevance, Pereira et al. [32] found that CB2 mediates retention of immature B cells in BM sinusoids. Inversely, then, lack of cannabinoid receptor would lead to higher B-cell counts in peripheral blood, consistent with our data for HSPCs. Schwarz et al. [22] and Schatz et al. [33] could show in the early 1990s that CB2 agonists inhibit lymphocyte proliferation *in vitro*, potentially explaining elevated lymphocyte levels found in CB2 knockout mice *in vivo* by us and others [34,35]. Our studies extend the previous characterization of the phenotype of CB2 knockout mice with the observation of increased numbers of baseline circulating immature hematopoietic cells (CFU-C). Endocannabinoids thus contribute, directly or indirectly, to HSPC retention in BM.

The only striking observation in the CB2^{-/-} mice is in bone marrow after G-CSF treatment: Mobilization experiments revealed a lesser depletion of HSPCs in the BM of CB2^{-/-} mice after G-CSF administration compared with WT mice (Fig. 4C). Analysis of the cell cycle on day 5 did not reveal significant differences in immature (Fig. 4E) or mature BM cell proliferation (data not shown). Possible explanations for this observation are not straightforward. Mathematically, the reduction of HSPC activity in bone marrow after G-CSF is due mostly to HSPC differentiation to precursor stage and not to egress, as only 1%–2 % of the total BM HSPC pool is mobilized into blood [3]. The possibility, therefore, that endocannabinoids elaborated

under G-CSF exert differentiation-promoting effects in CB2-competent mice, something that is not seen in the CB2^{-/-} mice, may be entertained but cannot be tested for lack of suitable compounds. In the course of transplantation experiments no functional differences between CB2-deficient and WT BM cells were found. The mild lymphocytosis was reestablished in WT hosts reconstituted with CB2^{-/-} BM similarly to complete CB2^{-/-} mice, pointing toward a strictly cell-intrinsic effect. While this article was undergoing revision, Khuja et al. [36] independently came to the same results and conclusions. Importantly, the kinetics of engraftment of CB2^{-/-} cells were indistinguishable from those of WT donor cells. Competitive transplantation experiments can decipher minor defects of stem cell function and thus would have directly addressed the competitiveness of CB2^{-/-} HSPCs with respect to BM niche invasion/engraftment. For lack of any suggestive phenotype of conventional transplants whatsoever, such studies were not performed, possibly limiting the definitiveness of the presented work.

We here show that CB2 receptor is largely dispensable for immature hematopoiesis in mice. In two different CB2 knockout models we found no impairment of HSPC function, neither under homeostatic conditions nor under stress conditions. CB2 receptor-deficient cells repopulate lethally irradiated recipients and establish functional hematopoiesis. All CB2-targeting small-molecule compounds tested here lack receptor specificity for hematopoietic cells and therefore need to be evaluated carefully for every application, using CB2-deficient cells as negative controls.

Conflict of interest disclosure

None of the authors declare potentially competing interests with respect to this article.

Author contributions

FH, SYL, FC, SO, KD, DC, GS, and BT performed experiments. ED, EW, and DK performed experiments and analyzed data. ED and HB planned experiments, co-wrote the article, and share overall responsibility for the studies. All authors read and approved the final version of the article.

References

1. Thomas ED, Lochte HL Jr, Ferrebee JW. Irradiation of the entire body and marrow transplantation: some observations and comments. *Blood*. 1959;14:1–23.
2. Calvi LM, Link DC. Cellular complexity of the bone marrow hematopoietic stem cell niche. *Calcif Tissue Int*. 2014;94:112–124.
3. Bonig H, Papayannopoulou T. Mobilization of hematopoietic stem/progenitor cells: general principles and molecular mechanisms. *Methods Mol Biol*. 2012;904:1–14.
4. Calvi LM, et al. Osteoblastic cells regulate the haematopoietic stem cell niche. *Nature*. 2003;425:841–846.
5. Nervi B, Link DC, DiPersio JF. Cytokines and hematopoietic stem cell mobilization. *J Cell Biochem*. 2006;99:690–705.
6. Karpova D, Bonig H. Concise review: CXCR4/CXCL12 signaling in immature hematopoiesis—lessons from pharmacological and genetic models. *Stem Cells*. 2015;33:2391–2399.
7. Broxmeyer HE, Orschell CM, Clapp DW, et al. Rapid mobilization of murine and human hematopoietic stem and progenitor cells with AMD3100, a CXCR4 antagonist. *J Exp Med*. 2005;201:1307–1318.
8. Bonig H, Watts KL, Chang KH, Kiem HP, Papayannopoulou T. Concurrent blockade of alpha4-integrin and CXCR4 in hematopoietic stem/progenitor cell mobilization. *Stem Cells*. 2009;27:836–837.
9. Howlett AC. The cannabinoid receptors. *Prostaglandins Other Lipid Mediat*. 2002;68/69:619–631.
10. Saito VM, Rezende RM, Teixeira AL. Cannabinoid modulation of neuroinflammatory disorders. *Curr Neuropharmacol*. 2012;10:159–166.
11. Leleu-Chavain N, Body-Malapel M, Spencer J, Chavatte P, Desreumaux P, Millet R. Recent advances in the development of selective CB(2) agonists as promising anti-inflammatory agents. *Curr Med Chem*. 2012;19:3457–3474.
12. Coke CJ, Scarlett KA, Chetram MA, et al. Simultaneous activation of induced heterodimerization between CXCR4 chemokine receptor and cannabinoid receptor 2 (CB2) reveals a mechanism for regulation of tumor progression. *J Biol Chem*. 2016;291:9991–10005.
13. Lattin JE, Schroder K, Su AI, et al. Expression analysis of G protein-coupled receptors in mouse macrophages. *Immunome Res*. 2008;4:5.
14. Ashton JC, Wright JL, McPartland JM, Tyndall JD. Cannabinoid CB1 and CB2 receptor ligand specificity and the development of CB2-selective agonists. *Curr Med Chem*. 2008;15:1428–1443.
15. Bingham B, Jones PC, Uveges AJ, et al. Species-specific in vitro pharmacological effects of the cannabinoid receptor 2 (CB2) selective ligand AM1241 and its resolved enantiomers. *Br J Pharmacol*. 2007;151:1061–1070.
16. Zhang HY, Shen H, Jordan CJ, et al. CB2 receptor antibody signal specificity: correlations with the use of partial CB2-knockout mice and anti-rat CB2 receptor antibodies. *Acta Pharmacol Sin*. 2019;40:398–409.
17. Buckley NE, McCoy KL, Mezev E, et al. Immunomodulation by cannabinoids is absent in mice deficient for the cannabinoid CB (2) receptor. *Eur J Pharmacol*. 2000;396:141–149.
18. Jiang N, Chen M, Yang G, et al. Hematopoietic stem cells in neural-crest derived bone marrow. *Sci Rep*. 2016;6:36411.
19. Lattin J, Zidar DA, Schroder K, Kellie S, Hume DA, Sweet MJ. G-protein-coupled receptor expression, function, and signaling in macrophages. *J Leukoc Biol*. 2007;82:16–32.
20. Galiegue S, Mary S, Marchand J, et al. Expression of central and peripheral cannabinoid receptors in human immune tissues and leukocyte subpopulations. *Eur J Biochem*. 1995;232:54–61.
21. Schwarz H, Blanco FJ, Lotz M. Anandamide, an endogenous cannabinoid receptor agonist, inhibits lymphocyte proliferation and induces apoptosis. *J Neuroimmunol*. 1994;55:107–115.
22. Derocq JM, Séqui M, Marchand J, Le Fur G, Casellas P. Cannabinoids enhance human B-cell growth at low nanomolar concentrations. *FEBS Lett*. 1995;369:177–182.
23. Pallavicini MG, Redfearn W, Necas E, Brecher G. Rescue from lethal irradiation correlates with transplantation of 10-20 CFU-S-day 12. *Blood Cells Mol Dis*. 1997;23:157–168.
24. Munro S, Thomas KL, Abu-Shaar M. Molecular characterization of a peripheral receptor for cannabinoids. *Nature*. 1993;365:61–65.
25. Klein TW, Newton C, Friedman H. Cannabinoid receptors and immunity. *Immunol Today*. 1998;19:373–381.
26. Valk P, Verbakel S, Vankan Y, et al. Anandamide, a natural ligand for the peripheral cannabinoid receptor is a novel synergistic growth factor for hematopoietic cells. *Blood*. 1997;90:1448–1457.
27. Cécyre B, Thomas S, Ptito M, Casanova C, Bouchard JF. Evaluation of the specificity of antibodies raised against cannabinoid

- receptor type 2 in the mouse retina. *Naunyn Schmiedebergs Arch Pharmacol.* 2014;387:175–184.
28. Ibrahim MM, Rude ML, Stagg NJ, et al. CB2 cannabinoid receptor mediation of antinociception. *Pain.* 2006;122:36–42.
 29. Hoggatt J, Pelus LM. Eicosanoid regulation of hematopoiesis and hematopoietic stem and progenitor trafficking. *Leukemia.* 2010;24:1993–2002.
 30. Yao B, Mackie K. Endocannabinoid receptor pharmacology. *Curr Top Behav Neurosci.* 2009;1:37–63.
 31. Jiang S, Fu Y, Williams J, et al. Expression and function of cannabinoid receptors CB1 and CB2 and their cognate cannabinoid ligands in murine embryonic stem cells. *PLoS One.* 2007;2:e641.
 32. Pereira JP, An J, Xu Y, Huang Y, Cyster JG. Cannabinoid receptor 2 mediates the retention of immature B cells in bone marrow sinusoids. *Nat Immunol.* 2009;10:403–411.
 33. Schatz AR, Lee M, Condie RB, Pulaski JT, Kaminski NE. Cannabinoid receptors CB1 and CB2: a characterization of expression and adenylate cyclase modulation within the immune system. *Toxicol Appl Pharmacol.* 1997;142:278–287.
 34. Buckley NE. The peripheral cannabinoid receptor knockout mice: an update. *Br J Pharmacol.* 2008;153:309–318.
 35. Ziring D, Wei B, Velazquez P, Schrage M, Buckley NE, Braun J. Formation of B and T cell subsets require the cannabinoid receptor CB2. *Immunogenetics.* 2006;58:714–725.
 36. Khuja I, Yekhtin Z, Or R, Almogi-Hazan O. Cannabinoids reduce inflammation but inhibit lymphocyte recovery in murine models of bone marrow transplantation. *Int J Mol Sci.* 2019;20(3):E668.